Molecular markers for natural and anthropogenic organic matter sources and distribution in aquatic systems from the Indian Subcontinent

Bulbul Mehta

A thesis submitted for the partial fulfillment of the degree of Doctor of Philosophy

Department of Earth and Environmental Sciences
Indian Institute of Science Education and Research Mohali
Knowledge city, Sector 81, SAS Nagar, Manauli PO, Mohali 140306, Punjab, India.

April 2023

DEDICATED
TO
MY FAMILY

Declaration

The thesis work has been done by me under the guidance of Dr. Anoop Ambili at the Indian Institute of Science Education and Research Mohali. The present work has not been submitted in part or in full for a degree, a diploma, or a fellowship to any other university or institute. Whenever contributions of others are involved, every effort is made to indicate this clearly, with due acknowledgement of collaborative research and discussions. This thesis is a bona fide record of original work done by me and all sources listed within have been detailed in the bibliography.

Bulbul Mehta

In my capacity as the supervisor of the candidate's thesis work, I certify that the above statements by the candidate are true to the best of my knowledge.

Dr. Anoop Ambili

Acknowledgement

The PhD thesis work has been accomplished at Department of Earth and Environmental Sciences, Indian Institute of Science Education and Research (IISER) Mohali, India. Firstly, I would like to express my deepest appreciation to my Supervisor Dr. Anoop Ambili (Assistant Professor), Department of Earth and Environmental Sciences, IISER Mohali for providing his constant guidance and suggestions in completion of my PhD journey. I wouldn't have been able to accomplish this feat within limited time frame without his endless endeavors and generous support. I am highly indebted to him as the way he rendered his help and provided me with all the facility required throughout is commendable. I would also like to express my special thanks of gratitude to my guide's better half (Mrs. Rimjhim Singh) and his two cute children (Anragya Ambili and Advaita Ambili) for their affection and care.

I would sincerely thank my doctoral committee members 'Dr. Baerbel Sinha' and 'Dr. Sunil K. Patil' from department of Earth and Environmental Sciences, IISER Mohali for their valuable inputs during my PhD. Also, I acknowledge 'Dr. Praveen Kumar Mishra' from Cluster University of Jammu and 'Dr. Sharmila Bhattacharya' from IISER Mohali for their assistance and knowledge.

I would extend my thanks to IISER Mohali (IISERM) and the Ministry of Human Resource Development (MHRD), Government of India for my Junior and Senior Research fellowships (JRF and SRF). Also, I would like to acknowledge my lab members Sunil and Ajay for the useful scientific discussions at the tea sessions.

Finally, words are insufficient to express gratitude to Almighty, Guruji and my cherished family members involving my father (Mr. Suresh Mehta), mother (Mrs. Pinky Mehta), sister (Sanskriti Mehta), brother-in-law (Sahil Mehta), brother (Chatenya Mehta) and niece (Abhedya Mehta) as without their faith and encouragement I wouldn't have been able to cross this path with conviction. I am always indebted to their tenderness and kindness. Finally, I dedicate my PhD thesis to my father and mother.

List of Publications

PhD work

Research Articles

Bulbul, M., Ankit, Y., Chirakkal, A., Anoop, A., Mishra, P.K., 2022. Understanding the present and past climate-human-vegetation dynamics in the Indian Himalaya: A comprehensive review. In: Advances in Remote Sensing Technology and the Three Poles 16 (247-256).

Bulbul, M., Ankit, Y., Basu, S., Anoop, A., 2021. Characterization of sedimentary organic matter and depositional processes in Mandovi estuary, Western India: An integrated lipid biomarker, sedimentological and stable isotope approach. Applied Geochemistry 131, 105041.

Bulbul, M., Bhattacharya, S., Ankit, Y., Yadav, P., Anoop, A., 2022. Occurrence, distribution and sources of phthalates and petroleum hydrocarbons in tropical estuaries (Mandovi and Ashtamudi) of western Peninsular India. Environmental Research 214, 113679.

Bulbul, M., Kumar, S., Ajay, K., Anoop, A., 2023. Spatial distribution and characteristics of microplastics and associated contaminants from mid-altitude lake in NW Himalaya. Chemosphere 138415.

Other Work

Ankit, Y., **Bulbul, M.**, Anoop, A., Mishra, P.K., 2022. Monsoon variability in the Indian subcontinent—A review based on proxy and observational datasets. In: Holocene Climate Change and Environment, 369-389.

Ankit, Y., Mishra*, P.K., **Bulbul, M.**, Anoop, A., Misra, S., Jamir, T., 2022. Hydroclimatic variability in northeast India during the last two millennia: sedimentological and geochemical record from Shilloi Lake, Nagaland. Palaeogeography, Palaeoclimatology, Palaeoecology 602, 111151.

Ankit, Y., Muneer, W., Gaye, B., Lahajnar, N., Bhattacharya, S., **Bulbul, M.**, Jehangir, A., Anoop*, A. and Mishra*, P.K., 2022. Apportioning sedimentary organic matter sources and its degradation state: inferences based on aliphatic hydrocarbons, amino acids and $\delta^{15}N$. Environmental research 205, 112409.

Table of Contents

Chapter 1

1.1 Introduction

The aquatic systems play critical role by acting as carbon sink and providing innumerable services to local and regional livelihoods, maintaining global climate conditions, and regulating heat budgets (Gnanamoorthy et al., 2020, Saranya et al, 2022). Moreover, the aquatic systems also serve as site for organic matter (OM) generation (Zhou et al., 2022). Traditionally, aquatic systems receive OM from various allochthonous (e.g., land-plants, watershed and anthropogenic activities) and autochthonous/in-situ sources (e.g., phytoplankton, algae, macrophytes, microbial activity) (Bruno et al., 2023). Understanding the source and composition of OM in an aquatic system is important, as they play a significant role in hypolimnetic oxygen content (Müller et al., 2012; Steinsberge et al., 2020), microbial community composition (Crump et al., 2003; Bertolet et al., 2019; Behera et al., 2022), and colonization of submerged plants (Silveira and Thomaz, 2015).

In addition to the natural OM sources, the human-induced activities involving tourism, mining, marine operations, ferries movement, domestic sewage, fishing, industrial waste, recreational activities, plastic waste, fossil fuel combustion have contributed to organic contamination in the aquatic ecosystems (Reshmi et al., 2015; Sreekanth et al., 2017). Notably, the rise in anthropogenic pressure has led to high nutrient loading, eutrophic conditions along with anoxia within the systems (Howarth et al., 2011). Further, the occurrence and composition of numerous emerging pollutants (e.g., microplastics, phthalates etc.) is a matter of rising concern, as the presence of these contaminants serves as major threat to aquatic organisms (Miller et al., 2021). The rise in urbanization and industrialization have resulted in the outspread of pollutants principally involving oil and plastic pollutants that have impacted the aquatic systems drastically (Sigler, 2014; Yang et al., 2015). The petroleum spillage in an ecosystem especially in the estuaries has also resulted in toxicological effects on the aquatic organisms (Yang et al., 2015).

Traditionally, molecular markers approach involving proxies based on *n*-alkanes is globally used to delineate the OM sources (Ficken et al., 2000). The *n*-alkanes are generally studied as they serve as effective tools due to their source specificity and resistance towards degradation (Ho and Meyers, 1994; Ankit et al., 2017). For instance, the short-chain, middle-chain and long-chain *n*-alkanes represent contribution from phytoplankton, submerged/floating

macrophyte and terrestrial plants, respectively (Ankit et al., 2017). Numerous *n*-alkane derived proxies including P-aqueous (P_{aq}), terrigenous/aquatic ratio (TAR), carbon preference index (CPI) and average chain length (ACL) have been used to understand the productivity changes as well as organic matter input from various natural sources (Bray and Evans, 1961; Poynter and Eglinton, 1990; Ficken et al., 2000; Mille et al., 2007). Furthermore, to have better understanding about OM sources and productivity changes, stable isotope signatures specifically $\delta^{13}C$ also serve as a useful variable (Liao et al., 2018). Among the anthropogenic markers, the petroleum such as hopanes, steranes (Fig. 1.1 a-b) and diasteranes are globally examined to detect the residues of oil contamination from marine operations (Volkman et al. 1992). These compounds are source-specific and have been valuable to understand the signatures of petroleum mixtures (Aeppli et al., 2014). The spectra for these compounds along with high unresolved complex mixtures are indicative of oil spillage in sediments (Venturini et al., 2008). Hopanes (m/z 191) are highly recalcitrant towards environmental degradation and these compounds change to 17α, 21β configuration and (22 R and 22 S) diastereoisomers upon catagenesis process (Bost et al., 2001). Likewise, cyclic molecules like steranes (m/z 217) are resistant towards biodegradation and modify to αββR and αββS isomers upon diagenesis (Peters et al., 2005). Similarly, the presence of diasteranes (m/z 259) also known as rearranged steranes suggest about extensive oil pollution in a system (Samelak et al., 2020).

In addition to petroleum contamination, microplastics (particles with size ranges in 1 μm – 0.5 mm) have captured considerable attention due to the concerns about the risk and possible adverse impacts on the ecosystem and human health (Wagner et al., 2014). The microplastics (MPs) tend to remain longer in the environment due to low degradation rates, thereby resulting in high environmental contamination (Lin et al., 2020). These particles cause potential threats to the aquatic organisms including reduced growth and reproduction issues (Dey et al., 2021). Moreover, MPs serve as medium for various chemical contaminants in the aquatic environments (Dehghani et al., 2017). Therefore, due to high negative impacts of MPs, it is important to study the distribution levels along with ecological risks. Furthermore, plastics also tend to contain toxic chemicals known as phthalic acid esters (PAEs or phthalates) (Fig. 1.2 a-c). Phthalates are plastic additives used in numerous industries such as cosmetics and medical devices (Staples et al., 1997; Gao et al., 2019). More recently, these compounds have received global significance as they have led to severe human health effects such as fertility issues and birth defects (Lottrup et al., 2006). Moreover, the phthalate compounds such as di-isobutyl

phthalate (DIBP) (Fig. 1.2b) and di(2-ethylhexyl) phthalate (DEHP) tend to cause reproductive and developmental toxicity (Ito et al., 2005).

In Indian subcontinent, only a handful of studies have examined the accumulation and source characterization of OM in sediments as well as identification and quantification of anthropogenically derived organic contaminants (Artifon et al., 2019). The limited studies encouraged me to focus my thesis on an integrated molecular and isotopic ($\delta^{13}C$) approach that helps to understand the natural and anthropogenic modifications in various ecosystems. I focused on estuaries i.e., Mandovi and Ashtamudi estuary and freshwater Himalayan lake i.e., Rewalsar lake, the study sites that are impacted by numerous anthropogenic activities. The organic matter sources were identified and petroleum contamination signatures were investigated from Mandovi estuary. Moreover, an intercomparison study was developed based on concentration levels of organic contaminants involving hopanes, steranes, diasteranes and phthalate compounds. Furthermore, the data retrieved from Mandovi estuary was compared with Ashtamudi estuary (Ramsar site, a wetland that is considered to be of international importance) to examine the extent of oil and plastic pollution levels in both the sites. Likewise, the occurrence and distribution of emerging class of pollutants such as microplastics (MPs) were investigated from highly sensitive mountainous lake (Rewalsar lake) in NW Himalayas. The examination of MPs in an ecosystem is of paramount significance as due to prolonged residence time and stable chemical properties, these particles tend to remain in the environment and are ingested by the aquatic organisms.

The research on lake and estuarine sediments was done keeping three broad goals in mind that involves:

- To use multiple proxies to have better understand about the organic matter accumulation and biogeochemical cycles.
- To delineate the natural and anthropogenic OM sources in aquatic systems using molecular markers.
- To understand the extent of pollution due to human-induced changes in the aquatic ecosystem.

1.2 Research objectives and thesis structure

The present thesis is divided into following ‘five’ chapters and examines numerous objectives listed within the respective chapters below.

1. Chapter 1 ‘Introduction’ provides information about the importance of organic matter source characterization to understand the biogeochemical cycles. Further, I have discussed the utilization of organic proxies for understanding the natural and anthropogenic changes in the aquatic systems. Notably, distribution of emerging contaminant specifically microplastics are commonly used to understand the anthropogenic impact in an aquatic ecosystem.

2. Chapter 2 discusses about the use of multiple proxies (molecular markers and carbon isotope) to determine the composition of organic matter within the Mandovi estuary, India. Further, lipid biomarkers (aliphatic hydrocarbons), sedimentological along with geochemical approach helped to understand the factors controlling organic matter distribution. Moreover, role of anthropogenic activities was also examined in the aquatic ecosystem.

   The objectives of present study are to:

   - decode OM input from natural and anthropogenic sources.
   - understand the circulation dynamics and depositional conditions in the Mandovi estuary
   - examine the factors controlling the OM distribution in the estuarine system.
   - investigate the petroleum biomarkers and hydrocarbon contamination in the system.

3. In Chapter 3, the occurrence and distribution of petroleum compounds was discussed and an intercomparison was done between Mandovi estuary and Ashtamudi estuary (Ramsar site). Likewise, the accumulation of phthalates was examined to delineate plastic pollution in both the study sites.

   The aims of the study are to:

   - evaluate phthalate esters in the surface sediments collected from two tropical estuaries.
   - investigate the accumulation of petroleum biomarkers in both the ecosystems.
   - determine the origin of the organic contaminants distribution into the system.
   - compare the level of pollution in both the estuaries on the basis of quantitative data.

4. In Chapter 4, the presence of another set of emerging contaminants such as microplastics (MPs) and a class of organic compounds such as phthalic acid esters (PAEs) were evaluated from the freshwater Rewalsar lake, Himachal Pradesh (India). Further, the morphology along with polymers were detected from sampling sites. Moreover, the potential sources responsible for spatial distribution of contaminants was also studied.

   The objectives are to:

   - understand the spatial distribution of MPs in water and sediment samples.
   - determine the concentration of phthalate compounds in the surface sediments.
   - delineate the sources behind accumulation of contaminants.
   - Compare the data with other study sites

5. Chapter 5 is the conclusion of our investigations and presents a comprehensive understanding about the contribution of OM from natural and anthropogenic sources in different aquatic environments. Further, it explains about rise in environmental risks due to high human intervention that has ultimately suggested adoption of monitoring programs as well as management strategies. The investigations regarding OM composition will help to understand the biogeochemical processes as well as carbon cycles. Also, the changes in OM influx and sources using molecular markers will help to understand about past climate and environmental conditions.

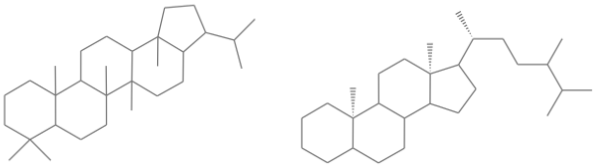

a) b)

Figure 1.1: Structure of a) hopane b) sterane compounds.

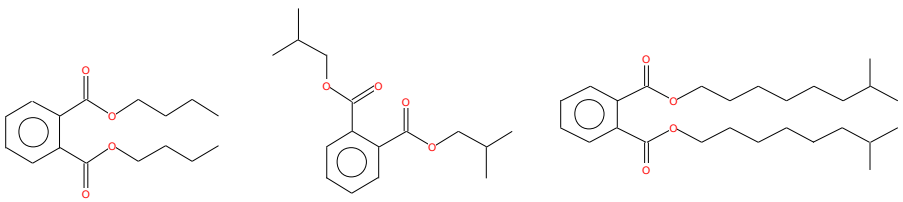

a) b) c)

Figure 1.2: Structure of a) dibutyl phthalate (DBP) b) di-isobutyl phthalate (DIBP) c) di-isononyl phthalate (DINP).

Chapter 2

Characterization of sedimentary organic matter and depositional processes in Mandovi estuary, western India: An integrated lipid biomarker, sedimentological and stable isotope approach*

*The contents of the chapter are published in the international peer reviewed journal 'Applied Geochemistry' as Bulbul et al., 2021.

Bulbul, M., Ankit, Y., Basu, S. and Anoop, A., 2021. Characterization of sedimentary organic matter and depositional processes in the Mandovi estuary, western India: An integrated lipid biomarker, sedimentological and stable isotope approach. Applied Geochemistry 131, 105041.

Mehta Bulbul[1], Yadav Ankit[1], Sayak Basu[1], Ambili Anoop[1]

[1]Indian Institute of Science Education and Research, Mohali 140306, India

2.1. Introduction

Estuaries form the transitional zone between marine and riverine environments and are sites of high organic matter (OM) production (Han et al., 2017). The circulation dynamics in an estuarine ecosystem is propagated by tidal advected currents in the lower reaches, and river influx in the upper reaches. This complex circulation pattern enhances OM dispersion and makes the system highly productive and sustainable (Malone et al., 1988; Geyer and MacCready, 2014). The OM in estuarine sediments is derived from both terrigenous sources and autochthonous marine components (Thornton and McManus, 1994; Ankit et al., 2017). The estuarine ecosystem also receives multiple organic pollutants from various anthropogenic sources as municipal and industrial wastewater effluents, and oil spills (Yuan et al., 2001). The intensified anthropogenic activities such as industrialization and urbanization in areas close to the estuarine systems lead to high nutrient concentrations resulting in eutrophication and hypoxia (Kumari and Rao, 2013; Ram et al., 2014 and references therein). The source apportionment of organic matter (*in situ* production versus terrestrial and anthropogenic OM contribution) is therefore important to understand the global carbon cycling (Ward et al., 2017; Bianchi and Allison, 2009) as well as the management of anthropogenic activities in a river-estuary system.

Stable isotope ratios of organic carbon ($\delta^{13}C_{org}$) are typically used to track OM sources in estuarine systems (Thornton and McManus, 1994; Zhou et al., 2006). However, post depositional alterations and multiple sources of OM can complicate the usefulness of the $\delta^{13}C_{org}$ as a source indicator in estuarine sediment (Ankit et al., 2017; Liao et al., 2018). The limitations of using bulk organic parameters can be overcome by using biomarkers (*n*-alkanes) to characterize specific sources of organic matter in an estuarine ecosystem (Wu et al., 2004; Ankit et al., 2017). The *n*-alkanes are frequently studied as source tracers due to their high preservation potential and resistance to diagenetic alteration (Ho and Meyers, 1994; Bourbonniere and Meyers, 1996). The *n*-alkane based indices are widely utilized to disentangle OM sources in sedimentary depositional environments (Bourbonniere and Meyers, 1996; Ficken et al., 2000; Ankit et al., 2017). The various *n*-alkane indices include i) the proxy ratio P-aqueous (P_{aq}), defined as the ratio of odd mid-chain alkanes (C_{23}+C_{25}) to odd mid and long-chain alkanes (C_{23}+C_{25}+C_{29}+C_{31}). Paq is used to discriminate between input from non-emergent plants (submerged and floating) represented by mid-chain homologues (C_{23} and C_{25}) and emergent aquatic, terrestrial plants constituted by the long-chain homologues (>C_{29})

(Ficken et al., 2000); ii) terrigenous/aquatic ratio (TAR), which estimates the contribution of long-chain *n*-alkanes ($C_{27}+C_{29}+C_{31}$) derived from terrestrial plant waxes and the short-chain *n*-alkanes ($C_{15}+C_{17}+C_{19}$) constituting microbial organism (Bourbonniere and Meyers, 1996; Mille et al., 2007); iii) carbon preference index (CPI) defined as the ratio of the odd number *n*-alkanes to even number *n*-alkanes that is used to determine the contribution from microbial, terrestrial and/or petrogenic hydrocarbons (Bray and Evans, 1961), iv) ACL (average chain length) defined as the average number of carbon atoms per molecule and is based on the abundance of odd carbon numbered higher plant-derived *n*-alkanes (Poynter and Eglinton, 1990). ACL is useful for distinguishing the organic matter input from marine and terrestrial sources, and assessing the degree of contamination in marine coastal waters due to human-induced activities (Jeng, 2006). Additionally, some other proxies were also used including NAR (natural *n*-alkanes ratio), which helps to discriminate the inputs from natural *n*-alkanes and petroleum-derived *n*-alkanes (Mille et al., 2007), isoprenoid ratios (pristane/phytane (Pr/Ph), Pr/*n*-C_{17}, Ph/*n*-C_{18}) that are used to evaluate the presence of oil and understand the relative biodegradation of *n*-alkanes (Mille et al., 2007). Likewise, the presence of unresolved complex mixture (UCM), which is defined as a rising baseline comprising of numerous unresolved peaks (Volkman et al., 1992), and hopanes are used to trace hydrocarbon contamination in the environment including oil spills (Saha et al., 2009; Maioli et al., 2011). The spatial distributions of aliphatic hydrocarbons and the presence of UCM and hopanes in surficial sediments supplemented by $\delta^{13}C_{org}$ and TOC content can help to identify OM sources, trace the impacts on the ecosystem and estimate the contamination levels in the system (Volkman et al., 1992; Ou et al., 2004). Furthermore, grain size analyses in sediments can also be used to assess the modern depositional pattern and the role of OM distribution in the estuary (Mayer, 1994).

Mandovi is a tropical estuary located on the western coast of the Indian subcontinent. The estuary is characterised by constant interactions of fluvial discharge and tidal modulations resulting in a unique tropical ecosystem. Over the past decades, research was focused on the physico-chemical parameters of water (Selvakumar et al., 1980; VishnuRadhan et al., 2015), mineralogy of surficial sediments (Bukhari and Nayak, 1996), heavy metals contamination (Veerasingam et al., 2015a), hydrological modelling (Vijith et al., 2016), and characterization of organic matter sources (Harji et al., 2008) from the Mandovi estuarine system. *n*-Alkane investigations have been also conducted but they are restricted to a few sites sampled on the upper reaches of the riverine side (Harji et al., 2008). An integrated approach involving the

qualitative and quantitative estimation of organic matter sources and distribution of organic pollutants across the basin is absent. The primary objective of our study is source apportionment of organic matter and interpretation of the natural and anthropogenic impact over an ecosystem using multiproxy data. The land use and land cover (LULC) changes in the vicinity of Mandovi estuary have also been evaluated to understand the effect of land-based human activities on anthropogenic OM inputs. Furthermore, the circulation dynamics and mixing of river water and open-ocean seawater in the estuarine system was also assessed using the $\delta^{18}O$ measurements in surface water. The aims for our study are to: (1) elucidate the applicability of $\delta^{13}C_{org}$ and TOC as indicators of OM sources across the estuary; (2) examine the depositional environment and assess the modern circulation dynamics (spatial inputs of freshwater and seawater) of the ecosystem; (3) investigate the *n*-alkane distribution and compute various *n*-alkane proxies for source apportionment and identification of anthropogenic activities across the estuary; (4) test the potential use of petroleum biomarkers as a tool to identify hydrocarbon contamination in the estuary; (5) determine land-use changes in the catchment over past decades to understand the catchment evolution and factors responsible for contaminant supply.

2.2 Regional setting

The Mandovi estuary (15° 25'-15°30' N; 73°45'-73°59' E) is a shallow tropical monsoonal estuary located along the central west coast of India (Fig. 2.1a). The main channel of Mandovi estuary is nearly 50 km long and 3.2 km wide with a total drainage area of ~1895 km^2 (Qasim and Gupta, 1981; Shetye, 1999). The width and average depth of the channel is 4 km (at mouth) and 5 m, respectively (Kessarkar et al., 2009). The cross-sectional area of the channel decreases upstream indicating the convergent nature of the ecosystem (Shetye, 1999; Vijith et al., 2016). The lithology in the Mandovi River catchment belongs to Precambrian metamorphic rocks overlain by laterites (Renjan et al., 2017). The estuary is influenced by tropical wet climate with three different seasons, namely: pre-monsoon (February–May), monsoon (June–September), and post-monsoon (October–January) (Fernandes and Nayak, 2009). The average rainfall (1981-1997) along the river course varies from nearly 661 cm/yr (upstream) to 286 cm/yr (downstream) (Shetye et al., 2007). The estuary is largely fed by the Mhadei River, and contributions from Khandepar, Valvat and Mhapsa tributaries account for 75 to 85% of the total annual discharge that occurs during the monsoon period (Vijith et al., 2016). The estuary is largely influenced by riverine freshwater inflow and land run-off from catchment areas during monsoons, whereas water level in the lower estuary is controlled throughout the year

by tidal currents (Shetye et al., 2007; Vijith et al., 2016). The water body behaves as a conduit by transporting all terrigenous sediments and runoff from adjacent plains and ghats into the sea. The stretches of the estuary are used for navigation purposes and for the transport of iron and manganese ores (Kessarkar et al., 2015). The lower estuary comprises of sandy beaches i.e., Miramar and Verem beaches on either side of the river mouth.

The upper and middle Mandovi estuary consists of many mangroves species such as *Acanthus ilicifolius, Rhizophora mucronata, Avicennia officinalis, Rhizophora apiculata, Sonneratia alba, Kandelia candel,* and *Excoecaria agallocha* due to low wave action and presence of nutrient-rich silt (Untawale et al., 1973; Singh et al., 2004). The lower estuary is characterised by seagrasses (Untawale et al., 1973; Untawale and Jagtap, 1977; Jagtap, 1991). The phytoplankton are crucial determinants of primary productivity in the ecosystem and the estuarine body is dominated by *Nitzschia* spp. and *Synedra* sp. in the freshwater zone, whereas the saline lower estuary is dominated by *Rhizosolenia* spp., *Coscinodiscus* spp., *Dinophysis* spp. (Madondkar et al., 2007). The dinoflagellate blooms of *Scrippsiella trochoidea* and *Skeletonema costatum* are abundant during the post-monsoon period (Parab et al., 2013).

The Mandovi estuary acts as a sink for natural hydrocarbons and organic contaminants and the coastal waters tend to have constant exposure to oil pollution (Raghavan and Furtado, 2000; Sousa et al., 2013). The anthropogenic fluxes derived from urbanisation, mining activities, extensive tourism, marine operations (e.g., tanker traffic, oil production), movement of water boats, ferries, etc. have resulted in intensified levels of hydrocarbon pollution in the ecosystem (Prajith et al., 2016; Raghavan and Furtado, 2000). Furthermore, surface sediments are highly contaminated with trace metals and its incorporation in the aquatic food web is a major concern (Veerasingam et al., 2015a).

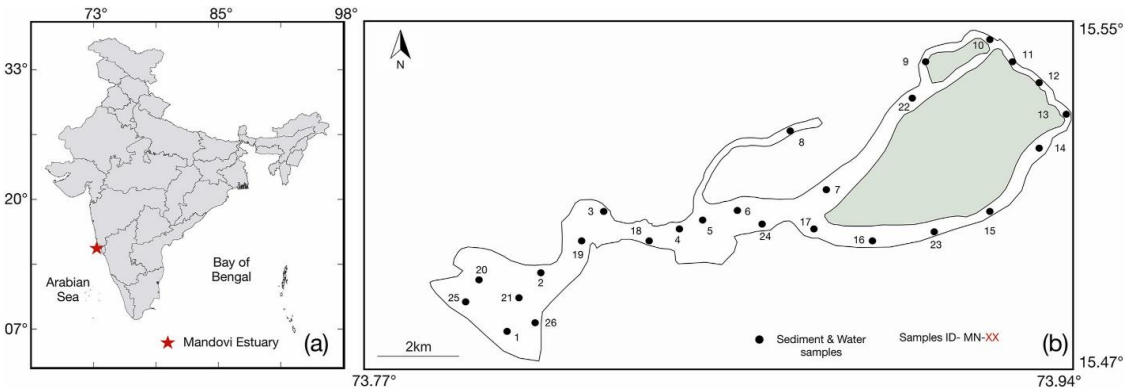

Figure 2.1. (a) Location of the study site (denoted with a 'red star'); (b) Map of study area including locations of sampling sites of sediment and water samples in the Mandovi estuary, western India.

2.3. Methodology

2.3.1. Field Sampling

Surface sediment samples (n = 26) were collected from Mandovi estuary during October 2018 using a Van Veen grab sampler with a penetration depth of 15-20 cm (Fig. 2.1b). The average sedimentation rate of ~1.42 cm/yr for Mandovi estuary (1980 AD onwards) was established by means of the radioactive $^{210}Pb_{excess}$ activity (Singh et al., 2014). Based on the estimated sedimentation rate, the retrieved modern surface sediments used in the present study represent a period of ~10-15 yrs. The samples were collected along the east-west transect covering lower, middle, and upper estuary. Additionally, surface water samples (n = 26) were also collected in polypropylene bottles (100 ml) from different sampling stations. The sediment and water samples were kept in a freezer (-20°C) prior to the analysis.

2.3.2. Laboratory analyses

2.3.2.1 Quality control and quality assurance

All glassware was rinsed sequentially with dichloromethane (DCM) and methanol, and then baked at 500°C for 8 h to avoid possible contamination. The high-performance liquid chromatography (HPLC) grade solvents (hexane, DCM and methanol) were used during extractions. The instrument was calibrated frequently with calibration standards and quality control procedures were strictly followed to ensure accuracy in extraction and separation procedure. Procedural and reagent blank samples were run to check for quantification and contamination. Procedural blanks indicated no interference with peaks of target compounds and reagent blanks that were run with all of the samples expressed signals < 0.5% of the sample signals. Prior to sample extraction, recovery experiment was performed and samples were spiked with recovery standard 5-α-cholestane (C8003-1G). The average recovery efficiency obtained was 80%. The identification of *n*-alkanes (m/z 57) was done using their mass spectra and quantification was carried out after using an external *n*-alkane standard (SIGMA-40147-U**)**. The hopanes (m/z 191) were quantified by comparing the integrated peak area of the selected ion with the peak area of analytical standard 17β(H),21β(H)-Hopane solution (SIGMA-07562).

2.3.2.2. Grain size analysis

The sediment samples (~ 2 g) for grain-size analysis were pre-treated with H_2O_2 (30%) to remove the organic matter incorporated in sediments. Furthermore, the samples were treated

with 1N HCl to eliminate detrital/authigenic carbonates. The samples after removal of carbonates and organic matter were centrifuged (using double distilled water) and decanted thrice to remove the excess acidic fraction. The grain-size analysis was carried out using laser particle size analyser (Malvern Mastersizer 3000) coupled to a Hydro EV (Extended Volume) wet dispersion unit with a standard operating procedure of 20 sec measurement time, obscuration of 5–20% and dispersion speed of 2500 rpm. The five measurement cycles were recorded for each sample and their mean value was considered. The grain-size distribution was intended for 100 grain-size classes (particle size ranging from 0.02 to 2000 μm) and the analytical error was less than 1%. The De Brouckere mean diameter (D[4,3]) was obtained and results are reported in volume percentage of sand, silt and clay according to textural class of grain size (Folk and Ward, 1957).

2.3.2.3. $\delta^{18}O$ analysis

The individual sample (~500 μL) for $\delta^{18}O$ analysis was equilibrated with CO_2+He for a duration of 18h. The $\delta^{18}O$ values were recorded via gas bench coupled to isotope ratio mass spectrometer (IRMS, Gas Bench II, MAT 253). The calibration of $\delta^{18}O$ values of water samples was done using the IAEA international standards (VSMOW-2, SLAP-2 and GISP-2) with respective values of 0‰, −55.5‰ and −24.8‰. The $\delta^{18}O$ values of internal laboratory standards used for the analysis were IISER-Dep (−9.8‰), IISER-Mid (−4.8‰) and IISER-Enr (−0.7‰). The isotopic data are reported against VSMOW. The monitoring of the instrument was done by running internal standards after every ten water samples and the routine precision of ± 0.06‰ was recorded. The reproducibility of measurements for $\delta^{18}O$ was better than 0.1‰.

2.3.2.4. TOC and $\delta^{13}C_{org}$ analyses

The powdered sediment samples (1-2 g each) were pretreated with 0.5 N HCl to remove the trace amount of authigenic carbonates. This procedure was repeated multiple times until the complete removal of carbonates. The HCl-treated samples were washed with Milli-Q water to remove excess chloride ions using centrifugation technique. The samples were oven-dried at 40°C for 8 hours. The carbonate-free samples were analysed via Continuous Flow Isotope Ratio Mass Spectrometer (CFIRMS, MAT 253) coupled with Con-Flow IV interface. The samples (~ 3–5mg each) were packed into pre-combusted tin capsules and introduced through an auto sampler into the pre-conditioned reactor of Elemental Analyzer (Flash EA 2000 HT) and CO_2 gas produced through the combustion was introduced into CFIRMS for isotopic analysis. The results are reported against VPDB. The calibration of $\delta^{13}C_{org}$ values of sediment

samples is done using the international standards IAEA-CH-3 and IAEA-CH-6 and internal standards (Sulphanilamide) to check the accuracy for CO_2 measurements with an external precision of ±0.1‰ (1σ). The precision and accuracy of $\delta^{13}C$ data is found to be better than 0.08‰. The TOC content is measured from the peak area that is obtained from the sum of the integrated signals m/z 44, 45 and 46 (Jensen, 1991). The measured total nitrogen (TN) content for most of the samples is below the instrument detection limit.

2.3.2.5. Extraction of soluble organic matter

The soluble organic matter from dried surface sediment samples (~10-15 g) was extracted using a solvent extractor (Buchi E-914) with a mixture of dichloromethane: methanol (93:7 ratio, respectively) following the protocols previously discussed elsewhere (Ankit et al., 2017; Misra et al., 2020; Bhattacharya et al., 2021). The instrument was programmed for two cycles at a maximum temperature ~ 100°C and pressure ~100 bars for a total duration of 40 min. The total lipid extract was concentrated using a multivap system (Buchi-multivap-P6) to remove the excess solvents at ~50°C for 5 hours. The saturated hydrocarbon was fractionated from total lipid extract by silica gel column chromatography (100-200 mesh, activated at ~250°C for 7 hours). The dead volume, which is the quantity of solvent required to completely wet the column, was calculated by introducing *n*-hexane into the silica column. The saturated fraction was eluted using *n*-hexane amounting to $3/8^{th}$ of the dead volume. The eluted fraction was concentrated to 0.2 ml using N_2 stream.

2.3.2.6. Gas chromatography mass spectrometry (GC–MS)

The saturated fraction (0.2 ml each) was transferred into GC vial and the fractionated aliquot was analyzed using Agilent 5977C mass spectrometer interfaced to a 7890B gas chromatograph (GC) following the method outlined in Misra et al. (2020). The GC was fitted with a non-polar capillary column (HP-5MS) (30m ×0.25mm i.d. × 0.25μm film thickness) and 1 μl of the sample was injected in splitless mode. The flow rate of the carrier gas (Helium) was maintained at 1ml/min. The initial temperature of GC oven was kept at 40°C that remained constant for 5 min and then ramped to 320°C at 4°C/min. The analysis was performed over the mass range of 40-600 Da in full scan mode and ion source operated at 70 eV. The data were processed using Agilent Mass Hunter Software and total ion chromatogram (TIC) was generated. The compounds were identified using published literature and NIST Library.

2.3.3. Statistical Analysis

2.3.3.1. Principal Component Analysis (PCA)

PCA analysis is an eigenvector based multivariate technique that reduces a large number of correlated variables to a small set of uncorrelated components (PCs) (Jolliffe and Cadima, 2016). The PCA analysis was carried out on geochemical (TOC, $\delta^{13}C_{org}$, *n*-alkane indices) and sedimentological parameters measured in our study to understand major factors controlling the organic matter distribution in the estuarine sediments and also investigating the inter-relationship between different proxies. PCA was performed using PAST 4.03 (Hammer et al., 2001). Correlation of various parameters was performed and results were considered statistically significant at $p < 0.05$. The spatial distribution maps were obtained using the kriging method in the Surfer15 graphics software program.

2.3.4. Land use and Land cover (LULC) classification

The decadal land use and land cover (LULC) changes in the region for the period 2001-2019 was studied using the Moderate Resolution Imaging Spectroradiometer (MODIS) Land Cover Type (MCD12Q1) version 6 data (Ma et al., 2019). The dataset is synthesised using supervised classification of MODIS reflectance data (Friedl et al., 2002, 2010) at a spatial resolution of 500 m under the International Geosphere Biosphere Programme (IGBP) classification scheme. The dataset is constructed for two-time steps of 2001 and 2019 to assess the relative change in the land cover types. The datasets have been downloaded from NASA Earth Data Search services (https://search.earthdata.nasa.gov/search). The raster data for the year 2001 and 2019 were processed for the study area using ArcGIS Desktop software- ArcMap (version-10.8.0.12790).

2.4. Results

2.4.1. Grain size variability and $\delta^{18}O$ values

According to the classification of Folk and Ward (1957), the grain size distribution of surface sediments is mainly characterized by sandy silt in the upper estuary and silty sand to sand in the lower estuary (Table 2.1) (Fig. 2.2). The De Brouckere mean diameter D[4,3] in surface sediments ranges from 42.2 to 291µm (average = 114.1 µm) (Fig. 2.3a). The percentage of silt varies from 0 to 62.4% (average = 30.7%) (Fig. 2.3b); clay from 0 to 12.5% (average = 6.1%) (Fig. 2.3c) and sand ranges from 25.1 to 100% (average = 63.2%) (Fig. 2.3d) (Table 2.1). The upper estuary is characterized by lower D[4,3] values, whereas higher D[4,3] values occur in

the lower estuary (Fig. 2.3a). Similarly, the clay and silt particles are pronounced in the upper estuary and sand particles are predominant in the lower estuarine system (Fig. 2.3b-d).

The $\delta^{18}O$ values of surface water range from -0.7 to 0.3‰ (mean = -0.2‰). The $\delta^{18}O$ results show an increasing trend from the upper to lower estuary (Fig. 2.3e). Water collected from the lower estuary has maximum $\delta^{18}O$ values that are similar to those of the seawater samples.

2.4.2. Total Organic Carbon (TOC) and $\delta^{13}C_{org}$ values

The TOC values range from 0.03 to 4.31%, with maximum value for sample station in upper estuary (MN-13) and lowest for the station (MN-26) in the lower estuary (Fig. 2.3f). The TOC content shows a declining trend from the upper to the lower part of the Mandovi system. The TOC and grain size parameter (D[4,3]) show high negative correlation ($r = -0.8$, $n = 26$, $p < 0.05$) (supplementary material Fig. S2.1a). The $\delta^{13}C_{org}$ values range from -22 to -27‰. The increasing $\delta^{13}C_{org}$ trend is obtained from upstream to downstream in the Mandovi estuary (Fig. 2.3g).

Table 2.1: *n*-alkane indices, bulk organics and sedimentological parameters, *n*-alkane (μg/g) and hopane (ng/g) concentrations of surface sediments from Mandovi estuary.

Sample ID	latitude	longitude	D [4,3]μm	$\delta^{13}C_{org}$(‰)	TOC(%)	Sand (%)	Silt (%)	Clay (%)	$\delta^{18}O$(‰)
MN-1	15.4844	73.8011	291	-24.1	0.04	100.0	0.0	0.0	0.2
MN-2	15.4981	73.8139	131	-25.7	0.33	84.8	12.7	2.5	0.3
MN-3	15.5050	73.8242	59.9	-26.6	2.66	32.9	55.9	11.2	0.2
MN-4	15.5056	73.8392	60.2	-26.0	2.42	38.9	50.9	10.2	0.1
MN-5	15.5097	73.8467	197	-24.9	0.28	89.6	8.6	1.7	-0.3
MN-6	15.5108	73.8572	122	-25.4	0.47	81.6	15.3	3.1	-0.1
MN-7	15.5119	73.8703	104	-26.5	0.97	72.0	23.3	4.7	-0.1
MN-8	15.5286	73.8717	66.6	-26.6	1.4	45.9	45.1	9.0	-0.5
MN-9	15.5456	73.9044	62.7	-26.7	4.01	40.9	49.2	9.8	-0.7
MN-10	15.5450	73.9161	61	-26.6	2.6	39.9	50.1	10.0	-0.4
MN-11	15.5394	73.9219	71.3	-24.7	3.21	37.4	52.2	10.4	-0.5
MN-12	15.5319	73.9294	58	-26.4	2.85	31.2	57.3	11.5	-0.7
MN-13	15.5286	73.9317	42.2	-26.7	4.31	25.1	62.4	12.5	-0.4
MN-14	15.5228	73.9244	57.2	-26.9	3.66	30.4	58.0	11.6	-0.2
MN-15	15.5117	73.9178	92.1	-26.5	1.33	69.0	25.8	5.2	-0.2
MN-16	15.5017	73.8794	81.3	-26.3	2.85	42.4	48.0	9.6	-0.5
MN-17	15.5042	73.8694	69.6	-26.6	2.09	38.3	51.4	10.3	-0.2
MN-18	15.5003	73.8422	110	-26.1	2.33	83.0	14.2	2.8	-0.1
MN-19	15.5031	73.8264	216	-23.9	0.1	92.8	6.0	1.2	-0.1
MN-20	15.4994	73.7886	141	-22.0	0.07	92.7	6.1	1.2	0.1
MN-21	15.4917	73.8028	136	-22.1	0.06	93.8	5.2	1.0	0.1
MN-22	15.5344	73.8950	61.3	-26.6	2.5	42.8	47.7	9.5	-0.7
MN-23	15.5019	73.8989	89	-27.0	0.71	60.9	32.6	6.5	-0.6
MN-24	15.5061	73.8628	132.0	-26.3	0.91	82.5	14.6	2.9	-0.2
MN-25	15.4972	73.7819	185	-21.9	0.05	95.1	4.1	0.8	0.2
MN-26	15.4825	73.8069	269	-21.6	0.03	99.2	0.7	0.1	0.2

Sample ID	TAR	P_{aq}	CPI	ACL	NAR	Pr/Ph	Pr/*n*-C_{17}	Ph/*n*-C_{18}	*n*-alkane conc.	Hopane conc.
MN-1	0.8	0.9	1.1	25.2	0.0	0.0	0.0	0.4	2.3	6.8
MN-2	7.9	0.5	8.6	27.3	0.7	2.5	0.7	0.3	3.5	50.7
MN-3	14.0	0.2	6.1	28.9	0.6	0.9	0.7	1.2	12.6	681.3
MN-4	12.3	0.2	6.7	29.2	0.6	1.2	0.5	0.5	16.0	375.9
MN-5	14.2	0.2	7.4	28.1	0.7	1.9	0.7	0.5	3.6	11.5
MN-6	1.1	0.6	4.4	26.7	0.4	1.1	0.1	0.2	3.7	33.7
MN-7	8.3	0.3	11.0	27.9	0.7	1.5	0.3	0.2	10.2	213.5
MN-8	32.4	0.2	13.3	28.4	0.8	2.3	0.5	0.3	9.2	293.6
MN-9	29.6	0.1	8.0	29.2	0.7	1.0	0.2	0.5	11.4	127.7
MN-10	27.2	0.1	6.7	29.2	0.7	1.3	0.6	0.8	25.4	382.8
MN-11	13.2	0.2	8.2	28.4	0.7	1.8	0.4	0.5	9.9	302.7
MN-12	20.5	0.1	8.0	28.9	0.7	1.7	0.4	0.2	17.3	191.0
MN-13	17.2	0.1	6.4	29.1	0.7	2.8	0.7	0.9	29.3	323.8
MN-14	35.7	0.1	7.8	29.2	0.7	1.2	0.2	0.4	15.8	443.9
MN-15	17.9	0.1	8.6	29.2	0.7	1.2	0.3	0.8	9.3	392.4
MN-16	22.7	0.1	7.3	29.2	0.7	0.8	0.5	0.6	8.1	154.3
MN-17	20.7	0.1	8.2	29.1	0.7	1.4	0.3	0.4	8.2	7.5
MN-18	5.6	0.2	7.1	28.8	0.6	0.0	0.0	1.0	10.1	205.3
MN-19	1.4	0.8	1.5	25.6	0.1	0.8	0.5	0.2	2.5	253.1
MN-20	0.4	0.8	1.7	25.0	0.2	0.5	0.3	0.3	2.3	420.0
MN-21	0.2	0.8	1.6	25.3	0.0	0.6	0.1	0.1	3.0	393.4
MN-22	35.1	0.3	5.5	28.2	0.6	1.0	0.6	0.8	6.8	12.3
MN-23	10.5	0.2	7.1	29.1	0.6	1.0	0.5	0.3	2.6	2.2
MN-24	15.1	0.2	5.1	28.6	0.6	1.2	0.5	0.7	11.0	4.1
MN-25	0.4	0.8	1.0	25.2	0.1	0.1	0.2	0.3	3.2	103.9
MN-26	0.1	0.9	1.1	25.0	0.0	0.0	0.0	0.4	2.9	4.6

Note: TAR= $(C_{27}+C_{29}+C_{31})$ /$(C_{15}+C_{17}+C_{19})$ (Bourbonniere and Meyers, 1996), Paq. = $(C_{23}+C_{25})$ / $(C_{23}+C_{25}+C_{29}+C_{31})$ (Ficken et al., 2000), CPI = $[(C_{25}+C_{27}+C_{29}+C_{31}+C_{33})$ / $(C_{24}+C_{26}+C_{28}+C_{30}+C_{32})$ + $(C_{25}+C_{27}+C_{29}+C_{31}+C_{33})/(C_{26}+C_{28}+C_{30}+C_{32}+C_{34})]$ / 2 (Bray and Evans, 1961), ACL = $(23 \times C_{23}+25\times C_{25}+27\times C_{27}+29\times C_{29}+31\times C_{31})$ / $(C_{23}+C_{25}+C_{27}+C_{29}+C_{31})$ (Poynter et al., 1989), NAR = [Σ *n*-alk(C_{19-32})-2Σ even *n*-alk(C_{20-32})] / Σ *n*-alk(C_{19-32}) (Mille et al., 2007)

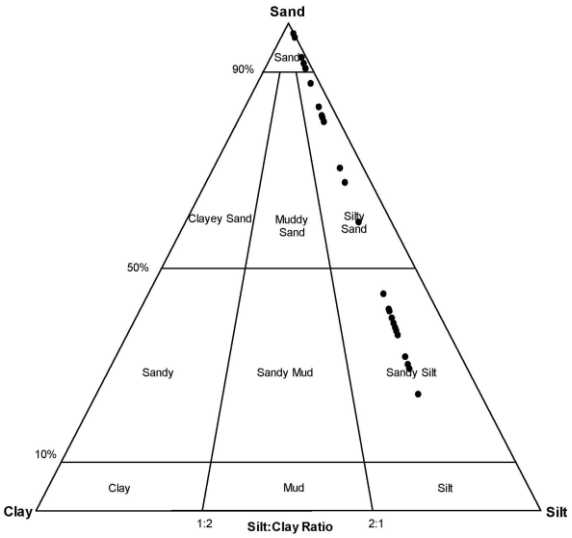

Figure 2.2: Ternary diagram showing classification of sand, silt and clay percentage proposed by Folk and Ward, 1957.

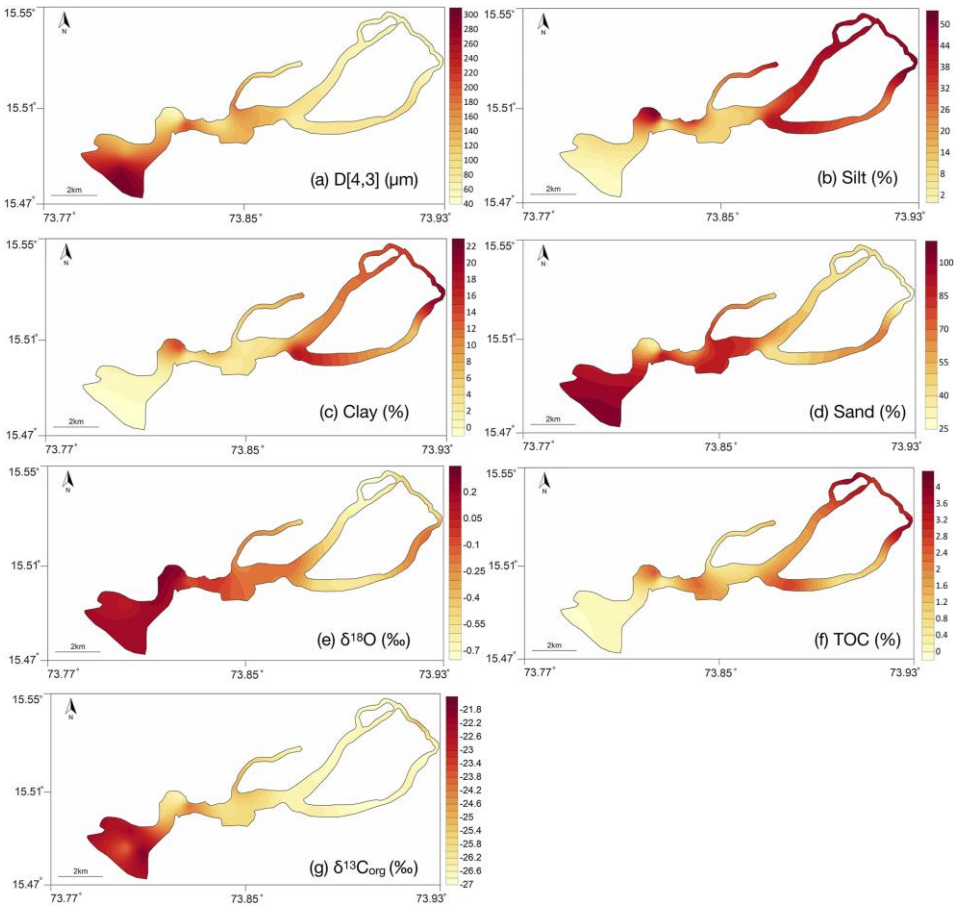

Figure 2.3: Spatial distribution of sedimentological and bulk organic parameters (a) D[4,3], (b) Silt (%), (c) clay (%), (d) sand (%), (e) $\delta^{18}O$ (‰), (f) TOC (%) and (g) $\delta^{13}C_{org}$ (‰).

2.4.3. Distribution of *n*-alkanes and hopane

The representative total ion chromatogram (TIC) of saturated hydrocarbon fraction of upper and lower estuary sediment samples are shown in Fig. 2.4 (a-b). The *n*-alkanes in the carbon number ranging from *n*-C_{11} to *n*-C_{35} are detected based on the mass fragment of m/z = 57. The total concentrations of *n*-C_{11}–*n*-C_{35} in the Mandovi estuary surface sediments varied from 2.3 to 29.3 μg/g (mean = 9.2 μg/g) (Table 2.1). The *n*-alkane concentrations were higher in the upper estuarine region and show positive correlation with silt ($r = 0.7$, $p < 0.05$) (supplementary material Fig. S2.2a) and clay ($r = 0.7$, $p < 0.05$) (supplementary material Fig. S2.2b). Furthermore, TIC reveals predominance of odd over even *n*-alkanes in riverine stations (Fig. 2.4a) and the presence of unresolved complex mixture (UCM) in the lower estuary stations (Fig. 2.4b). Acyclic isoprenoids (Pr and Ph) were identified by the selected ion chromatogram at m/z 57, followed by the major fragments at m/z 183 and m/z 197 (supplementary material Fig. S2.3).

The concentrations of hopanes (m/z 191) in the Mandovi surface sediments ranged from 2.2 to 681.3 ng/g-dry weight (Table 2.1). The hopane profiles in the estuarine sediments are characterized by the predominance of Ts: 18α(H), 22,29,30-trisnorneohopane; Tm: 17α(H), 22,29,30, trisnorhopane; 17α(H), 21β(H) C_{29} hopane; 17α(H), 21β(H) C_{30} hopane and C_{31}-C_{33} homohopanes (22S and 22R) (Fig. 2.4c).

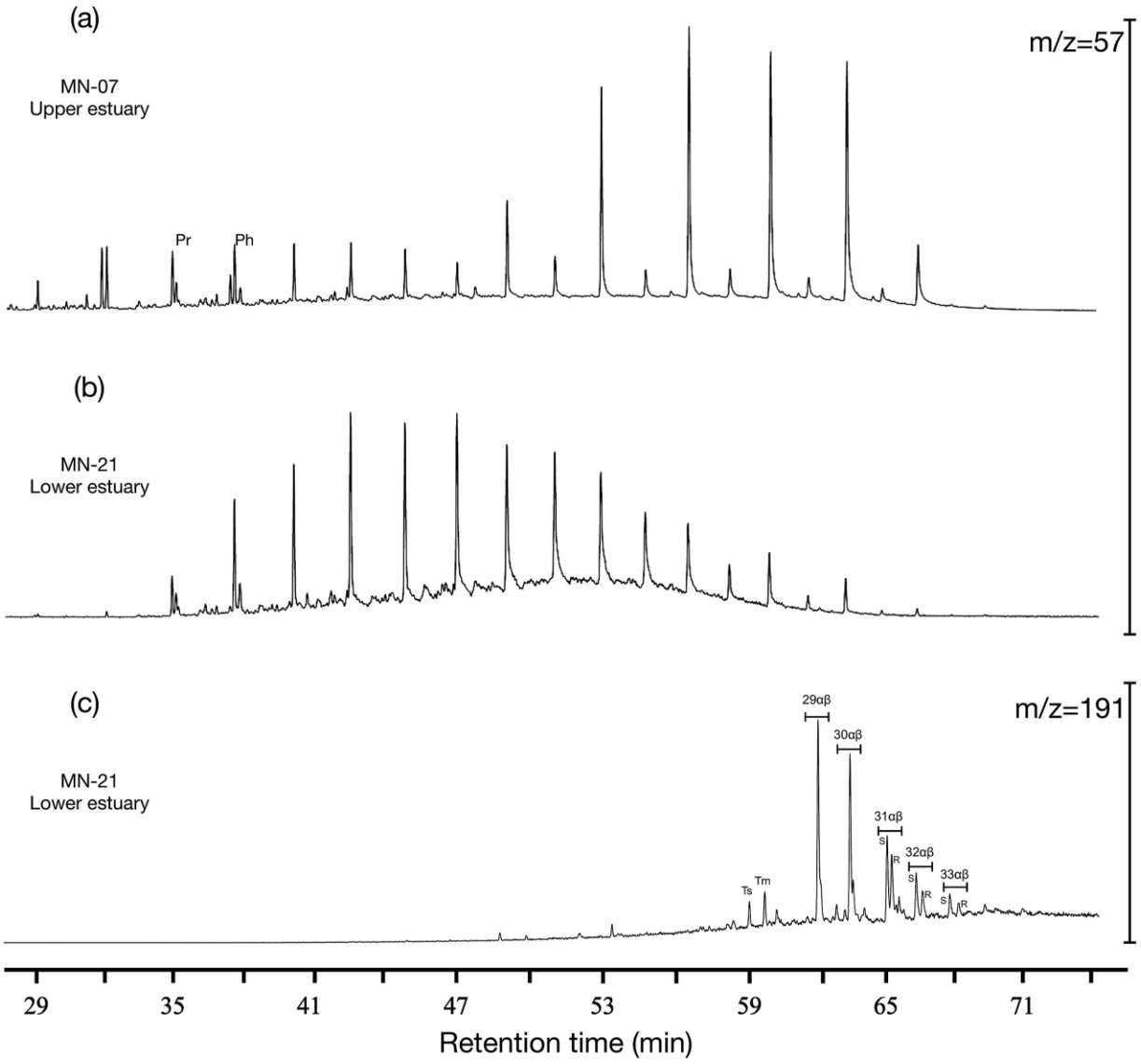

Figure 2.4: a-b) The representative total ion chromatogram showing the saturated hydrocarbon fraction of surface sediment from upper and lower Mandovi estuary. Please refer Figure 2.1b for location of sampling site, c) Mass fragmentogram of m/z = 191 (hopanes) of saturated hydrocarbon fraction from the surface sediment of lower estuary. Numerals refer to carbon numbers of hopane series; α, β = 17α(H), 21β(H)-hopanes; R and S = C-22 R and Sconfiguration; Ts=18α(H)-22,29,30-trisnorneohopane; Tm=17α(H)-22,29,30-trisnorhopane.

2.4.4. *n*-alkane and isoprenoid indices

The TAR index for the Mandovi surficial sediments varies from 0.1 to 35.7, indicating higher TAR values towards the proximity of the riverine system (Table 2.1) (Fig. 2.5a). The P_{aq} values of estuarine sediments range from 0.1 to 0.9 with elevated values observed towards a tidally

advected zone (Fig. 2.5b). The TAR and P_{aq} values show inverse correlation ($r = -0.8$; $n = 26$, $p < 0.05$) (supplementary material Fig. S2.1b).

The CPI values from the surface sediments range from 1.0 to 13.3 (Fig. 2.5c), whereas ACL values vary from 25.0 to 29.2 (Fig. 2.5d). The highest value of CPI is observed in the upper region towards riverside (MN-8), and minimum value is recorded in the lower estuary (MN-25). The CPI values show a decreasing trend from upper to lower estuary. The ACL values mirror the decreasing trend of CPI from upper to lower estuary. The highest value (29.2) for the ACL index is observed for river-borne sediments and the lowest value (25) for downstream sediments. The CPI and ACL are positive correlated ($r = 0.8$; $n = 26$ $p < 0.05$) (supplementary material Fig. S2.1c).

The NAR index shows a declining trend from upstream to the downstream region of the estuarine system with values ranging from 0 to 0.8 (Fig. 2.5e). The maximum NAR value is observed for stations in the upper reaches of the estuary, whereas the lowest value occur in the lower reaches of the estuary. The pristane/phytane (Pr/Ph) ratio for Mandovi estuary indicates a decreasing trend from the upper to the lower estuary. The Pr/Ph index ranges from 0 to 2.8 (Fig. 2.5f). The lowest value is recorded at seaside stations (Pr/Ph = 0), and the maximum value is observed for sampling stations in the upper estuary (Pr/Ph = 2.8). The isoprenoid ratios calculated from surface sediments show values of Pr/*n*-C_{17} (0-0.7) and Ph/*n*-C_{18} (0.1-1.2) (supplementary material Fig. S2.4a and b).

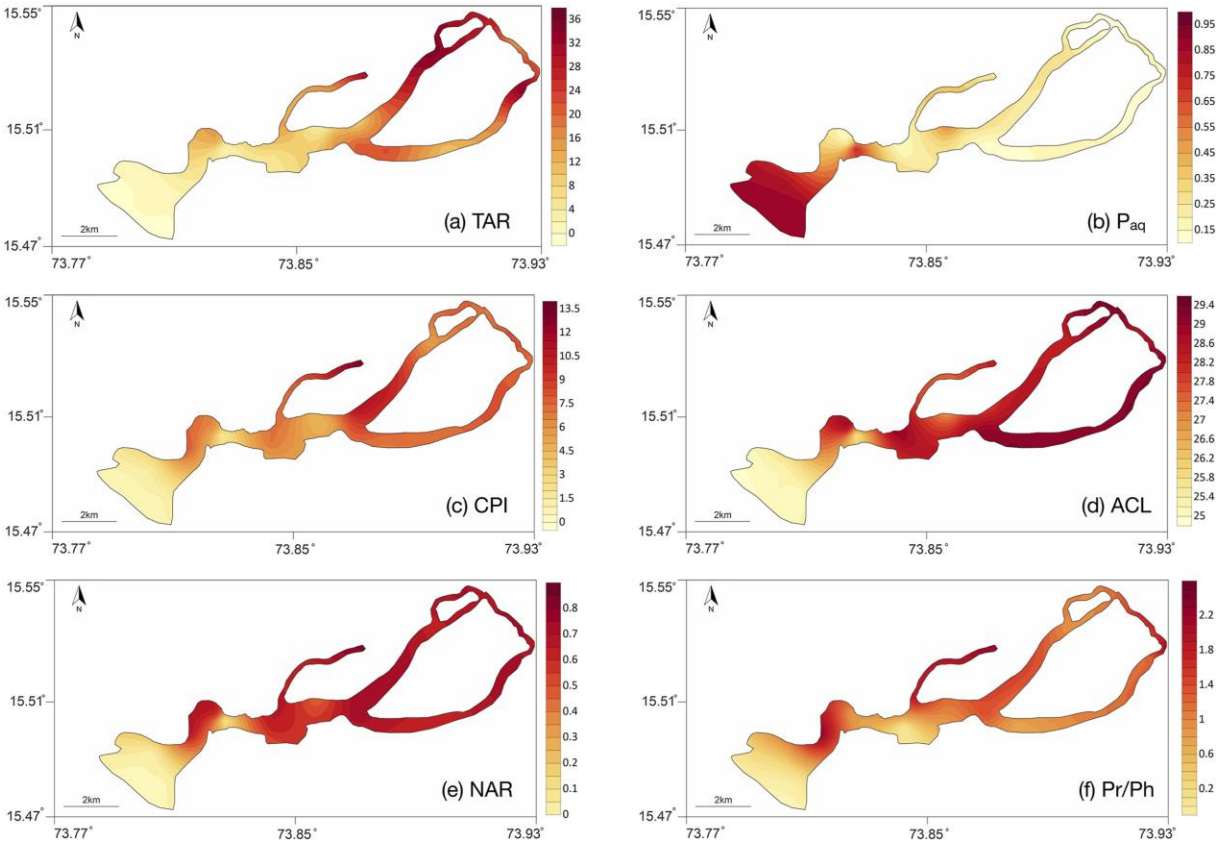

Figure 2.5. Spatial distribution of aliphatic hydrocarbon indices (a) TAR, (b) Paq, (c) CPI, (d) ACL, (e) NAR and (f) Pr/Ph ratio.

Note: TAR= $(C_{27}+C_{29}+C_{31})$ /$(C_{15}+C_{17}+C_{19})$ (Bourbonniere and Meyers, 1996), Paq. = $(C_{23}+C_{25})$ / $(C_{23}+C_{25}+C_{29}+C_{31})$ (Ficken et al., 2000), CPI = [$(C_{25}+C_{27}+C_{29}+C_{31}+C_{33})$ / $(C_{24}+C_{26}+C_{28}+C_{30}+C_{32})$ + $(C_{25}+C_{27}+C_{29}+C_{31}+C_{33})$/$(C_{26}+C_{28}+C_{30}+C_{32}+C_{34})$] / 2 (Bray and Evans, 1961), ACL = $(23 \times C_{23}+25\times C_{25}+27\times C_{27}+29\times C_{29}+31\times C_{31})$ / $(C_{23}+C_{25}+C_{27}+C_{29}+C_{31})$ (Poynter et al., 1989), NAR = [Σ *n*-alk(C_{19-32})-2Σ even *n*-alk(C_{20-32})] / Σ *n*-alk(C_{19-32}) (Mille et al., 2007)

2.4.5. Principal component analysis

PCA was performed on the datasets containing TOC (%), $\delta^{13}C_{org}$ (‰), D[4,3], sand (%), silt (%), clay (%), TAR, CPI, ACL, NAR, Pr/Ph and P_{aq}. The analysis performed on various parameters in the study revealed two principal components (PC1 and PC2) that explain the cumulative variance of 86.9 % in the dataset (Fig. 2.6). The PC1 component accounts for 77.2% of the total variance and demonstrates high positive loadings for TOC (%), silt (%), clay (%), TAR, CPI, ACL, NAR, Pr/Ph, whereas high negative loadings are observed for $\delta^{13}C_{org}$ (‰), D[4,3], sand (%) and P_{aq}. The PC2 only accounted for 9.7% of the total variance and is characterised by moderate positive loadings for CPI and Pr/Ph.

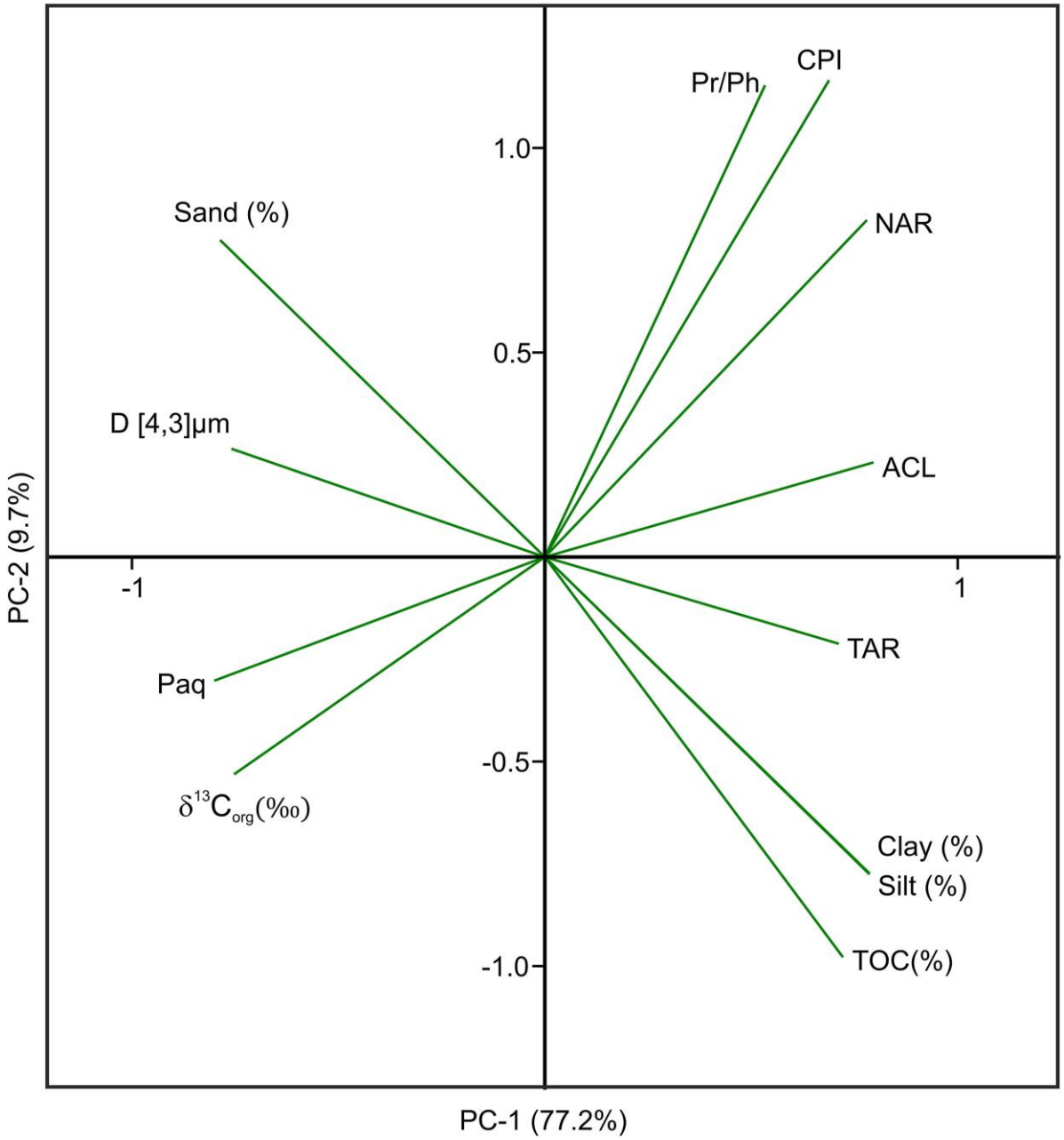

Figure 2.6: Plots of variable loadings from PCA of geochemical and sedimentological variables from Mandovi estuary.

2.5. Discussion

2.5.1. Modern circulations and sediment distribution processes

The Mandovi estuary as a tropical monsoonal estuary, is characterised by high river discharge during periods of active monsoon (June to September) which substantially modulates the salinity conditions in the system (Vijith et al., 2009). The water samples were collected during

the onset of monsoon withdrawal (early October) when the freshwater inflow was high; the estuary retained the salt wedge characteristics, and salinity levels started migrating upstream (Qasim and Gupta, 1981; Vijith et al., 2009). Generally, lower isotopic values mark the high influx of freshwater and higher values reflect saline water circulation (Deshpande et al., 2013; Ghosh et al., 2013). The low $\delta^{18}O$ values in the upper estuary can be attributed to high freshwater inflow into the system. The overall impact of runoff is higher at the head as compared to the mouth due to convergent nature of the Mandovi estuary (Shetye and Vijith, 2013). The maximum $\delta^{18}O$ values in the lower reaches can be explained by high evaporation in the Arabian Sea that increases the salinity field in coastal waters. The high intrusion rates of saline water extend farther into the estuary due to tidal currents (that also corresponds to differential mixing of freshwater and seawater in the middle of the estuarine system) (Shetye et al., 2007). A mass-balance model has been further utilized to examine the mixing trajectory as $\delta^{18}O$ and the contribution of seawater and river water is calculated using a single isotope two source linear mixing model equation,

$$\delta^{18}O_{sample} = x^* \delta^{18}O_{river} + (1-x)^* \delta^{18}O_{sea}$$

The $\delta^{18}O$ of two end-members controlling the circulation dynamics are $\delta^{18}O_{river}$ (-0.7 ‰) and $\delta^{18}O_{sea}$ (0.3‰). The results show most of the stations in the lower estuary receive contribution from seawater (70-100%), whereas nearly all the stations proximal to fluvial settings have high freshwater input (70-100%). The middle estuary is characterised by the mixing of river water and open-ocean seawater (Fig. 2.3e).

The grain size distributions have been widely used for understanding the hydrodynamic characteristics as well as the sediment transport and deposition processes (Allen, 1971; Visher, 1969; Mishra et al., 2019). The sediments deposited in the estuary are controlled by riverine inputs, which depends on various geomorphological factors that include flow velocity and channel length, and marine sediments transported by tidal currents (Sündermann and Feng, 2004; Dessai et al., 2009). The grain size data of Mandovi estuary reveal distinct sedimentary dynamics i.e., accumulation of coarser particles (sand) in tidal advected region, fine particles in the river-influenced region (clay and silt) and fine to coarse particles (silt-sand) in the mid-section of the estuary. A similar distribution has also been exhibited by other estuaries such as the Tamaki Estuary (Abrahim et al., 2007) and Ashtamudi Estuary (Mishra et al., 2019). The depositional pattern reflects high energy, less violent and calm hydrodynamic conditions in lower, middle, and upper estuary, respectively. The high energy conditions can also be

supported by wave spectra generated due to strong monsoon winds over the open sea (Shetye et al., 2007). Furthermore, due to the high affinity of aliphatic hydrocarbon concentrations with fine sediment fractions (Kennicutt II et al., 1987a), upstream stations with silt-clay textures show higher hydrocarbon concentrations while downstream stations express lower values.

2.5.2. Characterization and source apportionment of organic matter

The organic carbon isotope composition ($\delta^{13}C_{org}$) is often used for source characterization of organic matter in estuaries (Schubert and Calvert, 2001). The organic matter distribution in the tropical estuarine ecosystem is controlled by two major sources (terrestrial and marine) and four principal pathways that include two distinct terrestrial sources viz. the C3 pathway (-23 to -30‰; Smith and Epstein, 1971) and C4 pathway (−9 to −16‰; Pancost and Boot, 2004); marine source pathways viz. macrophytes and marine plankton (-19 to -22‰ ; Fry and Sherr, 1989), and seagrasses (-3 to -23‰; Hemminga and Mateo, 1996). The range of $\delta^{13}C_{org}$ values observed in our study region (-22 to -27‰) is in good agreement with previous data reported from the region (–21.6 to –27.2‰; Shynu et al., 2015, -23.1 to -28.2‰; Pradhan et. al, 2014) as well as other estuarine systems (e.g., Pearl estuary (Yu et al., 2010), Zhangjiang estuary (Li et al., 2018)). The $\delta^{13}C_{org}$ values from the Mandovi estuary indicate organic matter contribution from terrestrial C3 plants in the upper and middle estuarine ecosystem. The accumulation of terrigenous organic carbon can possibly be explained by riverine transport of catchment vegetation (e.g., mangroves) and terrestrial soils along with leaf litter derived from the Western Ghats (Sundarapandian and Swamy, 1999). The decrease of $\delta^{13}C_{org}$ values in the lower estuary show that organic matter is sourced from marine input and is further supported by the dominance of seagrasses and marine phytoplankton in the coastal waters (Jagtap, 1991). Additionally, the positive correlation of organic carbon with clay (r = 0.9) and silt (r = 0.9) and negative correlation with sand (r = -0.9) indicates that grain size distribution plays a major role in influencing the distribution of OM in the study area.

Furthermore, several *n*-alkane indices have been utilized for the identification and quantification of OM sources (Yamada and Ishiwatari, 1999; Ankit et al., 2017). The estimation of terrestrial and aquatic OM sources is carried out using *n*-alkane indices such as TAR and P_{aq}. P_{aq} <0.1 indicates the dominance of terrestrial plants, 0.1-0.4 corresponds to emergent macrophytes and 0.4-1 indicates submerged/floating plants (Ficken et al., 2000). The inverse correlation of TAR and P_{aq} and elevated TAR values in the upper estuary indicate higher terrestrial input from the watershed sources in the form of land derived plant waxes that can

also be explained by enhanced terrestrial contribution from various river tributaries of Mandovi (Khandepar, Sinquerim, Assonora and Valvanti). The higher values of P_{aq} in the lower estuary suggest that aquatic organic matter predominates over terrigenous organic matter. This interpretation was further corroborated by $\delta^{13}C_{org}$ data indicating high contribution of OM from marine source in lower estuary and dominance of terrigenous OM in the upper estuary.

2.5.3. Assessment of natural versus anthropogenic organic matter sources

A number of *n*-alkane indices such as CPI, ACL, Pr/Ph ratio, NAR, Pr/*n*-C_{17}, Ph/*n*-C_{18} along with presence/lack of UCM can help to evaluate the natural and anthropogenic sources of OM input in the Mandovi estuary (Ten Haven et al., 1987; Jeng, 2006; Mille et al., 2007). CPI value close to unity suggests possible presence of petroleum-derived *n*-alkanes and recycled OM (Kennicutt II et al., 1987b; Le Dréau et al., 1997; Mille et al., 2007) and higher CPI values (4-10) suggest terrestrial contribution (Wang et al., 2003). The CPI data obtained from the lower estuary indicate hydrocarbons in marine sediments are probably derived from petrogenic sources. In contrast, *n*-alkanes in middle and upper estuary are mainly derived from terrigenous sources that can also be explained by the predominance of odd over even *n*-alkanes (C_{24}-C_{32}) (Fig. 2.4a) thereby indicating the input of waxes derived from higher land plants (Eglinton and Hamilton, 1967; Wang et al., 2003). The ACL value decreases if petrogenic hydrocarbons are introduced into sediments and the *n*-alkane trend is C_{25}>C_{27}>C_{29}>C_{31}alkanes (Jeng et al., 2003; Jeng, 2006). The ACL data derived from stations proximal to sea have relatively lower values of ACL (25-25.3) and C_{25}>C_{27}>C_{29}>C_{31} trend, reflecting high contamination from petroleum-derived hydrocarbons (Fig. 2.5d). ACL and CPI show a positive correlation (r = 0.8) (supplementary material Fig. S2.1c) and highlight the fact that petrogenic hydrocarbons are higher in the lower estuary and terrigenous hydrocarbons in upper and middle estuary. A similar observation of seaward decrease of ACL and CPI values indicating intense petrogenic hydrocarbon contamination was also reported from the Tyne estuary (Ahad et al., 2011), Ashtamudi estuary (Ankit et al., 2017), and estuaries of Malaysia (Keshavarzifard et al., 2020).

The NAR proxy is widely used to delineate the natural and anthropogenic sources in aquatic systems (Mille et al., 2007). The NAR ratio equivalent to 0 indicates petroleum hydrocarbons contamination, whereas a ratio close to one suggests organic input from land and marine plants (Mille et al., 2007; Ines et al., 2013; Zrafi et al., 2013). The NAR ratio for all the stations range between 0.1-0.8 except for the seaward locations, which has a ratio equal to 0 highlighting the intensified levels of petrogenic *n*-alkanes in the lower estuary and natural *n*-alkanes in the

middle and upper estuary. Likewise, isoprenoid ratios (Pr/Ph, Pr/*n*-C_{17}, Ph/ *n*-C_{18}) are also useful indicators for identifying petroleum contamination (Hwang et al., 2002; Zaghden et al., 2005; Mille et al., 2007). The pristane and phytane are produced from catalytic hydrogenation of phytadienes or from oxidation (Pr) /reduction (Ph) of the phytol chain of chlorophyll in immature sediments (Peters and Moldowan, 1993). Pristane is primarily found in biota (zooplankton, marine animals) (Volkman et al., 1992) and phytane tends to be a major component of crude oil (Steinhauer and Boehm, 1992). The Pr/Ph ratio close to or <1 indicates contamination from petroleum hydrocarbons and crude oils (Blumer et al., 1963; Gao and Chen, 2008), and the ratio above 1 reflects uncontaminated sediments (Steinhauer and Boehm, 1992). The low Pr/Ph ratio (0-0.8) in the lower estuarine samples suggests that this section is more prone to petroleum contamination. Furthermore, the other diagnostic ratios (Pr/*n*-C_{17}, Ph/ *n*-C_{18}) are also used for identification of oil contaminants and differentiation of fresh and degraded petroleum hydrocarbons (Hwang et al., 2002). The ratios with values >1 imply high degradation of isoprenoid hydrocarbons (Hwang et al., 2002; Zhang et al., 2021). The values obtained for most of the stations from the Mandovi estuary are close to 1 and suggest petroleum contamination in the estuary is relatively fresh. Another evaluation tool to distinguish the source of hydrocarbon is by investigating the presence of UCM and petroleum biomarkers. UCM mainly comprises the homologues of branched and cyclic hydrocarbons and indicates the contamination from petroleum sources (Volkman et al., 1992; Gogou et al., 2000). UCM is known to be highly resistant to degradation, and thereby tends to remain longer in the environment than *n*-alkanes (Bouloubassi and Saliot, 1993; Jeng, 2006). The presence of unimodal distribution and a distinct hump in lower stations (Fig. 2.4b) reflects the signatures of petroleum-derived hydrocarbons from anthropogenic sources indicating contamination from oil residues (Brassell and Eglinton, 1980).

Likewise, hopanes are used as molecular markers of petroleum contamination owing to their high resistance to degradation in environments (e.g., Wang et al., 1994; Zakaria et al., 2002). These biological markers mainly exhibit distributions of structural and stereochemical isomers in oils (Peters and Moldowan, 1993). Hopanes are slightly modified during diagenesis and catagenesis with an unstable 17β, 21β to a more stable 17α, 21β configuration and biological configuration of hopanes (22R) gets converted to a mixture of diastereoisomers (22R and 22S). Diagenetic configurations reflect thermal maturity of OM and petroleum by-products (Rogge et al., 1993, Beiger et al., 1996). Low concentrations of hopanes were observed in the upper section of the estuary and concentrations increased significantly downstream indicating high

anthropogenic activities. Hopanes upstream are possibly derived from terrigenous component (urban and domestic sewage input, tourism activities), whereas the sources for downstream stations are leakages from crude oil transfer, tankers etc. (Raghavan and Furtado, 2000; Veerasingam et al., 2015b). The *n*-alkane and hopane concentrations in sand dominated estuarine regions are low as sand particles tend to have less specific surface area along with low residual capacity for hydrocarbons (Kennicutt II et al., 1987a; Fine et al., 1997; Veerasingam et al., 2015b). The combined multiproxy results strongly suggest that the OM contribution to lower estuary sediments is via anthropogenic sources i.e., petroleum and crude oil, whereas the middle and upper sections in the estuary are mostly influenced by natural sources.

2.5.4. Association of various ecological indicators using multivariate analyses

Chemometric method (e.g., principal component analysis) has widespread environmental implications and this statistical technique is normally applied to multidimensional dataset having complex inter-relationships among variables. The spatial distribution of organic matter in estuarine systems are mostly controlled by changes in natural and anthropogenic OM sources (Medeiros and Bícego, 2004), and the depositional conditions are largely governed by river-tidal processes (Sundar and Shetye, 2005). The scatter plot has been used in the present study to investigate the association between multidimensional variables (Fig. 2.6). PC1 demonstrates positive loadings comprising mainly TOC (%), silt (%), clay (%), CPI, NAR, TAR, ACL and Pr/Ph. The predominant contribution to the variance in PC1 was due to the influence of CPI, NAR, ACL and Pr/Ph related to anthropogenic sources. Positive association is also found between the TOC content and silt and clay content suggesting that grain size parameters play a crucial factor in controlling organic matter distribution in the Mandovi estuary. Interestingly, the TAR with positive loading denotes terrestrial contribution to the estuarine system. Conversely, PC1 in the negative direction shows P_{aq} and $\delta^{13}C_{org}$ belong to aquatic source indicators. The PCA analysis provides potential associations among the various ecological parameters and their utility as key indicators for estimation of OM sources in an estuarine environment. Moreover, the integrated use of various bulk parameters (grain size, $\delta^{13}C_{org}$ and TOC), and molecular (*n*-alkanes) techniques provide an accurate estimation of OM sources and avoid potential biases.

2.5.5. Effects of climate and land use/land cover change on OM distribution

The combined effect of increasing human disturbance and climate change exert controls on the abundance and distribution of OM in sediments (Zhang et al., 2013; Zhang et al., 2020). The use of inorganic fertilizers and human population growth in the watershed results in anthropogenically induced increase in primary productivity (cultural eutrophication) in coastal environments (Zimmerman and Canuel, 2000). Likewise, the anthropogenic modification of the catchment also accelerate the transportation of terrestrial material to the estuarine system (Zhang et al., 2013). The *n*-alkane concentration in the Mandovi estuary ranged from 2.3 to 29.3 μg/g with an average of 9.2 μg/g. The concentration of *n*-alkanes from Mandovi estuary are comparable to those obtained from other estuaries including Ashtamudi Estuary (0.42 to 6.6 μg/g) (Ankit et al., 2017), Cochin Estuary (6.03 to 43.23 μg/g) (Gireeshkumar et al., 2015), Pearl River estuary (3.43 to 8.46 μg/g) (Gao et al., 2007), and Changjiang estuary (2.20 to 11.82 μg/g) (Bouloubassi et al., 2001). Interestingly, present study shows a fivefold increase in *n*-alkane concentration in the Mandovi estuarine system compared to previously reported *n*-alkane concentration (0.8-3.2 μg/g) (Harji et al., 2008). The LULC changes have been evaluated to understand the possible role of anthropogenic activities in increasing the levels of organic matter input in the Mandovi estuary.

The spatial trends and total area of LULC changes in the vicinity of Mandovi estuary for the 2001-2019 period have been used to understand the anthropogenic impact in the region (Fig. 2.7). The results show significant changes in the LULC category 'Built-up land', representing land covered by buildings and other man-made structures over the years. The LULC showed an increase in built-up area by 650 ha over the past 20 years at an average rate of 34 ha/year. The LULC changes obtained from the study site over a period of 20 years (2001-19) signifies an increase in anthropogenically induced perturbations (urbanisation, extensive tourism and marine operations) resulting in the discharge of organic pollutants, municipal-industrial wastewater effluents and oil spills. Additionally, the increase in precipitation and high discharge rates in the region may further facilitate the transportation of terrestrially-derived pollutants into the estuary, thereby degrading the ecosystem. The results from the present study are expected to help policymakers and environmentalists in developing a strategic framework for urban management and planning, and formulating a workable mechanism to prevent further environmental degradation in a delta-estuary system.

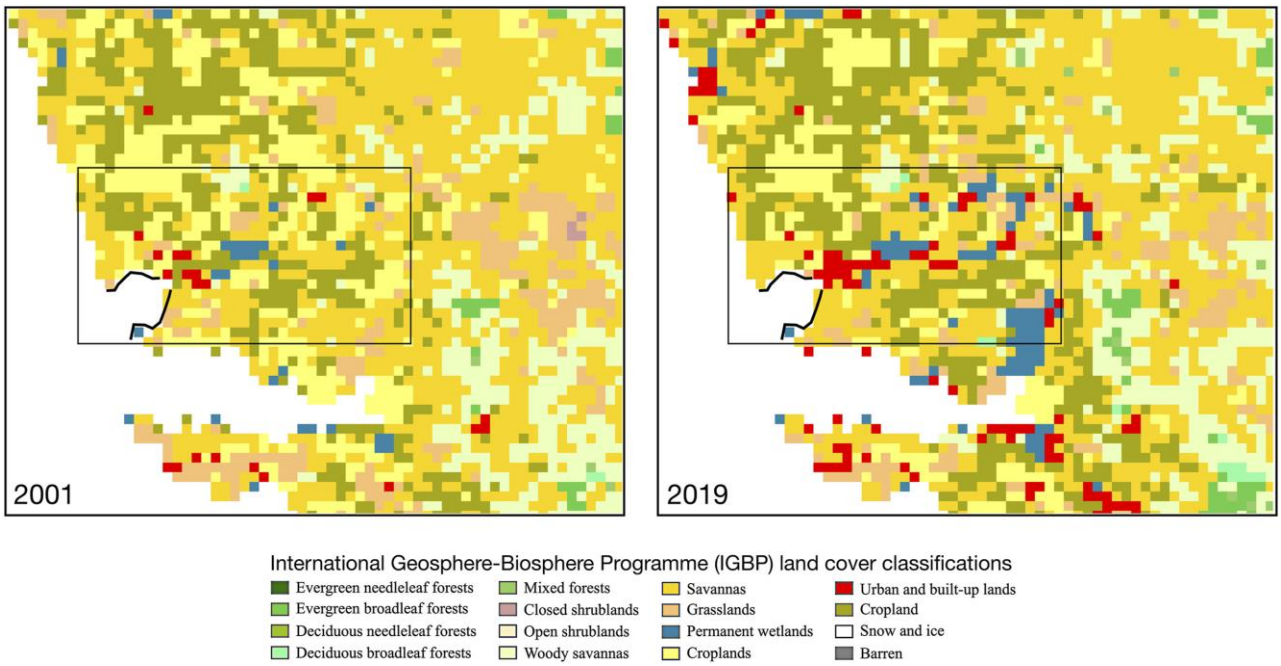

Figure 2.7: Featured Land-Use/Land-Cover (LULC) Change in the Mandovi estuary catchment, Goa for period 2001-2019.

2.6. Conclusions

Here we present the results of a multiproxy study to characterise the organic matter sources, understand its distribution and composition in surface sediments from the tropical Mandovi estuary in western India. The bulk parameters (TOC and $\delta^{13}C_{org}$), lipid (*n*-alkane) distribution and indices were evaluated to understand the productivity changes in the ecosystem and anthropogenic OM contribution in the basin. The $\delta^{13}C_{org}$, P_{aq} and TAR reflects the relative contributions from terrigenous and marine sources. The presence of UCM, hopanes, ACL, NAR, CPI and Pr/Ph indicate the presence of petroleum hydrocarbons derived from anthropogenic activities in the lower estuary. The correlation of TOC and grain size parameters indicates the role of grain size in controlling the organic matter distribution in the Mandovi estuary. Furthermore, the $\delta^{18}O$ values demonstrate the circulation dynamics of riverine freshwater and oceanic saline water in the upper, middle and lower reaches. The multiple ecological indicators established in this study are useful in understanding the historical variations of organic matter inputs as well as their sources, and in reconstructing their paleoenvironmental and paleoecological conditions.

Chapter 3

Occurrence, distribution and sources of phthalates and petroleum hydrocarbons in tropical estuarine sediments (Mandovi and Ashtamudi) of western Peninsular India*

*The contents of this chapter are published in the international peer reviewed journal 'Environmental Research' as Bulbul et al., 2022.

Bulbul, M., Bhattacharya, S., Ankit, Y., Yadav, P. and Anoop, A., 2022. Occurrence, distribution and sources of phthalates and petroleum hydrocarbons in tropical estuarine sediments (Mandovi and Ashtamudi) of western Peninsular India. Environmental Research 214, 113679.

Mehta Bulbul[1], Sharmila Bhattacharya[1], Yadav Ankit[1], Pushpit Yadav[1], Ambili Anoop[1]
[1]Indian Institute of Science Education and Research, Mohali 140306, India

3.1. Introduction

Estuaries are centers for intense urban development and expansion (Ridgway and Shimmield, 2002) in addition to being one of the most densely populated regions worldwide (Van Leussen and Dronkers, 1988). Approximately 50% (3.5 billion people) of the world's population inhabit within 200 kilometers of coastline (Kummu et al., 2016). The progressive increase of anthropogenic perturbations such as waste disposal, sewage discharges, industrialization, tourism, shipping, marine transportation, commercial fishing, petroleum spills and incomplete combustion of fossil fuels deteriorate aquatic environment and alter the structure of biotic communities (Kennish, 2002; Nogales et al., 2011). Among the different pollutants, the accumulation of organic contaminants is a matter of growing concern, as these hydrophobic chemical markers are major threats to the estuarine environment (Miller et al., 2021). The occurrence of organic pollutants, notably phthalates and fossil fuel hydrocarbons, remains a serious issue especially in highly sensitive and vulnerable ecosystems (Rhind, 2009; Paluselli et al., 2018). Hence, these organic pollutants are required to be carefully monitored to develop appropriate mitigation strategies.

Phthalates are widely used plastic additives or plasticizers that are known to improve the flexibility of the plastic products (Gao et al., 2019). These ubiquitous synthetic compounds are also tremendously used in lubricants, cosmetics, industries, personal care products and pharmaceuticals (Staples et al., 1997). Owing to their extensive usage (6 to 8 million tons yr^{-1}) (Net et al., 2015a; Kaewlaoyoong et al., 2018) and physicochemical properties, these compounds have been profoundly detected in different environmental matrices such as sediments (Zeng et al., 2009a), surface water (Clara et al., 2010), soil (Niu et al., 2014), air (Yang et al., 2020) and biota (Kim et al., 2011; Liu et al., 2012). Since these emerging contaminants (PAEs) are not chemically bound to plastic polymers, therefore they leach, or migrate and enter into aquatic ecosystems through various pathways (industrial and domestic wastes, sewage sludge, surface runoff etc.) (Kastner et al., 2012; Liu et al., 2013; Net et al., 2014). These organic contaminants also cause serious health effects in humans such as fertility, organ damage, postnatal development alterations and birth defects (Lottrup et al., 2006; Guerrero-Bosagna and Skinner, 2014). At the experimental level, some phthalates such as DIBP has been observed as a male reproductive toxicant (Yost et al., 2019), while DEHP, a phthalate compound used in PVC medical devices, migrates to surrounding media such as blood, plasma and result in reproductive and developmental toxicity (Ito et al., 2005).

Therefore, PAEs are considered as environmental hormones, whose accumulation in environment result in ecotoxicological effects.

Similar to PAEs, hydrocarbon pollution also poses a major threat to estuarine ecosystem (Gilde and Pinckney, 2012). These components are readily adsorbed on the particulate matter and are anthropogenically derived from multiple sources such as domestic, petrogenic, industrial discharges and pyrogenic (Volkman et al., 1992; Medeiros and Bícego, 2004). Petrogenic sources including lubricating oil, diesel fuel, asphalt and kerosene contribute significant hydrocarbon inputs consisting of complex assemblage of chemicals that get accumulated in bottom sediments (Zaghden et al., 2005). The *n*-alkane distribution and its related indices such as carbon preference index (CPI) and unresolved complex mixtures (UCM) are used to ascertain oil contamination (Venturini et al., 2008). The CPI records the relative proportion of odd and even carbon-numbered *n*-alkanes and helps to differentiate between biogenic and petrogenic sources of petroleum (Bray and Evans, 1961; Vaezzadeh et al., 2015). Another quintessential signature of petrochemical input especially into surface sediments is the UCM (Silva et al., 2013; Adeniji et al., 2017). It occurs as a huge hump in total ion chromatograms (TIC) of analyzed soluble fraction of organic matter (OM) in sediments comprising a complex mixture of branched and cyclic compounds that remains unresolved by capillary columns in gas chromatography mass spectrometry (GC-MS) (Ventura et al., 2008; Silva et al., 2013). Further, to confirm oil pollution in recent sediments, characteristic petroleum biomarkers such as hopanes, steranes and diasteranes serve as reliable tools since these are recalcitrant toward environmental alteration and degradation (Peters et al., 2005; Aeppli et al., 2014).

The assessment of organic contaminants in the Indian estuaries has become extremely crucial in the wake of rapid urbanisation and industrialization. Numerous studies have largely examined PAEs occurrence and distribution in rivers and lakes worldwide (Teil et al., 2007; Zeng et al., 2009b). However, there has been limited research on concentration and distribution of PAEs and hydrocarbon contamination from Indian estuaries (Ramzi et al., 2018). Ashtamudi estuary is a Ramsar wetland located along the southwest coast of India, while Mandovi estuary is a tropical estuary in central west coast of India (Alagarsamy, 2006; Sinclair et al., 2021). Both the estuaries have been receiving a high influx of pollutants from industrial discharge, sewage inputs, marine transportation, dredging and fishing activities, waste disposal, shipping, agricultural practices and recreational activities (Shynu et al., 2012; Mote et el., 2015; Reshmi et al., 2015; Chinnadurai et al., 2020). In this study, surface sediments from multiple estuaries (Ashtamudi and Mandovi) in Indian subcontinent were evaluated for concentration levels,

distribution characteristics and pollution sources of petroleum hydrocarbon and PAEs. Furthermore, the impact of total organic carbon (TOC) on the accumulation of different organic contaminants in the sediments was also examined from the estuaries. Previous investigations from both the study sites have focussed on metal contamination and OM source characterisation (Harji et al., 2008; Veerasingam et al., 2015a; Ankit et al., 2017; Mishra et al., 2019; Hussain et al., 2020; Bulbul et al., 2021); however no systematic study has been conducted on occurrence and spatial distribution of phthalate esters from both the estuaries. The assessment of pollution status of the estuaries will result in building management strategies as well as monitoring techniques for maintaining the ecosystem health. Hence, the primary objectives of the present study are to: 1) examine spatial distribution of PAEs and discuss the possible sources responsible for introducing phthalates in both tropical estuaries; 2) assess detailed information on the occurrence and origin of different petroleum hydrocarbons: hopanes, steranes and diasteranes; 3) study effects of TOC content on contaminants accumulation in the sediments; 4) compare the pollution status based on quantitative assessment of the phthalates and petroleum markers.

3.2. Materials and Methods

3.2.1. Study Sites

The Ashtamudi estuary (8°53′-9°02′ N, 76°31′-76°41′E) is located near Kollam city (south coast of India) and acts as an interface between the Arabian Sea (south) and the Kallada River (north) (Fig. 3.1a). Ashtamudi estuary is 16 km long, 3.2 km wide and has a depth ranging from 1 to 5.5 m (Fig. 3.1b). While Mandovi estuary (15° 25’-15°30’ N, 73°45’-73°59’ E) is situated near Panjim city (west coast of India) and lies between Sahyadris (Western Ghats) and Arabian Sea (Fig. 3.1a). The estuary is approximately 50 km long (Shetye, 1999), 3.2 km (downstream) to 0.25 km (upstream) wide with an average depth of 5 m (Kessarkar et al., 2009) (Fig. 3.1c). The upper part of both the systems is characterised by abundant terrestrial load, whereas lower part is marine influenced (Maya et al., 2011; Anooja et al. 2013; Ankit et al. 2017). Both the estuaries have enhanced anthropogenic influences from multiple activities that include marine operations, ferries movement, municipal sewage, urban development, fishing, recreation, effluents from industries (plastic, glass, paint, and pigment) and combustion of fossil fuels in vehicles (Nair et al., 1984a; Jennerjahn et al. 2008; Babu et al., 2010; Veerasingam et al., 2015b; Antony and Ignatius, 2016; Prajith et al., 2016; Raghavan and Furtado, 2000; Sreekanth et al., 2017). The untreated anthropogenic pollutants generated from both the ecosystems have

disturbed its equilibrium, thereby causing serious threats to biota (Sitaram, 2014; VishnuRadhan et al., 2015).

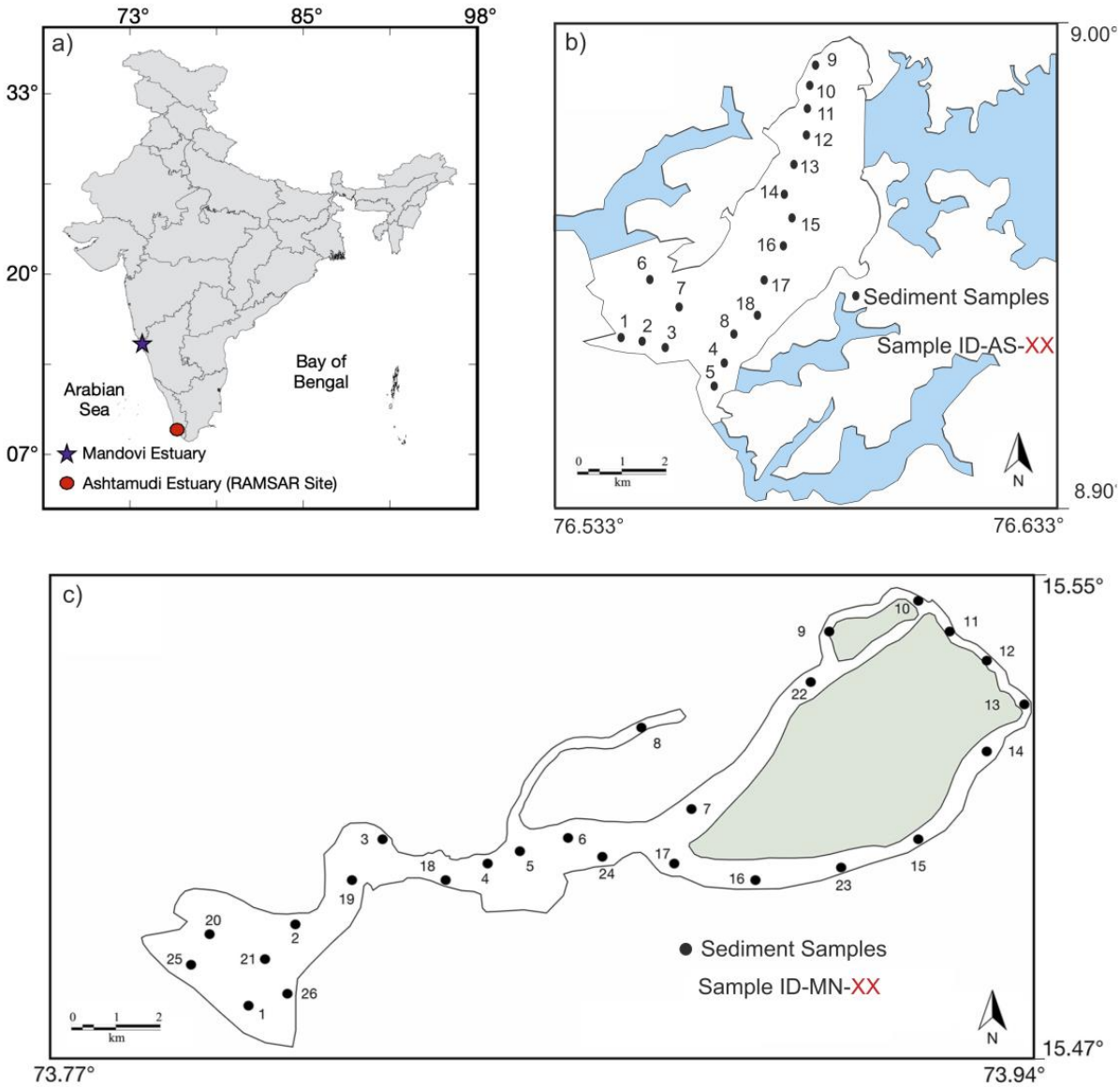

Figure 3.1: (a) Location of the study areas (denoted with 'star' and 'circle') (b) Map of study site showing sediment sampling stations in the Ashtamudi estuary, south-west coast of India. (c) Map of study area exhibiting sediment sample locations in the Mandovi estuary, central west coast of India.

3.2.2. Sample collection

The surface sediment samples were collected from Ashtamudi (n=18) (Fig. 3.1b) and Mandovi (n=26) (Fig. 3.1c) estuaries in October, 2018 using Van Veen stainless steel grab sampler with a penetration depth of 15–20 cm. The collected sediment samples were then transferred to pre-

rinsed glass jars. The field sampling covered lower, middle and upper estuary of both ecosystems. After collection, samples were stored in a freezer (-20°C) prior to the analysis.

3.2.3. TOC analysis

For TOC analysis, the sediment samples (1–2 g each) were powdered using a pestle and mortar and pre-treated with 0.5 N HCl for complete removal of inorganic carbon. The samples were centrifuged (~3000 rpm) to remove acid from the sediments and oven-dried at 30°C for 2-3 days. The de-carbonated samples (~3–5 mg each) were packed in tin capsules and analysed using elemental analyser (Flash EA 2000 HT). The standard deviation observed for replicate analysis was 0.15%.

3.2.4. Extraction procedure for PAEs and petroleum hydrocarbons

The oven-dried (<30°C, 2-3 days) sediment samples (10–15 g) were powdered using a pestle and mortar. The soluble OM (250 mL) was extracted with the help of pressurized solvent extractor (Buchi E-914). The instrument operated for two cycles at T~100°C, P~70 bars and total extraction time of ~40 min. The protocols for extraction of PAEs and aliphatic hydrocarbons were followed according to Ajay et al. (2021) and Bulbul et al. (2021), respectively. PAEs were extracted using dichloromethane (DCM) as solvent (Net et al., 2015b; Ramzi et al., 2018), while aliphatic hydrocarbons were extracted with a mixture of DCM: methanol (MeOH) (93:7 ratio, respectively). The extract (250 mL) was concentrated to 1 mL using multi evaporation system (Multivap P-6, Buchi). Column chromatography was performed using activated silica gel (100–200 mesh, 14 g, activation temperature 450°C for 8 h). The saturated fraction was eluted with *n*-hexane (HX), while the polar fraction (PAEs) was separated from total extract using DCM and MeOH (1:1). The eluted fractions were further condensed to 0.5 mL vials under purified N_2 stream and transferred to GC vials prior to instrumental analysis.

3.2.5. Instrumental analysis

The aliphatic hydrocarbons and PAEs were analyzed using Agilent gas chromatograph (7890B) interfaced to mass spectrometer (5977C) following the procedure outlined in Bulbul et al. (2021) and Ajay et al. (2021), respectively. Sample (1 μl) was injected from automated liquid sampler (GC-ALS) in splitless mode. Analyte separation was attained with capillary column (HP-5MS) (30 m × 0.25 mm i.d. × 0.25 μm film thickness). Helium was used as carrier gas with a flow rate of 1 mL/min. GC oven programmed from 40° to 320°C at a ramp rate of

4°C/min and ion source operated at 70 eV. TIC were produced and the targeted compounds were determined using published literature and NIST library. The petroleum biomarkers (terpenoid compounds) were identified in the saturated hydrocarbon fraction and phthalate compounds were detected in the polar fraction of the Ashtamudi and Mandovi sediment samples. The PAEs are detected using the diagnostic base peak in the selected ion chromatogram at *m/z* 149 which is typical for many phthalates. Additionally, (DEHP) is characterized by the major fragments in the selected ion chromatograms at *m/z* 167 and *m/z* 279 (Fig. 3.2, Supplementary Fig. S3.1). Hopanes and steranes were detected in all samples by ion monitoring using m/z 191 and 217, respectively. The presence of a prominent mass fragment at *m/z* 259 in addition to the *m/z* 217 allowed the identification of the diasteranes.

3.2.6. Quality assurance and quality control

The quality control protocols were strictly followed during sample collection, storage, extraction procedure and GC analysis. During sampling and laboratory analyses, plasticware was excluded to avoid possible contamination. The pre-treatment process of the samples was carried out on a clean workbench. The GC-MS instrument was calibrated regularly with HX (Sigma-34859) and the glassware used for experimental work was subsequently washed with DCM and MeOH and then baked at 500°C for 8 h. The high-performance liquid chromatography grade solvents (HX, DCM and MeOH) were used for processing of the samples. A procedural blank and reagent blank were analyzed after a batch of three samples to improve the precision of the experimental data. For the blank process, powdered pre-combusted sand (90-100 g, 450°C for 8 h) was extracted alongside samples in order to eliminate probability of background signals. The concentration of phthalates was based on calibration curve method and quantification was performed using various concentrations of DBP (99%, Sigma-524980) as an analytical standard. The recovery experiment for PAEs was conducted as mentioned in Ajay et al. (2021) and samples were spiked with internal standard deuterated DEHP (SIGMA-617180), and the recovery ranged from 90.0 to 94.0%. Further, procedure adopted for recovery of aliphatic hydrocarbons was according to Bulbul et al. (2021), and the average recovery obtained was 80%.

3.3. Results

3.3.1. Spatial distribution of PAEs in the two estuaries

A total of 5 PAEs comprising the di-isobutyl phthalate (DIBP), DBP, an isomer peak for DBP, DEHP, di-isononyl phthalate (DINP) are identified in the sediment samples from Ashtamudi estuary (Fig. 3.2, Supplementary Table S3.1). The relative distribution of phthalates towards marine (AS-1) and the riverine zone (AS-9) of Ashtamudi estuary are shown in Fig. 3.2a-b. The concentration of the $\sum_5$PAEs ranges from 7.77 to 1478.2 ng/g (mean= 371.8 ng/g); the highest concentration of $\sum_5$PAEs is found in the riverine sampling site for AS-12 (1478.2 ng/g), followed by middle section AS-18 (676.9 ng/g) (Fig. 3.3a, Supplementary Fig. S3.2a) (Table 3.1). The relative contribution of the phthalate compounds shows DBP and DINP serve as dominant compounds in the Ashtamudi sediments (Fig. 3.3a). The predominance of the DINP compound toward the marine side is noteworthy. Correlation analysis conducted for PAEs indicate a positive correlation between DIBP and DBP ($r=0.9$, $p< 0.05$) and DEHP and DBP ($r=0.9$, $p< 0.05$). TOC concentrations of Ashtamudi samples lie within the range of 1.13–9.49%, and relatively weak correlation was observed between TOC (%) and $\sum_5$PAEs ($r=-0.02$, $p< 0.05$) (Table 3.1).

In the Mandovi estuarine samples, phthalates including diethyl phthalate (DEP), DIBP, DBP, an isomer peak for DBP, DEHP and di(2-ethylhexyl) terephthalate (DEHTP) are detected (Fig. 3.4, Supplementary Fig. S3.1 and Table S3.2). The significant differences in the Mandovi sediment samples compared to Ashtamudi estuary are the absence of the DINP and the presence of DEHTP along with DEP. The concentration of the $\sum_6$PAEs range from 60.1 to 271.9 ng/g (mean= 117.3 ng/g) in the Mandovi estuary (Table 3.2), indicating higher concentration in upper and middle estuarine sampling sites (MN-6 and MN-24) (Fig. 3.3b, Supplementary Fig. S3.2b). The characteristic chromatograms depicting the phthalates distribution in lower (MN-1) and upper (MN-14) end of the Mandovi estuary are shown in Fig. 3.4(a-b). The relative contribution of the phthalate compounds indicates DIBP and DBP are dominant compounds in the Mandovi sediments (Fig. 3.3b). A positive correlation has been obtained between DIBP and DBP ($r=0.8$, $p< 0.05$), and DEHP and DBP ($r=0.9$, $p< 0.05$). Further, insignificant correlation was observed between TOC (%) and $\sum_6$PAEs ($r=0.1$, $p< 0.05$) of Mandovi sediments (Table 3.2).

Table 3.1: Summary of ∑PAEs (ng/g), diasterane (ng/g), sterane (ng/g), hopane (ng/g), petroleum biomarkers (∑PBs) (ng/g) concentrations, TOC (%) and *n*-alkane index (CPI) of surface sediments from Ashtamudi estuary.

Sample ID	Lat	Lon	DIBP	DBP	DEHP	DINP	∑PAEs	Diasterane	Sterane	Hopane	∑PBs	CPI	TOC
AS-1	8.9345	76.5481	79.1	116.7	117.2	311.3	624.4	30.4	30.9	57.5	118.8	0.989	3.79
AS-2	8.9350	76.5486	2.64	3.85	1.28	n.d.	7.77	n.d.	n.d.	0.177	0.177	0.732	1.81
AS-3	8.9322	76.5496	46.5	69.4	23.2	n.d.	139.1	n.d.	n.d.	n.d.	n.d.	0.644	8.34
AS-4	8.9280	76.5688	6.43	12.2	5.96	72.8	97.4	0.518	0.518	0.787	1.82	0.719	2.76
AS-5	8.9237	76.5658	91.1	163.5	79.0	n.d.	333.5	116.6	121.5	363.2	601.3	0.642	1.13
AS-6	8.9513	76.5533	24.8	49.0	24.6	292.3	390.7	17.2	17.6	43.2	78.0	2.02	1.30
AS-7	8.9465	76.5612	76.3	91.8	65.7	360.0	593.8	7.08	7.12	14.0	28.2	1.11	3.21
AS-8	8.9351	76.5707	76.8	102.2	75.4	301.8	556.3	37.7	41.1	137.8	216.7	1.63	9.14
AS-9	9.0008	76.5911	27.6	31.8	31.3	n.d.	90.7	3.19	3.22	8.08	14.5	1.75	3.20
AS-10	8.9962	76.5853	39.4	59.5	19.4	n.d.	118.4	3.40	3.41	4.48	11.3	1.84	3.08
AS-11	8.9911	76.5838	48.4	48.0	24.0	286.8	407.1	34.7	36.0	92.9	163.5	3.17	9.49
AS-12	8.9834	76.5828	515	739.9	223.7	n.d.	1478.2	12.2	12.2	47.0	71.4	1.64	1.38
AS-13	8.9770	76.5809	71.7	71.7	23.2	n.d.	166.6	34.1	36.2	134.5	204.7	1.90	1.45
AS-14	8.9723	76.5831	27.7	72.4	23.8	n.d.	123.9	34.0	37.4	317.2	388.6	2.27	1.24
AS-15	8.9653	76.5822	109	98.8	25.5	n.d.	233.5	30.3	34.2	201.2	265.6	2.47	1.29
AS-16	8.9575	76.5799	50.9	76.3	74.5	300.3	502.0	36.1	37.9	124.1	198.1	2.73	1.39
AS-17	8.9485	76.5757	32.5	60.7	29.2	29.1	151.5	42.7	45.2	161.5	249.4	1.83	1.39
AS-18	8.9412	76.5728	93.2	133.3	93.9	356.6	676.9	34.9	35.9	70.4	141.2	2.28	1.26

n.d.- not detected

Table 3.2: Summary of of ∑PAEs (ng/g), diasterane (ng/g), sterane (ng/g) and petroleum biomarkers (∑PBs) (ng/g) concentration of surface sediments from Mandovi estuary. Hopane concentrations (ng/g) and TOC (%) are reported from Bulbul et al. (2021).

Sample ID	Lat	Lon	DEP	DIBP	DBP	DEHP	DEHTP	∑PAEs	Diast.	Ste.	Hop.	∑PBs	TOC
MN-1	15.4844	73.8011	15.0	15.6	30.4	15.1	15.0	91.1	2.28	2.33	6.80	11.4	0.038
MN-2	15.4981	73.8139	15.0	20.4	33.4	16.4	15.2	100.3	10.1	10.4	50.7	71.2	0.332
MN-3	15.5050	73.8242	15.1	20.8	30.7	17.3	15.0	98.9	20.8	40.1	681.3	742.2	2.66
MN-4	15.5056	73.8392	18.8	28.1	38.6	20.8	18.8	125.0	17.7	24.7	375.9	418.3	2.42
MN-5	15.5097	73.8467	n.d.	18.8	37.5	18.8	18.8	93.8	11.4	11.7	11.5	34.6	0.280
MN-6	15.5108	73.8572	19.3	114.3	42.9	24.5	19.0	219.8	11.9	12.7	33.7	58.2	0.467
MN-7	15.5119	73.8703	18.8	25.7	38.8	19.3	18.8	121.4	14.7	19.1	213.5	247.4	0.971
MN-8	15.5286	73.8717	18.8	19.2	37.7	19.1	18.8	113.6	15.2	20.2	293.6	328.9	1.40
MN-9	15.5456	73.9044	18.8	22.0	37.9	19.8	18.8	117.2	18.9	26.7	127.7	173.2	4.01
MN-10	15.5450	73.9161	18.8	32.7	38.6	21.6	19.0	130.6	18.7	25.5	382.8	427.0	2.60
MN-11	15.5394	73.9219	18.8	22.6	38.0	19.7	18.8	118.0	14.1	18.2	302.7	335.0	3.21
MN-12	15.5319	73.9294	18.8	21.1	38.2	20.5	18.8	117.3	16.2	24.9	191.0	232.1	2.85
MN-13	15.5286	73.9317	18.8	20.0	37.7	19.4	18.8	114.7	23.0	33.8	323.8	380.6	4.31
MN-14	15.5228	73.9244	18.9	22.1	38.0	19.9	18.9	117.8	17.4	26.2	443.9	487.5	3.66
MN-15	15.5117	73.9178	18.8	22.2	38.2	20.5	18.9	118.6	14.2	17.6	392.4	424.2	1.33
MN-16	15.5017	73.8794	19.0	19.5	37.8	19.0	18.8	114.1	14.6	21.1	154.3	190.0	2.85
MN-17	15.5042	73.8694	18.8	22.2	38.2	20.0	18.8	117.9	18.2	25.4	7.50	51.1	2.09
MN-18	15.5003	73.8422	18.8	23.7	38.1	20.5	19.0	120.0	18.6	24.5	205.3	248.5	2.33
MN-19	15.5031	73.8264	n.d.	15.6	30.5	18.2	15.2	79.5	9.37	9.59	253.1	272.1	0.101
MN-20	15.4994	73.7886	n.d.	16.2	30.2	15.6	15.1	77.0	9.08	9.07	420.0	438.1	0.066
MN-21	15.4917	73.8028	n.d.	16.6	30.8	16.7	15.1	79.1	9.11	9.12	393.4	411.7	0.062
MN-22	15.5344	73.8950	n.d.	51.9	39.6	25.2	15.6	132.3	10.5	10.7	12.3	33.5	2.50
MN-23	15.5019	73.8989	18.8	24.3	38.2	20.6	18.9	120.8	2.86	2.86	2.20	7.96	0.712
MN-24	15.5061	73.8628	15.6	115.1	87.7	38.1	15.5	271.9	3.14	3.75	4.10	11.0	0.909
MN-25	15.4972	73.7819	n.d.	16.8	30.5	16.1	15.1	78.4	10.1	12.4	103.9	126.3	0.051
MN-26	15.4825	73.8069	n.d.	15.0	30.0	15.1	n.d.	60.1	2.29	2.33	4.60	9.19	0.026

n.d.- not detected, Diast.- Diasterane, Ste.- Sterane, Hop.- Hopane

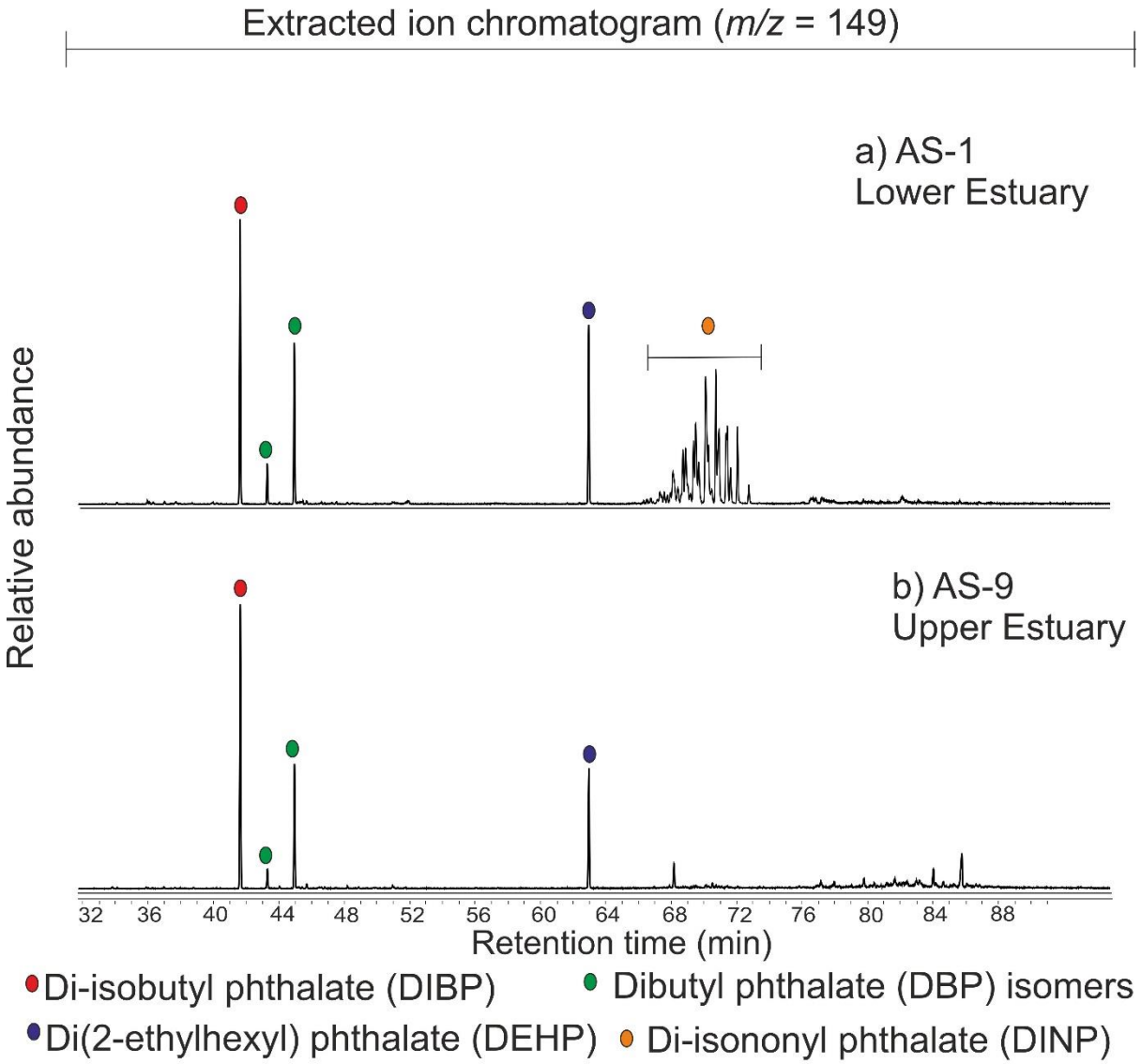

Figure 3.2: Selected ion chromatogram at *m/z* 149 constituting different PAEs in sediments collected from lower (AS-1) (a) and upper (AS-9) (b) end of the Ashtamudi estuary.

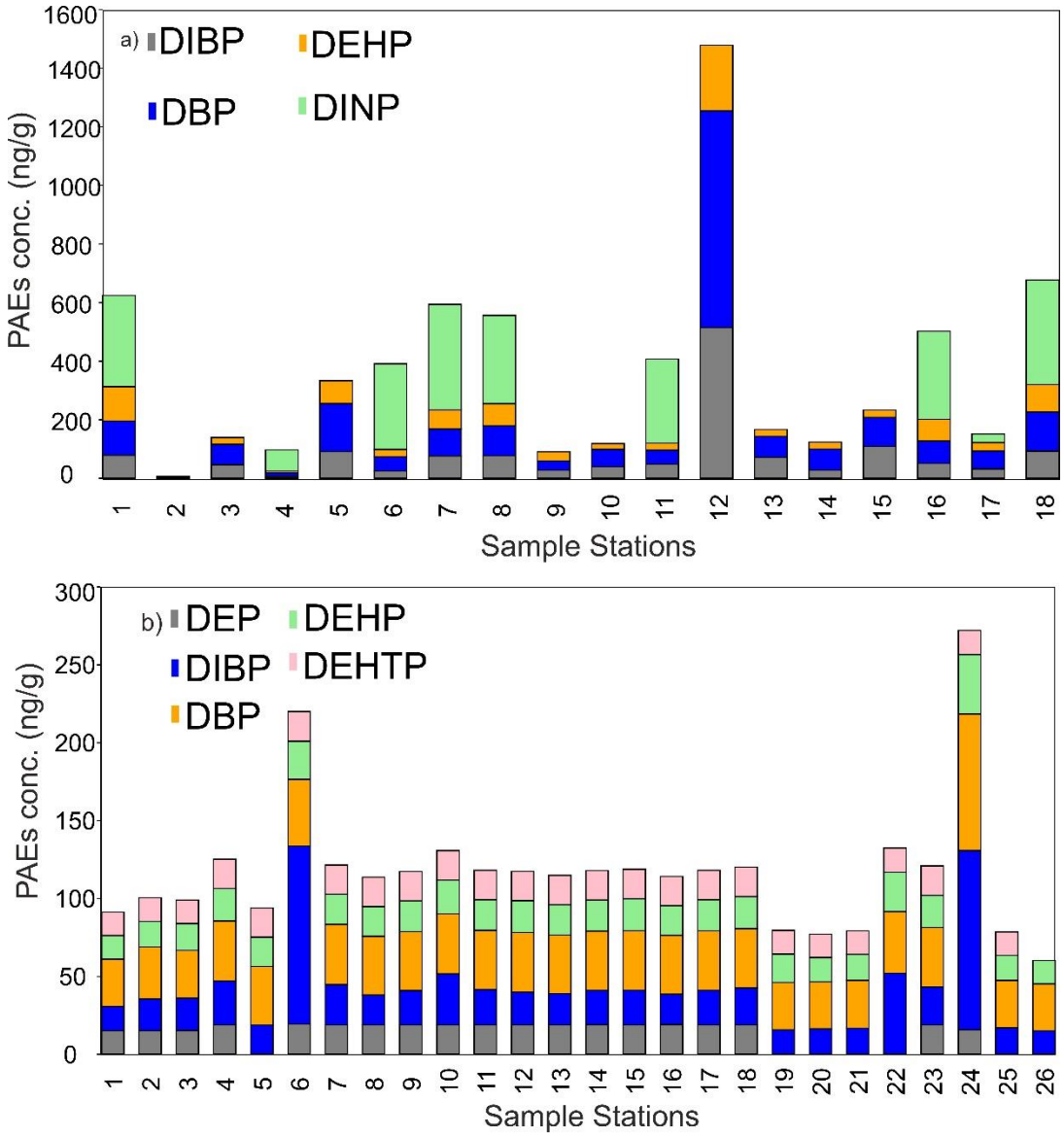

Figure 3.3: PAEs concentrations in sediment samples from various sampling sites of Ashtamudi estuary (a) and Mandovi estuary (b).

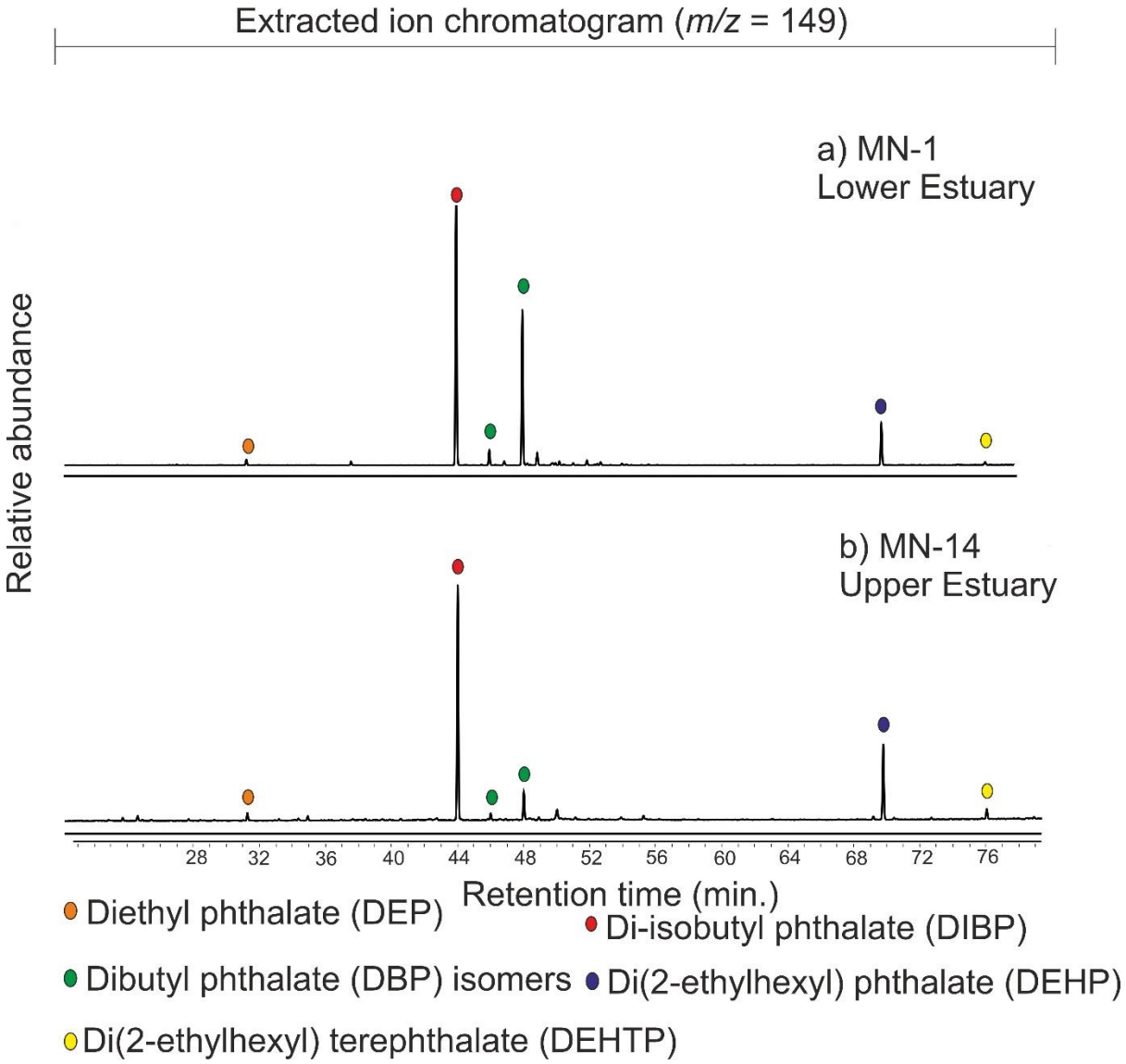

Fig. 3.4: Selected ion chromatogram at *m/z*149 showing various PAEs in sediments obtained from lower (MN-1) (a) and upper (MN-14) (b) reaches of the Mandovi estuary.

3.3.2. Distribution of aliphatic hydrocarbons in estuaries

3.3.2.1. *n*-Alkanes

The representative TIC of the saturated hydrocarbon fractions of lower and upper estuarine samples from Ashtamudi estuary are shown in Supplementary Material Fig. S3.3. The *n*-alkanes are detected in the selected ion chromatogram at *m/z* 57. In Ashtamudi estuary, resolved aliphatic hydrocarbons consist of *n*-C_{16} to *n*-C_{33} *n*-alkanes. The Ashtamudi sediments close to the marine side are characterized by lack of any carbon preference and display a unimodal distribution of the *n*-alkanes (CPI~1; Table 3.1) (Supplementary Material Fig. S3.3a).

However, the sediment samples obtained from the upper estuarine region exhibit distinct odd-over-even carbon preference for the *n*-alkanes and depict a bimodal distribution (Supplementary Material Fig. S3.3b). The presence of high UCM in the lower parts of the Ashtamudi estuary is observed and this is clearly depicted by samples AS-1 (Supplementary Material Fig. S3.3a), while the sediment samples closer to the riverine setting (AS-14) exhibit TIC with negligible UCM (Supplementary Material Fig. S3.3b). Notably, the UCM intensity decreases with increasing distance of the recovered sediment samples from the open sea. The UCM pattern obtained from the Ashtamudi estuary is comparable with the pattern observed in Mandovi samples collected from the region closer to the marine side (Bulbul et al., 2021).

3.3.2.2. Petroleum biomarkers

A wide spectrum of hydrocarbon biomarkers specifically the terpenoid compounds are present in the sediment samples retrieved from Ashtamudi and Mandovi estuaries (Supplementary Tables S3.3 and S3.4). Steranes and diasteranes ranging between C_{27} to C_{29} are identified in sediments retrieved from both the sites. The Ashtamudi sediments also comprise a moderate abundance of hopanes such as the C_{27} hopanes -trisnorhopane (Tm) and trisnorneohopane (Ts), C_{29} hopane, C_{30} hopane and $C_{31,}$ C_{32}, C_{33} homohopanes occurring as the 22S and 22R doublets. The hopane profiles are similar to that obtained from the samples of the Mandovi estuary (Bulbul et al., 2021).

The concentration of hopanes, steranes and diasteranes in the Ashtamudi surface sediments ranged from n.d.-363.2 ng/g, n.d.-121.5 ng/g and n.d.-116.6 ng/g, respectively (Table 3.1). Likewise, the concentration of steranes and diasteranes in the Mandovi estuary ranged from 2.33 to 40.1 ng/g and 2.28 to 23.0 ng/g, respectively (Table 3.2). Notably, the relative contribution of the petroleum markers suggests hopanes are dominant in the Ashtamudi (Supplementary Material Fig. S3.4) as well as Mandovi surface sediments (Supplementary Material Fig. S3.5). Moreover, the respective total concentration of petroleum biomarkers from Ashtamudi estuary and Mandovi estuary varies between n.d.-601.3 ng/g (mean= 153.0 ng/g) (Fig. 3.5a) and 7.96 to 742.2 ng/g (mean= 237.4 ng/g), respectively (Fig. 3.5b). Further, weak correlation was observed between TOC% and total concentration of petroleum biomarkers for Ashtamudi estuary (-0.22, $p< 0.05$) and Mandovi estuary ($r=0.4$, $p< 0.05$).

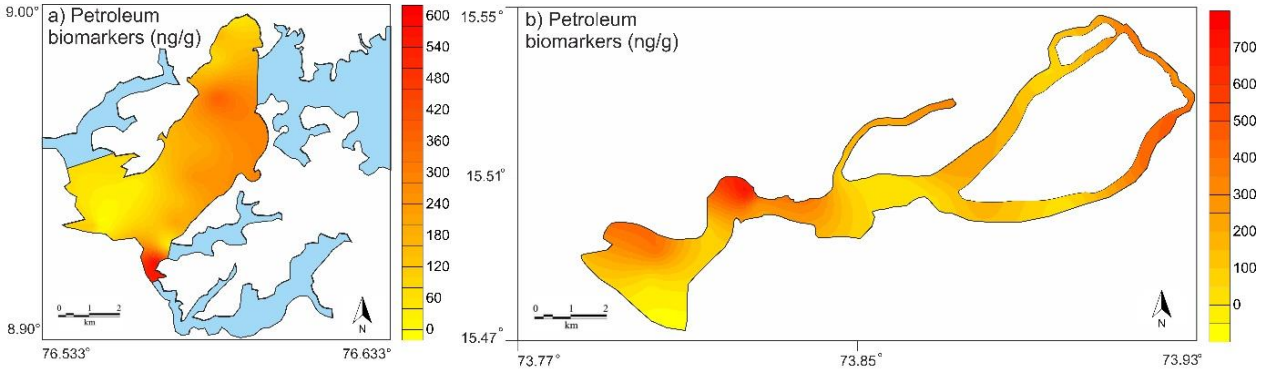

Figure 3.5: Spatial occurrence of petroleum biomarkers (diasteranes, steranes and hopanes) (ng/g) in Ashtamudi estuary (a) and Mandovi estuary (b).

3.4. Discussion

3.4.1. Spatial distributions of PAEs

The phthalate compounds detected in Ashtamudi estuary are DIBP, DBP, DEHP and DINP (DINP is present in the marine sediments) (Fig. 3.2a-b, Supplementary Material Fig. S3.1), whereas phthalates comprising DEP, DIBP, DBP, DEHP and DEHTP are spatially distributed in Mandovi sediments (Fig. 3.4a-b, Supplementary Material Fig. S3.1). DBP and DIBP serve as dominant PAEs in the Mandovi estuary (Fig. 3.3b), while DINP and DBP are dominant phthalates in the Ashtamudi estuary (Fig. 3.3a). The accumulation of DBP, DINP and DIBP, DBP in the respective estuaries might be associated with their long-term usage and disposal close to the regions. DBP is used as a plasticizer in rubber and plastic products containing polyvinyl chloride and also as solvent and fixative in various products such as paints, cosmetics and coating of medicines and food supplements (Chen et al., 2005, Borch et al., 2006). DIBP is used as a replacement compound for DBP in manufacturing industries due to similarity in the application properties and hence a surge in this compound has been observed through biomonitoring studies (Zota et al., 2014). The DINP found in the Ashtamudi sediments recovered from the marine side is an essential component of paints and coats used in the boating vessels (Przybylinska and Wyszkowski, 2016; Schrank et al., 2019). DEHP is used in the manufacturing of a variety of products such as clothing, car and building products, medical devices and food packaging (Heudorf et al., 2007). Furthermore, DEHP is also used in the manufacturing of polyvinyl chloride (PVC) products in order to attain desired stability (Bernard et al., 2014). DEHTP is used as alternative plasticizer for ortho-phthalate such as DEHP and this replacement compound is used in various products like consumer goods, medical devices and food contact materials (Biedermann-Brem et al., 2008). DIBP, DBP and

DEHP are dominant in the upper estuarine region of both the estuaries. A positive correlation among DIBP, DBP and DEHP in both the studied regions implies a common source. DEP observed in Mandovi sediments has numerous industrial uses and this compound is used as solvent in cosmetic ingredients (Barse et al., 2007).

Interestingly, the $\sum_5$PAEs observed in the Ashtamudi estuary is 3 order of magnitude higher than the Mandovi estuary (Table 3.1 and 3.2). The Ashtamudi estuary is used as a waste sink and receives anthropogenic influx from various sources such as corporation's sewage-treatment plant located near the bank, and other dumping sites (Sitaram, 2014). The waste generated mainly includes solid and domestic plastic containers and bags, and the accumulation of plastic waste has turned out to be the major threat (Sitaram, 2014; Joy and Paul, 2021). Likewise, Mandovi estuary receives industrial wastes from plastic, glass, paint and pigment manufacturing industries (Samant et al., 2018). Other sources include garbage from domestic houses, hotels, casinos and marine activities (Gupta et al., 2021).

PAEs were detected in the entire transect of both the estuarine ecosystem indicating that they are ubiquitous contaminants in the studied systems. However, the higher concentration of total PAEs has been observed in upper and middle part of both the estuaries. The PAEs distribution is substantially influenced by multiple factors such as hydrodynamic condition, river runoff, human activities and physico-chemical properties of the compounds (Sun et al., 2013; Li et al., 2017). To investigate the role of physico-chemical parameter (such as TOC) over PAEs accumulation, correlation analysis was performed between ∑PAEs and TOC%, and weak correlation has been noticed for Mandovi estuary ($r=0.1$, $p< 0.05$) and Ashtamudi estuary ($r=-0.02$, $p< 0.05$) thereby reflecting that TOC has negligible role over the PAEs distribution. Moreover, previous investigations have suggested a close relationship between anthropogenic activities and outspread of the plastic-derived chemicals in the estuarine environment (Lubecki and Kowalewska, 2019).

Notably, distribution pattern of the plastic debris is largely influenced by the hydrodynamics, seasonal variations, wind regimes and ocean currents (Veerasingam et al., 2016). During wet periods, high freshwater influx carries significant amount of plastic debris into the estuarine system resulting in higher accumulation (Gupta et al., 2021). Thus, the relative dominance of PAEs in upper and middle reaches of both the systems indicate high input of land-based domestic and industrial plastic waste that is further favoured by high precipitation regime. Moreover, the higher concentration of phthalates in the Ashtamudi estuary (a Ramsar wetland)

suggests the presence of a vast amount of plastic waste being disposed off irresponsibly at the banks that is severely polluting the ecosystem.

3.4.2. Petroleum contamination

The petroleum pollution in an ecosystem can be assessed by utilising the combined approach based on distribution of the *n*-alkanes profile, diagnostic ratio (CPI), nature of baseline humps (UCM) and presence of petroleum biomarkers (Petersen et al., 2017; Venturini et al., 2008). In the sediments, the functionalized compounds such as acids and alcohols usually produced as even carbon chains are diagenetically altered through removal of the carboxylic acid or the hydroxyl groups to form *n*-alkanes (Peters et al., 2005). The preference for the odd carbon number and bimodal distribution occurs if the terrestrial OM input is high (Eglinton and Hamilton, 1967) and such pattern has been observed in the upper end of Ashtamudi estuary (Supplementary Material Fig. S3.3b). The dominance of terrestrial OM is due to contribution from various river tributaries and local vegetation sources (Ankit et al., 2017). The *n*-alkane pattern with no noticeable even/odd preference for carbon chain length reflects fossil fuel inputs (Mille et al., 2007) and such unimodal distributions are noticed in the lower estuary (Supplementary Material Fig. S3.3a). The intensified pollution level in the coastal environment was further corroborated by examining the CPI values and UCM pattern (Venturini et al., 2008). *n*-Alkanes produced from the epicuticular waxes of vascular plants give rise to high CPI values, while petrochemically derived *n*-alkanes exhibit CPI values close to 1 (Mille et al., 2007; Venturini et al., 2008). In this study, low CPI values (~1) accompanied by very high UCM in the lower estuarine samples imply a significant contamination of the sediments by petrochemical substances (Supplementary Material Fig. S3.3a). On the contrary, higher CPI values in the upper estuarine samples indicate dominant input of terrestrial vegetation sources (Table 3.1).

The petrogenic hydrocarbons towards the marine side is also substantiated by the detection of diagnostic petroleum-derived compounds (Aeppli et al., 2014). The hydrocarbon compounds such as hopanes and steranes are diagenetically and/or catagenetically produced from the precursor functionalized compounds that are lipid remnants of organisms constituting the petroleum. Biological hopanoids and steroids typically comprise the ββ (Seifert and Moldowan, 1980) and ααα*R* configurations, respectively (Mackenzie and McKenzie, 1983). With increasing diagenesis, the hopanoids alter to βα and αβ configurations and the steranes convert to αββ*R* and αββ*S* isomers (Seifert and Moldowan, 1980; Mackenzie et al., 1982).

Thus, the stabilities of the isomers of compounds with same molecular masses can be effectively used to discriminate between biogenic and diagenetic products (Mackenzie et al., 1980). Hopanes are present with βα and αβ configurations, while steranes profile is dominated by peaks of αββR and αββS isomers in both the estuaries, thereby indicating petroleum by-products (Seifert and Moldowan, 1980; Mackenzie et al., 1982; Mackenzie and McKenzie, 1983). Further, diasteranes (rearranged steranes) also serve as useful indicator of petroleum contamination in the urban coastal areas (Medeiros and Bícego, 2004). The petroleum compounds are present in lower concentrations in the sediments collected from the uppermost parts of both estuaries (Fig 3.5a-b, Supplementary Material Figs. S3.4 and S3.5). Comparing both the systems, petroleum biomarkers are detected in substantial abundance in Mandovi estuary thus further validating the extensive petroleum pollution (Fig. 3.5b) (Supplementary Material Fig. S3.5). Moreover, the poor correlation between TOC and petroleum biomarkers for Mandovi ($r=0.4$, $p< 0.05$) and Ashtamudi estuary ($r=-0.22$, $p< 0.05$) indicates minimal impact of TOC over petroleum hydrocarbons distribution. Oil pollution in lower and middle part of Ashtamudi estuary can be attributed to vessel spill, and seepage from oil pipelines or from fishing crafts (Nair et al., 1984b; Santhosh and Badusha, 2017; Zachariah and Johny, 2009). Also, the intense fishing activities have led to rise in the utility of mechanized crafts and country crafts fitted to outboard engines that dispose of diesel and kerosene and pollute the estuarine ecosystem at an alarming rate (Raghunathan, 2007; Santhosh and Badusha, 2017). Oil spillage from fishing crafts is regarded as one of the main sources of petroleum pollution with the Neendakara fishing harbour being the busiest fishing hub and located at the mouth of the Ashtamudi estuary (Kumar et al., 2012). Likewise, the petroleum pollution in lower and middle reaches of the Mandovi estuary has been attributed to boating, iron ore mining, tourism activities and oil spillage from tankers (Veerasingam et al., 2015b). Further, rainfall data of more than 100 years have depicted an intensified monsoon in the region (Potdar et al., 2019) that facilitated the transportation of the terrestrially-derived hydrocarbon pollutants from the nearby localities into the estuary. Several accidents of tankers carrying oil along the route between Goa and the Middle East countries have led to the surge in the concentrations of the crude oil hydrocarbons in the estuary (Vethamony et al., 2007).

3.4.3. Comparison with other estuarine systems

The level of PAEs reported from the present study has been compared with previously reported PAEs abundance in various aquatic environments including lakes, rivers and estuaries. The concentrations of phthalates have been documented from India in Kaveri River (south India;

Selvaraj et al., 2015), Cochin estuary (south west coast of India; Ramzi et al., 2018), Gomti River (North India; Srivastava et al., 2010) (Supplementary Table S3.5). The PAEs concentrations are also reported from Pearl River estuary (Li et al., 2016) and Guanting Reservoir (Zheng et al., 2014), Jinshan (Zhang et al., 2003) in China (Supplementary Table S3.5). The systematic data on PAE distribution from both the estuaries suggest that phthalate concentration of Ashtamudi estuary has exceeded Kaveri Indian riverine estuary (Selvaraj et al., 2015), though the value is lower than that reported from Pearl River estuary, Gomti river, Cochin estuary and Guanting Reservoir. Further, the values reported for DEP and DBP from Mandovi estuary are higher than those in the Kaveri River. The concentration for DBP and DEHP from Mandovi estuary are comparable to the values reported from Jinshan, Shanghai. DBP, DEHP concentrations from Ashtamudi estuary are higher than those in the Kaveri River, Jinshan (Shanghai). Further, our study shows that the riverine transport is the major pathway of phthalate contamination in Ashtamudi and Mandovi estuaries, similar to other estuarine systems (eg., Zheng et al., 2014; Ramzi et al., 2018).

3.4.4. Environmental risk assessment

PAEs are man-made chemicals and its presence in the environment is concerning as its accumulation in the sediments may pose risk to aquatic organisms. These pollutants have major impact on coastal ecosystem and threaten top consumers in the food chain (Yang et al., 2012). Experimental studies have revealed that some metabolites of phthalates are estrogenic and have harmful effect on endocrine glands. The environmental risk limits (ERLs) based on (eco)toxicology and environmental chemistry data were derived and reported for DBP as well as DEHP in sediments and fresh soils (Van Wezel et al., 2000). The calculated ERLs for DBP and DEHP were 700 ng/g and 1000 ng/g respectively (Liu et al., 2014). ERL for other phthalate compounds is absent, therefore the risk assessment in Mandovi and Ashtamudi sediments was adopted based on DBP and DEHP. In the present work, the average concentrations for DBP and DEHP from Ashtamudi estuary were 111.16 ng/g and 53.39 ng/g, respectively while the values for DBP and DEHP for Mandovi estuary were 38 ng/g and 19.9, ng/g respectively. The measured values are lower than ERL, thereby suggesting low ecological risk of both compounds. However, the ERL of remaining phthalate compounds remain unknown. In spite of the lower concentrations of DBP and DEHP, the overall presence of PAEs necessitates adoption of relevant environment management strategies in order to control further accumulation in both the systems.

3.5. Conclusions

The present study provides primary systematic data on the concentration and distribution of phthalates and petroleum markers examined in the surface sediments of Ashtamudi and Mandovi estuaries. The results indicate that upper and middle part of both the ecosystems are highly influenced by plastic-derived chemicals. The *n*-alkane profile, UCM pattern and hydrocarbon terpenoids clearly suggest that the lower tidal advected and middle zones of both estuaries are immensely affected by abundant contaminants derived from spillage of petroleum. The data also highlights intensified plastic pollution in a Ashtamudi estuary (a Ramsar site) that is responsible for providing innumerable ecosystem services to the community. The comparison data on PAE suggest that the concentration levels found for DBP as well as DEHP in Ashtamudi estuary are comparable to that obtained in Kaveri River, Jinshan (Shanghai) and Guanting Reservoir. Although the calculated values are lower than ERL, the adverse ecotoxicological effects of PAEs and their metabolites accentuate immediate adoption of pollution control strategies to reduce mounting stresses on the aquatic environments due to increased contaminants runoff. Additionally, crude oil contamination that has equally impacted the health of valuable ecosystems implies a need of long-time monitoring of hydrocarbon pollution in the estuarine environments. Therefore, the present investigation will provide a baseline study and allow an exclusive survey to understand the changing dynamics of estuaries.

Chapter 4

Spatial distribution and characteristics of microplastics and associated contaminants from mid-altitude lake in NW Himalaya*

*The contents of this chapter are published in the international peer reviewed journal 'Chemosphere' as Bulbul et al., 2023.

Bulbul, M., Kumar, S., Ajay, K., Anoop, A., 2023. Spatial distribution and characteristics of microplastics and associated contaminants from mid-altitude lake in NW Himalaya. Chemosphere 138415.

Mehta Bulbul[1], Sunil Kumar[1], Kumar Ajay[1], Ambili Anoop[1]

[1]Indian Institute of Science Education and Research, Mohali 140306, India

4.1. Introduction

In recent years, there has been growing concern regarding the impacts of plastic pollution in aquatic ecosystems (Andrady, 2015; Ivleva et al., 2017; Green, 2020; Napper and Thompson, 2020). The global production of plastic materials was 348 million tons in 2017 (Plastics Europe, 2018), while only 20% entered waste stream management (Cole et al., 2011; Plastics Europe, 2019). Once released into the environment, the plastic materials undergo significant degradation resulting from the action of physical, chemical, and biological drivers (Andrady, 2015; Zhang et al., 2021). The degradation and disintegration of plastics generate particles with dimensions <5 mm defined as microplastics (MPs), classified as contaminants of emerging concern (Wagner et al., 2014; Andrady, 2015; Sedlak, 2017).

The stable chemical properties, resistant to degradation and long residence time results in the widespread distribution of MPs in global waters and sediments (Hopewell et al., 2009; Andrady, 2015). Based on their sources, MPs are classified into primary MPs that are originally manufactured at those size, while secondary MPs originate by fragmentation/weathering or photodegradation of larger plastic particles (Lambert et al., 2017; Díaz-Mendoza et al., 2020). Moreover, morphological characteristics differentiate MPs into fibre, fragments, foam, films and spherical (beads and pellets) (Baldwin et al., 2016; Zhang, 2017; Karthik et al., 2018), whereas chemical properties categorize MPs mainly into polyethylene (PE), polypropylene (PP), and polystyrene (PS), polyvinyl chloride, nylons, and polyethylene terephthalate (Lambert et al., 2017; Sharma and Chatterjee, 2017).

The MPs in aquatic systems pose potential dangers as microplastic ingestion have been recorded by wide variety of aquatic organisms (Jabeen et al., 2017; Pannetier et al., 2020) resulting in physiological disorders (Ma et al., 2020; Pannetier et al., 2020). Additionally, MPs also serve as a vector to transport heavy metals and persistent organic pollutants (Dehghani et al., 2017) and pose threat to humans due to their ability to persist through food chain. Apart from the direct effects of MPs, plastics also contain hazardous chemical additives such as phthalic acid esters or phthalates (PAEs) that are used as plasticizers (Kueseng et al., 2007; Ajay et al., 2021). These toxic chemicals were added to improve various mechanical properties including elasticity and flexibility of plastic products (Kueseng et al., 2007; Hahladakis et al., 2018). PAEs are considered as environmental priority pollutants and endocrine disrupting contaminants due to their cytotoxicity and estrogenic effects (Harris et al., 1997; Swan, 2008; Mankidy et al., 2013). These chemical contaminants have high octanol-water partition

coefficients, due to which they are detected in sorbents including sediment organic matters, soil etc. (Verla et al., 2019; Atugoda et al., 2021).

The Indian Himalayan region is one of the most heavily populated mountainous areas in the world. The aquatic systems in this region offer series of ecosystem services and functions such as water for household consumption and agricultural purposes, reservoirs of biodiversity and wetland products, and recreation and tourism (Joshi and Joshi, 2019; Dar et al., 2021; Ghosh, 2021). In spite of its socio-economic and ecological importance, the Himalayan lakes are subjected to various anthropogenic alterations and receive plastic waste by the means of industrial and sewage discharges, urban runoff and wind-blown deposition (Ajay et al., 2021; Pastorino et al., 2022). Despite a significant amount of research undertaken on MPs pollution in the marine environment (Thompson, 2015; Wang et al., 2016; Saha et al., 2021; Venkatramanan et al., 2022), there are limited studies on MPs distribution in freshwater environment especially in the Indian subcontinent (Sarkar et al., 2020, Vanapalli et al., 2021). Moreover, to date, integrated studies on MPs and PAEs in freshwater environment from the Indian subcontinent have been restricted to an investigation from Renuka Lake (Ajay et al., 2021). In this study, we present the abundance and distribution of both MPs and its contaminants (PAEs) in a mid-altitude Rewalsar Lake located in the North-Western Indian Himalaya. The overarching aims of the present research are to i) assess the extent of microplastic pollution in Rewalsar Lake surface water and sediments; and ii) determine the spatial distribution and potential sources of microplastics; iii) characterize the distribution levels and environmental risk assessment of PAEs in the sediments.

4.2. Study Area

Rewalsar (31º37’30” N, 76º49’15” E), a freshwater lake, is located in Mandi district, Himachal Pradesh (India) at an altitude of 1400 m above mean sea level (Fig. 4.1a and 4.1b). The oval-shaped lake has maximum length of 225 m, 160 m breadth and a large catchment area of ~1.17 km^2 (Das and Haake, 2003; Sarkar et al., 2016). The Rewalsar Lake is characterised by an average water depth of ~4 m (Jindal et al. 2014). The lake is fed by three seasonal inlet streams in northern side and catchment runoff (Gaury et al., 2018). Additionally, sewage water also enters the lake through overflow and leakage (Jindal et al., 2014). The mean annual rainfall received by the region is ca. 124 cm with contribution mostly from the Indian summer monsoon (Sarkar et al., 2016).

The Rewalsar Lake is used for several purposes like supply of drinking water, agricultural and urban irrigation, recreational and religious activities (Thakur et al., 2013; Gaury et al., 2018). However, in recent years, lake is highly contaminated due to the increase of human inhabitation in its catchment, and religious activity that includes artificial feeding of fishes (Kashyap et al. 2015). In particular, the eastern and western shore of lake are influenced by anthropogenic settlements including bathing ghat, gurudwara, temple and bus stand resulting in increased pollution. The physicochemical analyses (Total Dissolved Solids, Biological Oxygen Demand, Nitrate, Chloride etc.) of Rewalsar Lake showed significant degradation of water quality (Thakur et al., 2013; Jindal and Thakur 2013). Likewise, the temporal assessment of heavy metals concentration in water samples also shows values well above permissible limits as per US Environmental Protection Agency (USEPA), 2010 and WHO, 2010 (Kashyap et al. 2015). Moreover, the high human intervention in the region has led to fish-killing mechanism (Kumar and Mahajan, 2020).

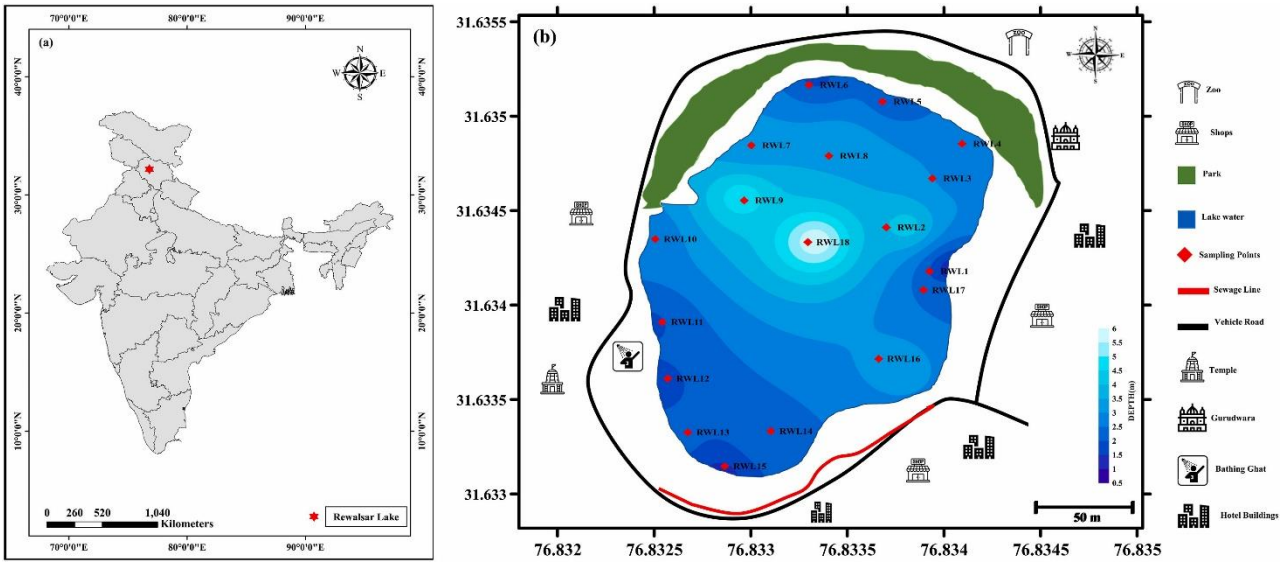

Fig. 4.1: (a) The map showing location of Rewalsar Lake (denoted with 'star'); (b) Lake bathymetry and surface water and sediment sample locations in the Rewalsar Lake, NW Himalaya.

4.3. Materials and Methods

4.3.1. Field sampling

The surface water and sediments samples from Rewalsar Lake were collected from eighteen sampling stations using a water sampler (Uwitec, Austria) and Van Veen grab sampler, respectively (Fig. 4.1b). The bathymetric survey was performed with the help of GARMIN

GPSMAP 585 plus echo sounder. At all stations, 2 L of collected water samples were transferred into pre-cleaned glass bottles without filtering. Likewise, approximately 1 kg of the sediments were taken from each station, and kept in an aluminium foil bag. MPs abundance was measured from both the media i.e., sediments and water, while the PAEs concentrations were computed from the sediment samples. The PAEs analysis was not conducted in water samples due to limited sample availability after the MPs extraction (replicate analysis was performed for each sample).

4.3.2. Microplastics extraction and analysis

The MPs from water and sediment samples were extracted following the methodology outlined in Ajay et al. (2021) with minor modifications. The water sample (~1000 ml) was homogenized by shaking the container, and was extracted using a filtration unit (MERCK MILLIPORE). The filtration was carried out using a glass fibre filter paper (47 mm diameter, Whatman CAT no. 1820-047) having pore size of 0.2 µm. The filter papers were kept in glass Petri-dishes until further analyses.

For sediments samples, the wet surface sediments were air-dried and 100 gm of each sample was used. Further, organic matter was removed from the sediment using hydrogen peroxide and Fenton's reagent. After digestion of organic matter, the solution was filtered using 4.75 mm mesh size sieve. Thereafter, density separation was performed, and sample solution was mixed with salt solution of zinc chloride ($ZnCl_2$) for separation of MPs. $ZnCl_2$ was preferred for density flotation because of its good recovery for high-density polymers (Van Cauwenberghe et al., 2015; Rodrigues et al., 2018). After the settling of sediment debris, the supernatant was filtered through a Whatman glass fibre filter. All glass fibre filters were then carefully placed in covered and labelled Petri-dishes.

The visual identification and screening of morphological characteristics of MPs were performed using Nikon SMZ- 10 stereoscopic zoom microscope coupled with an illuminator. The morphological features were classified into fibre, fragments, pellets/beads, foam, and films. Further, samples were analysed for polymer composition of microplastic particles using micro-Raman spectrometer (Renishaw InVia) linked with three different excitation laser sources of 514, 633 and 785 nm. The spectroscopic analysis was undertaken on selected number of MPs particles (n = 300). The spectral range of MPs scanning in Raman spectroscopy was in the range of 500–3200 cm^{-1}. The polymer type of each measured sample was identified by comparison with available literature.

4.3.3. Plasticizers extraction and analysis

The PAEs extraction from sediment samples was in accordance with the procedure described elsewhere (Ajay et al., 2021; Bulbul et al., 2022). The dried sediment samples (8-10g) were extracted via pressurized liquid extraction (Buchi Speed Extractor, E-914) using DCM (three cycles, 20 min each). The instrument was programmed at T~100°C, P~70 bars with an extraction duration of 1 h. The extract was concentrated to 1ml with the help of a Buchi Multivapor P-6 system. Silica gel column chromatography was performed on the extract, and polar fraction (phthalates) was isolated using DCM/methanol (1:1; v/v). Further, the eluted polar fraction was concentrated to 0.5 ml, and transferred into autosampler vial for GC-MS analyses. The aliquots were analyzed using an Agilent 7890B gas chromatograph (GC) interfaced to a 5977C mass spectrometer.

4.3.4. Quality control

Throughout the sampling and laboratory analysis, a series of quality measures were followed to prevent potential contamination of the samples from airborne microplastic particles. The plastic-free cotton laboratory coats, masks, and nitrile gloves were worn during field sampling and laboratory experiments. Prior to analyses, the glasswares were cleaned, solvent-rinsed and baked to avoid cross-contamination. Thereafter, glasswares were dried in a muffle furnace (500 °C for 8 h), and then wrapped in aluminium foil. Milli-Q water was used for sample preparation, and the filtered samples were stored in glass Petri-dishes. The HPLC grade organic solvents (dichloromethane (DCM) and hexane) were used for conducting various experiments.

The extraction of MPs and preparation of $ZnCl_2$ solution was carried out at room temperature. The density of the prepared $ZnCl_2$ solution (1.6–1.7 kg/L) was continuously monitored using specific gravity hydrometer. The procedural blanks (pre-combusted quartz sand and MilliQ water) were also included during MPs extraction to check for background contamination from laboratory sources. Further, replicate analyses for each samples were also conducted for both the media so as to confirm the reproducibility and terminate probable background signals. The relative error of replicate analyses was found to be low ≤5%, and the average of these analyses was considered to present the abundance of microplastic data.

The calibration of GC-MS was done with hexane, and reagent blanks were run after two samples. For PAEs, laboratory procedural blanks (baked pre-combusted sand) was also extracted along with the sediment samples to ensure that any background signals were negligible. The concentrations of targeted phthalates in the blank samples were less than

detection limit indicating a lack of contamination during sample processing. The detailed procedures for PAEs recovery have been described in Bulbul et al. (2022), and 92.0% mean recovery was obtained in this study. The concentration values of phthalates were derived using calibration curve method and standard (EPA 506 Phthalate Mix 40077-U) was used to elucidate the elution pattern of phthalates with retention time.

4.3.5. Statistical analysis

The concentration of MPs in water and sediment samples is reported in particles per liter (particles L^{-1}) and particles per kilogram of dry sediment (particles kg^{-1} d. w.), respectively. Further, the concentration of phthalates is expressed as μg/g dw. The spatial interpolation of MPs and associated compounds was carried out using kriging interpolation method (Golden Software licensed program Surfer 15). The stacked plots were obtained using PAST software Version-4.03 (Hammer et al. 2001). The correlation analysis was conducted to examine the relationship between MPs and PAEs content in surface sediments with $p<0.05$ considered as statistically significant.

4.4. Results and discussion

4.4.1. Concentration and distribution of microplastics in surface water and sediments samples

Microplastics were ubiquitous in Rewalsar Lake as these particles were detected in all the sampling stations in both the media. The abundance of MPs in surface water ranged from 13 to 238 particles L^{-1}, while the concentration in sediments samples varied from 750 to 3020 particles kg^{-1} d.w (Table 4.1). The average concentrations are registered higher for sediments (1449 particles kg^{-1} d.w) as compared to water samples (130 particles L^{-1}) (Supplementary Fig. S4.1). The high concentration of MPs in water samples was recorded for sample RWL-1 (238 particles L^{-1}) followed by RWL-3 (235 particles L^{-1}) and lowest for sample RWL-13 (13 particles L^{-1}) (Fig. 4.2a). For surface waters, the highest abundance of MPs was observed in samples from shallow water (water depth of ≤ 3 m) sites in the western and eastern part, while lowest level of MPs was found in the sites in the south-western part of the lake. On the other hand, high abundance of MPs in sediments was observed in sampling station RWL-10 (3020 particles kg^{-1} d.w) followed by RWL-17 (2000 particles kg^{-1} d.w), while low concentration was noticed for station RWL-16 (750 particles kg^{-1} d.w) (Fig. 4.2b). For sediments, highest abundance of MPs was observed in the western margin of the lake, followed by eastern region.

The lowest concentration of MPs in sediments was recorded in the northern and southern parts of the lake.

The spatial distribution of MPs in water and sediments are mainly influenced by human activities (Zheng et al., 2020; Ajay et al., 2021). The major anthropogenic activities in this region include tourism, recreational boating, industries, fisheries and agriculture practices. Based on the concentration levels in the sediments and water, the margins of lake basin are dominated by MPs input. The sites RWL-1 and RWL-3 are situated close to settlements including hotels and related hospitality infrastructure, while RWL-10 and RWL-17 are towards bathing site and hotel buildings respectively. Additionally, the domestic sewage effluents, high level of tourist activities and surface runoff from inhabited areas may serve as non-point sources of microplastic pollution, thereby becoming dominant threat to the lake system. On the other hand, the southern and northern regions were characterized with lower level of local human activities (Fig. 4.1b). The results indicate that the intensity of human activities had an obvious correlation with MP abundance.

Furthermore, MPs abundance do not show significant correlation ($r^2 = 0.22$) between surface water and sediment samples. The insignificant correlation was mostly attributed to different residence times of MPs in each environment (Kowalski et al., 2016; Teng et al., 2020). A variety of factors (e.g., water quality, hydraulic conditions, particle density) is known to influence the residence time of MPs in the water column (Kowalski et al., 2016; Yan et al., 2021). The physical behaviour that includes shape, particle size and density influences the settling of MPs (Kowalski et al., 2016; Yang et al., 2022). Furthermore, the biofouling mechanism i.e., the microbial colonization that tends to enhance the density while decrease buoyancy of MPs, may also result in sinking of MPs in the sediments (Cózar et al., 2014; Andrady, 2015). Therefore, MPs in the sediments integrate relatively long-term influence of anthropogenic emissions, while surface water only represent short-term changes (less than a year) (Hitchcock, 2020; Teng et al., 2020). Further, the total microplastic abundance in surface water and sediments showed no pattern with water depth or distance from shoreline. Overall, our results indicated an insignificant correlation between water depth and MPs in water ($r^2 = 0.12$) and sediments ($r^2 = 0.02$).

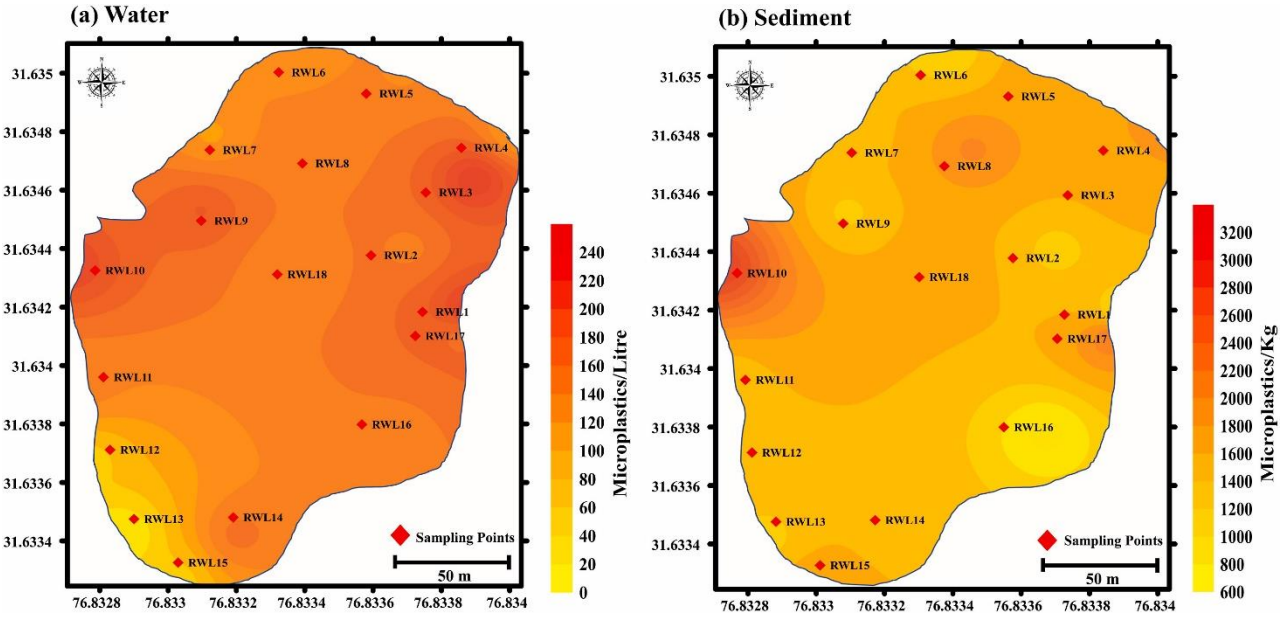

Fig. 4.2: Spatial occurrence of microplastics in Rewalsar Lake surface water (a) and surface sediments (b).

Table 4.1: Summary of microplastic abundance in surface water and sediments, DIBP, DBP, DEHP and $\sum_3$PAEs concentrations in sediment samples (μg/g) from Rewalsar Lake.

			Water Samples	Sediment Samples				
Sample ID	Lat	Long	MPs abundance (particles/L)	MPs abundance (particles/kg dw)	DIBP	DBP	DEHP	ΣPAEs concentration (μg/g dw)
RWL-1	31.6342	76.8339	238	950	0.43	0.55	1.31	2.29
RWL-2	31.6344	76.8337	135	1120	0.44	0.34	3.22	4.00
RWL-3	31.6346	76.8339	235	1480	0.42	0.55	1.51	2.49
RWL-4	31.6348	76.834	89	1730	0.49	0.55	1.78	2.82
RWL-5	31.635	76.8337	118	1540	0.47	0.61	2.96	4.03
RWL-6	31.6351	76.8334	102	1020	0.53	0.57	1.47	2.57
RWL-7	31.6348	76.8331	97	1340	0.62	0.58	1.37	2.57
RWL-8	31.6348	76.8335	131	1840	0.46	0.54	1.34	2.34
RWL-9	31.6345	76.8331	181	1160	0.51	0.56	1.53	2.60
RWL-10	31.6344	76.8327	216	3020	0.42	0.55	1.15	2.13
RWL-11	31.6339	76.8327	132	1270	0.52	0.55	1.15	2.23
RWL-12	31.6337	76.8328	53	1250	0.71	0.61	1.64	2.95
RWL-13	31.6334	76.8328	13	1140	0.43	0.54	0.97	1.93
RWL-14	31.6334	76.8332	146	1350	0.51	0.76	1.26	2.53
RWL-15	31.6332	76.833	48	1590	0.36	0.52	1.06	1.95
RWL-16	31.6338	76.8337	133	750	0.48	0.55	1.17	2.20
RWL-17	31.6341	76.8339	152	2000	0.43	0.54	1.19	2.17
RWL-18	31.6343	76.8334	120	1530	0.29	0.51	0.89	1.69

4.4.2. Sources of microplastics

The shapes of the observed MPs were sorted into pellets/beads, fragment, fibre, film and foam (Fig. 4.3). The most common shapes of MPs in water and sediments samples were pellets/beads accounting for 71.70% and 64.11% respectively (Fig. 4.4). The beads mainly originate from cosmetics and personal care products, such as facial scrubs, hand-cleansers, soaps, toothpaste and shaving foam (Baldwin et al., 2016; Cheung and Fok, 2017). Likewise, pellets are mostly used in beauty and cleaning products (Warrier et al., 2022). The anthropogenic activities including bathing and washing clothes and use of cosmetic products could be responsible for generation of large proportion of pellets/beads in Rewalsar Lake. The proportion of fragment recorded in water and sediment samples were 26.34% and 22.35%, respectively (Table 4.1). Fragments are primarily resulted from the breakdown of larger plastic items i.e., this shape type could be directly sourced from fragmentation of packing bags, plastic containers and other daily used plastic materials (Baldwin et al., 2016; Meng et al., 2020). The concentration of films (0.04%), foam (0.38%) and fibre (1.54%) were relatively lower in water samples (Fig. 4.4a-b). Likewise, the films, foam and fibre show relatively low concentration in sediment samples with values of 4.79%, 3.95%, 4.79% respectively. The films are mainly derived from discarded bags and packing and agricultural plastic film, while foam from food packaging and construction materials (Kyrikou and Briassoulis, 2007; Nor and Obbard, 2014). The fibre shaped MPs originate from synthetic fabrics, ropes and fishing lines (Napper and Thompson, 2016). Plastic fibres may also enter through domestic sewage line connected to the lake system by the means of laundry water of synthetic clothes. The predominance of pellets with size mostly less than 3 mm in Rewalsar Lake may pose a higher environmental risk to organisms due to their greater exposed surface area resulting in increased adsorption of hydrophobic organic pollutants (Frias et al., 2010; Tan et al., 2019). Further, the high percentage of pellet-sized MPs in the present study may also results in accidental ingestion for aquatic organisms by mistaking them for food (Cole et al., 2013; Lin, 2016).

Further, polymer composition can be used to trace the source of MPs (Yuan et al., 2019; Ajay et al., 2021). The polymers identified in the sediment and water samples were mainly polypropylene, polyethylene and polystyrene, derived from primary and secondary MPs (Fig. 4.5). The polypropylene is detected based on Raman peaks recorded from 500 and 1500 cm^{-1} and 2600 to 3000 cm^{-1}. Different vibrations including C–C backbone stretching, $–CH_2$ and $–CH_3$ deformation are observed from 500 to 1500 cm^{-1}, while $–CH_2–$ and $–CH_3$ stretching

vibrations from 2600 to 3000 cm^{-1}. The respective frequencies that occur in polystyrene spectrum are 1637 cm^{-1}, 2935 cm^{-1}, and 2885 cm^{-1} assigned to C=C styrene, symmetric and antisymmetric CH_2 valency vibrations. The CH_2 deformation between 500 to 1500 cm^{-1} and stretching mode 2600 to 3000 cm^{-1} are indicative of polyethylene (Dąbrowska, 2021). Polyethylene is the most abundant synthetic polymer due to its wide applicability, and is used in products such as packing bags, plastic containers, toys and other household items (Royer et al., 2018). Likewise, owing to excellent physical and chemical properties, polypropylene is extensively used to manufacture various plastic tools, fishing nets, textile coverings, while polystyrene are commonly used in production of disposable plastic products and packaging applications (Vianello et al., 2013; Kim, 2017; Letcher, 2020).

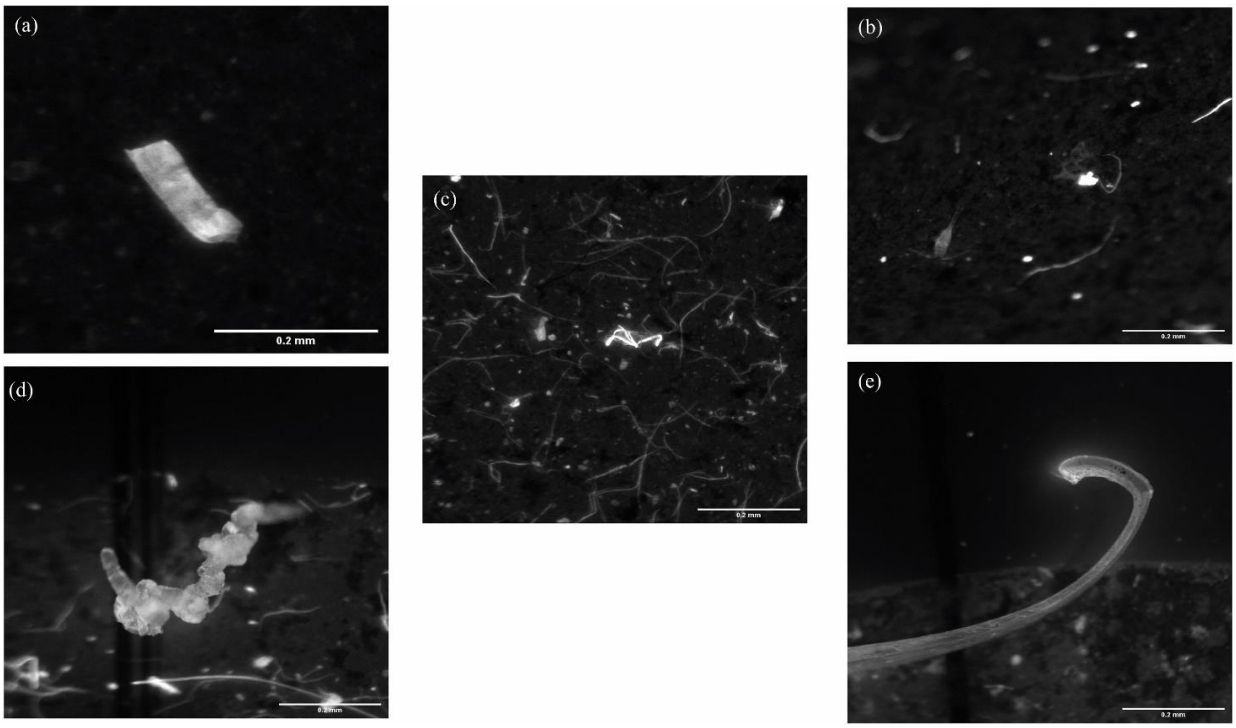

Fig. 4.3: The microplastic particle type in the study area; (a) film, (b) pellet/beads, (c) fragments, (d) foam, and (e) fibre.

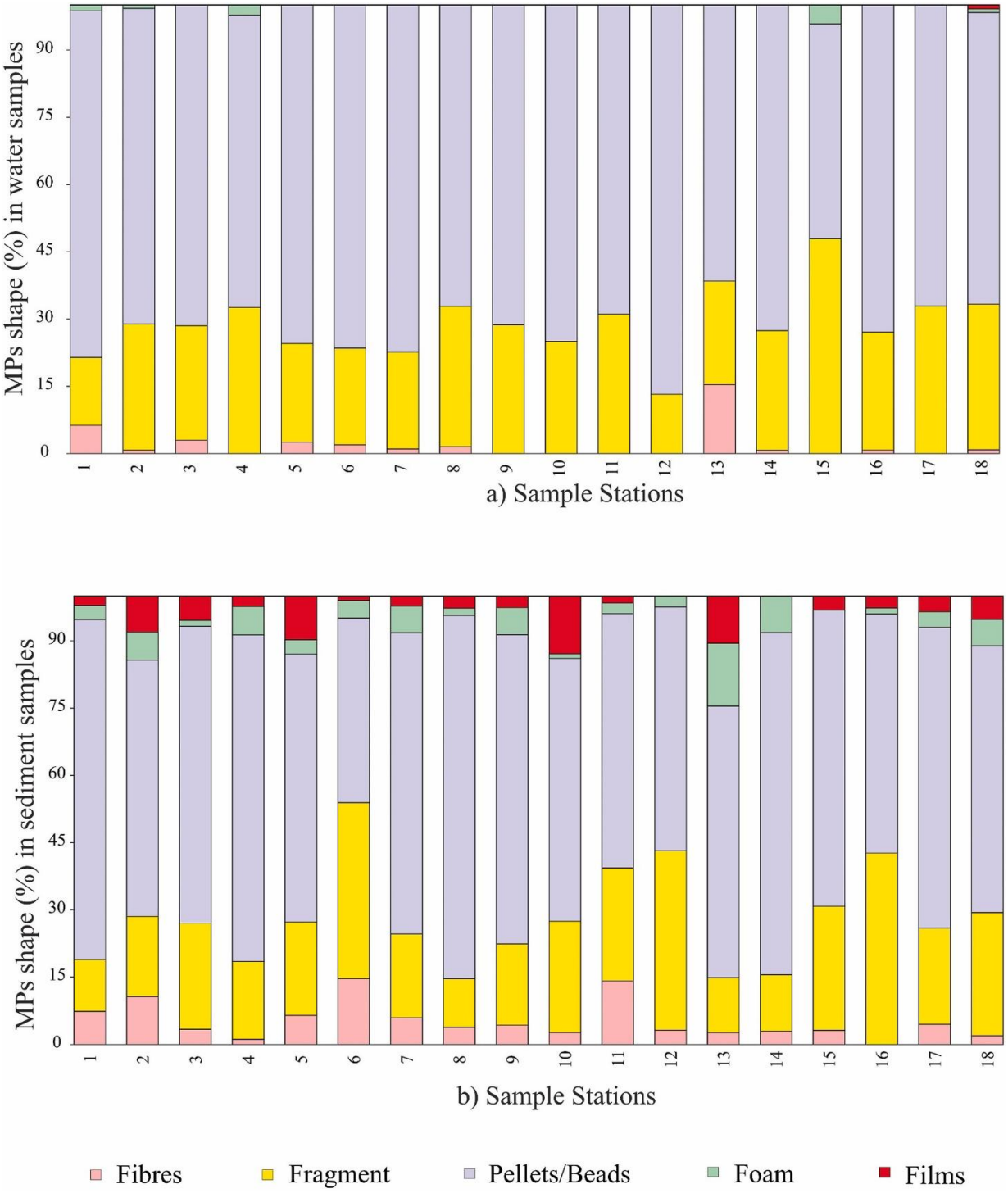

Fig. 4.4: Stacked bar chart representing particle type abundance at various locations in water samples (a) and sediment samples (b).

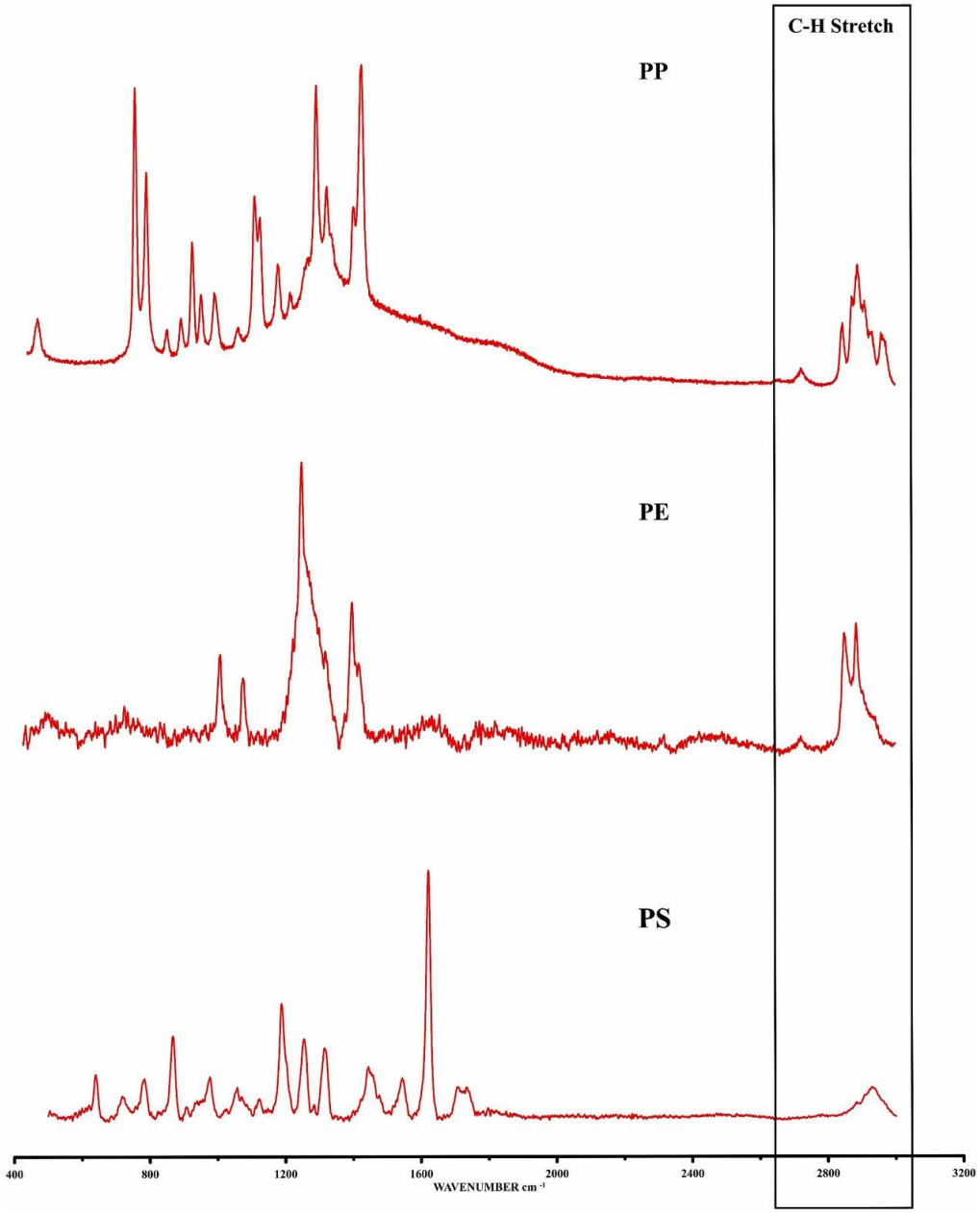

Fig. 4.5: Raman spectra of the representative microplastics from Rewalsar Lake.

4.4.3. Concentration of phthalates in sediments

The concentrations of phthalates measured in surface sediment collected from Rewalsar Lake were summarized in Table 4.1. A total of 3 PAEs including di-isobutyl phthalate (DIBP), dibutyl phthalate (DBP) and its isomer, and di(2-ethylhexyl) phthalate (DEHP) were detected in Rewalsar lake surface sediments. Phthalate compounds (DIBP and DBP) was identified based on the characteristic m/z 149 and m/z 223 fragment ions, while DEHP was monitored using m/z 149, m/z 167 and m/z 279 diagnostic ions (Fig. 4.6, Supplementary Table S4.1). The concentration of PAEs ranged from 1.69 μg/g to 4.03 μg/g in Rewalsar surface sediments.

Among identified phthalates, DEHP showed the highest concentrations followed by DBP and DIBP (Fig. 4.7). The concentrations of DEHP, DBP and DIBP in sediment samples varied from 0.89-3.22 μg/g (average: 1.50 μg/g), 0.34-0.76 μg/g (average: 0.56 μg/g), and 0.29-0.71 μg/g (average: 0.47 μg/g), respectively.

4.4.4. Distribution pattern and potential sources of phthalates

The overall concentrations of Σ_3PAEs in Rewalsar lake sediment exhibits considerably less variability with average value of 2.53 ± 0.62 μg/g (Table 4.1). The highest concentration is observed for station RWL-5 (4.03 μg/g) followed by RWL-2 (4.00 μg/g). The correlation analysis conducted between DIBP and DBP ($r=0.4$, $p< 0.05$) and DIBP and DEHP ($r=0.2$, $p< 0.05$) indicate weak relationship among individual compounds of phthalates, thereby suggesting different sources. The DEHP is a high molecular weight phthalates widely added to variety of consumer products such as building materials, food packaging, children's products and medical devices (Heudorf et al., 2007). On the other hand, DBP and DIBP are low molecular weight phthalates commonly found in cosmetics and personal care products such as nail polishes, perfumes and deodorants (Zota et al., 2014; Koniecki et al., 2011). The occurrence of phthalate compounds in the Rewalsar Lake are attributed to high tourist influx, sewage outflow and developmental activities.

Further, the correlation analysis was also conducted between MPs pollution (particles kg^{-1} d.w) and PAE congeners (μg/g) in the surface sediments in order to examine the potential relationship between two pollutants (Supplementary Fig. S4.2). A weak relationship ($r=-0.2$, $p< 0.05$) was observed between MPs abundance and Σ_3PAEs in sediment. Few studies based on the positive correlation between MPs and PAEs have shown the utility of PAEs as a proxy for MPs contamination in the environment (Ramirez et al., 2019; Ajay et al., 2021; Mohammadi et al., 2022). In contrast, numerous investigations have documented an absence of a clear correlation between total PAEs and MPs similar to this study (Montoto-Martínez et al., 2021; Schmidt et al., 2021). The poor correlation are mostly attributed to release of PAEs into the environment since PAEs are not covalently bonded to the plastic materials (Yan et al., 2022; Saliu et al., 2022). The environmental parameters such as temperature and salinity have found to effect the leaching of PAEs from plastics materials (Dhavamani et al., 2022; Mohammadi et al., 2022). Additionally, plastic properties particularly particle size can also influence PAEs migration as PAEs diffuse higher from smaller particles as compared to larger particles (Talsness et al., 2009; Yan et al., 2021). The high abundance of small particles principally

beads/pellets reported from the Rewalsar Lake may result in high rates of phthalates diffusion. The other possible reason behind lack of correlation is the use of PAEs as additives for non-plastic sources such as oil residues, detergents and pharmaceuticals (Garcia-Garin et al., 2022, Lodi et al., 2022). Furthermore, Li et al. (2021) documented that inconsistent correlations may also arise from the difference in units of MPs (particles/kg) and PAEs (µg/g) in sediments as MPs (particles/kg) contribute in number while PAEs (µg/g) in sediments majorly contribute as mass to the system. Collectively, these factors may contribute to the observed weak relationship between MPs abundance and Σ_3PAEs in Rewalsar surface sediments.

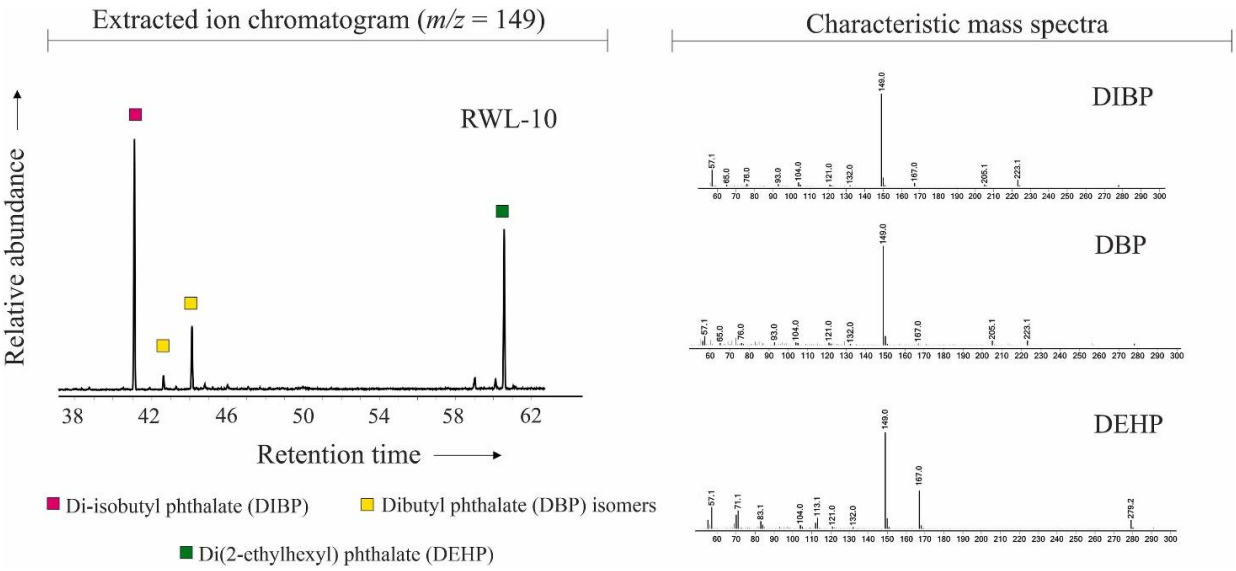

Fig. 4.6: Selected ion chromatogram at m/z 149 and characteristic mass spectra showing various phthalate esters in surface sediments.

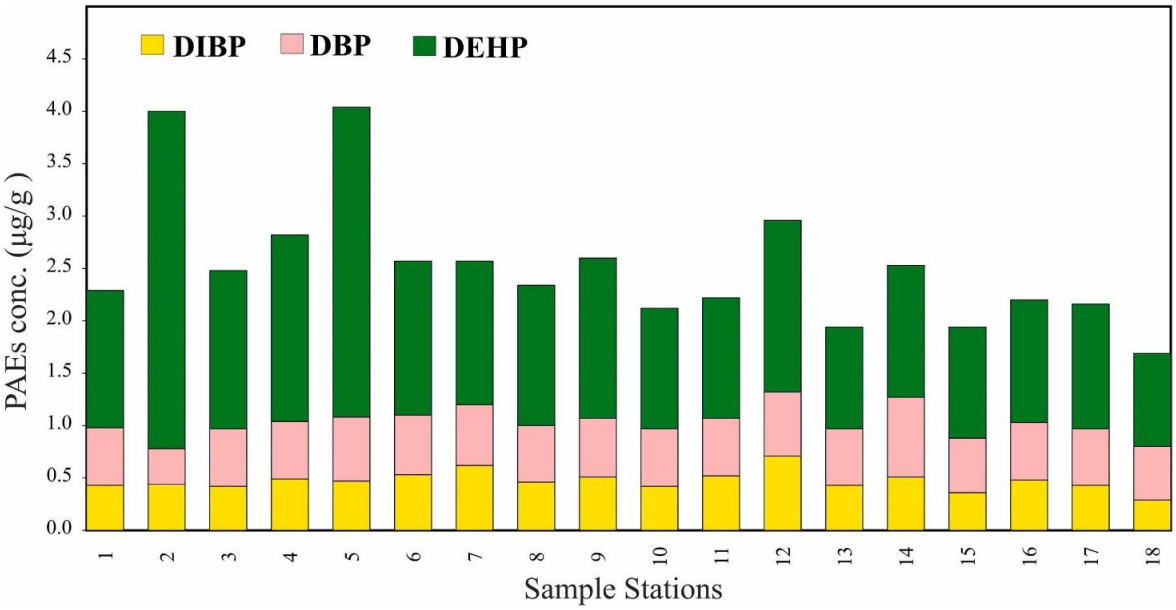

Fig. 4.7: Stacked bar chart showing phthalate concentrations (µg/g) at different sampling locations.

4.4.5. Comparison with Indian lakes and environmental risk assessment

The MPs occurrence in inland waters from Indian subcontinent are shown in Table 4.2. However, comparison of MPs data from different regions is difficult due to the difference in sampling and sample processing methodologies, size limits and reporting units (Campanale et al., 2020; Oni et al., 2020). Nevertheless, the comparison of the present study with other investigations on MPs pollution in freshwater lake system in Indian subcontinent shows that the level of MPs in Rewalsar sediments and water samples was several order of magnitude higher than Manipal Lake (South India; Warrier et al., 2022), Red Hills Lake (Tamil Nadu; Gopinath et al., 2020), Veeranam Lake (South India; Manikanda Bharath et al., 2021), Anchar Lake (NW Himalaya; Neelavannan et al., 2022), and Renuka Lake (Himachal Pradesh; Ajay et al., 2021) (Table 4.2). Further, the abundance of MPs pollution in the Rewalsar Lake is exceedingly high in comparison with other global mountain lakes (Fig. 4.8 and Table 4.2). Therefore, systematic data pinpoint that present study site is the most contaminated Indian lake that further signal the immediate adoption of risk assessment to investigate the impact on ecosystem.

Further, the various PAEs have received considerable attention due to their endocrine-disrupting effects and harmful consequences on human health. Biomonitoring studies imply human exposure to DIBP results in reproductive toxic effects in males (Chen et al., 2020). Likewise, DEHP are neurotoxic and can lead to hyperactivity disorder risks in humans, while DBP are associated with high estrogenic activity and developmental effects (Hong et al., 2005). Consequently, six of PAEs including DBP, DIBP and DEHP have been listed as priority pollutant by the USEPA (Das et al., 2021). Further, the environmental risk limits (ERLs) have also been developed for DBP and DEHP in sediments, and respective values for DBP and DEHP was 0.7 and 1.0 $\mu g \cdot g^{-1}$ respectively (Van Wezel et al., 2000). In this study, DBP concentration (mean= 0.56 μg/g) is lower than the ERL, while the DEHP levels (mean=1.50 μg/g) in the Rewalsar sediments exceeded the ERL. Overall, the high values of DEHP in the lake basin urge control on human interference in order to cease accumulation of plastic derived chemicals and preserve the aquatic system.

Table 4.2: Summary of microplastics abundance in water and sediments measured in Indian and global mountain lake systems.

S. No.	Location	Sample media	Microplastic Abundance (mean)	Polymer Type	Ref.
1	Manipal Lake, Karnataka, India	Water	0.423 particles/L	PET, CE	Warrier et al., 2022
2	Red Hills Lake, Tamil Nadu, India	Water, Sediment	5.9 particles/L, 27 particles/kg	HDPE, LDPE, PP, PS	Gopinath et al., 2020
3	Veeranam Lake, South India	Sediment	309 items/kg	NY, PE, PS, PP, PVC	Manikanda Bharath et al., 2021
4	Anchar Lake, NW Himalaya, India	Sediment	606 particles/kg	PA, PET, PP, PS, PVC	Neelavannan et al., 2022
5	Renuka Lake, Himachal Pradesh, India	Water, Sediment	21 ± 13 particles/L, 180 ± 143 particles/kg	PS, PP, PE	Ajay et al., 2021
6	Rewalsar Lake, Himachal Pradesh, India	Water, Sediment	130 particles/L, 1449 particles/kg	PS, PP, PE	This study
7	Pangong Lake, Indian Himalaya	Sediment	160–200 MP/kg	PE, PP, PS, PET, PMMA	Tsering et al., 2022
8	Tsomoriri Lake, Indian Himalaya	Sediment	960–1440 MP/kg	PE, PP, PS, PET, PMMA	Tsering et al., 2022
9	Tsokar Lake, Indian Himalaya	Sediment	160–320 MP/kg	PE, PP, PS, PET, PMMA	Tsering et al., 2022
10	Gangtang Co, China	Sediment	406.85 ±262.18 items/kg	PA, PET	Liang et al., 2022
11	Yibug Caka, China	Sediment	2643.65 ±1716.25 items/kg	PA, PET	Liang et al., 2022
12	Tangqung Co, China	Sediment	269.26 ±371.98 items/kg	PA, PET	Liang et al., 2022

13	Dagze Co, China	Sediment	507.51 ±543.06 items/kg	PA, PET	Liang et al., 2022
14	Chaxiabu Co, China	Sediment	701.89 ±227.02 items/kg	PA, PET	Liang et al., 2022
15	Guojialun Co, China	Sediment	185.55 ±265.56 items/kg	PA, PET	Liang et al., 2022
16	Pongcê Co, China	Sediment	250.12 ±412.68 items/kg	PA, PET	Liang et al., 2022
17	Bangkog Co, China	Sediment	297.39 ±61.87 items/kg	PA, PET	Liang et al., 2022
18	Gogen Co, China	Sediment	640.94 ±157.7 items/kg	PA, PET	Liang et al., 2022
19	Bobsêr, China	Sediment	143.45 ±268.38 items/kg	PA, PET	Liang et al., 2022
20	Yangnapeng Co, China	Sediment	17.22 ±29.66 items/kg	PA, PET	Liang et al., 2022
21	Angdaer Co, China	Sediment	389.03 ±505.71 items/kg	PA, PET	Liang et al., 2022
22	Dzhulukul, Russia	Water	5 items/L	ND	Malygina et al., 2021
23	Talmen, Russia	Water	8 items/L	ND	Malygina et al., 2021
24	Dimon, Italy	Snow	0.11 ± 0.19 items/L	PET	Pastorino et al., 2021
25	Sassolo, Switzerland	Water	2.6 items/L	PB, PE, PET, PMMA, PP, PS	Negrete et al, 2020

ND: not determined; PA: polyamide; PMMA: poly(methyl methacrylate); PE: polyethylene; PET: polyethylene terephthalate; PP: polypropylene; PS: polystyrene; PVC: polyvinyl chloride; CE: cellulose; PE: polyethylene; NY: nylon; HDPE: high-density polyethylene; LDPE: low-density polyethylene (LDPE); PB: poly (1-butene)

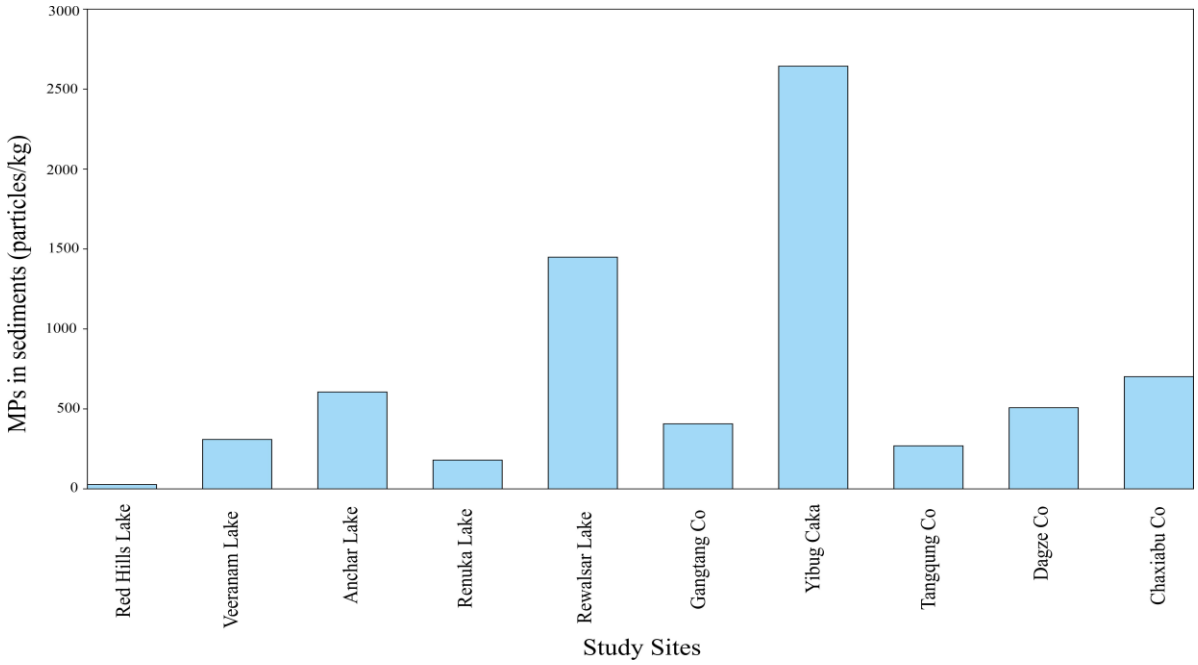

Fig. 4.8: Stacked bar chart showing microplastics abundance in the sediment media (particles/kg) measured in Indian and global mountain lake systems.

4.5. Conclusions

The concentration, spatial distribution and sources of MPs and associated pollutants were investigated in mid-altitude Rewalsar Lake in North-western Himalaya. Notably, the current investigation unravels primary combined data on distribution and concentration levels of MPs and PAEs. The results showed concentration of MPs in water is 13-238 particles L^{-1}, while concentration in sediments ranged from 750 to 3020 particles kg^{-1}. Moreover, majority MPs are present in the form of pellets and fragments in both the media. Further, the major polymer compositions detected in water and sediment samples were polypropylene, polyethylene, and polystyrene. The MPs data show widespread distribution in the whole basin with intensification at the margins thereby pointing to crucial role of anthropogenic sources located throughout. The comparison data from numerous lake systems mark that Rewalsar Lake is most impacted by microplastic pollution. The concentration of the three PAEs (Σ_3PAEs) in the sediment ranged from 1.69 µg/g to 4.03 µg/g dw. Further, DEHP in sediments exceeded the environmental risk levels thereby highlighting intensified accumulation of pollutants in the system. Overall, presence MPs along with phthalates in the ecosystem calls for implementation of the several management strategies for the conservation of aquatic ecosystems. Moreover, monitoring programs should be fostered in order to control the outspread of emerging pollutants and impact on biota.

Chapter 5

Conclusions

The aquatic environments including lakes and estuaries receive OM from terrigenous, aquatic and marine components as well as anthropogenic sources. However, among the numerous components human induced activities have majorly impacted the aquatic environment. Notably, OM source identification is important in order to better understand the global carbon budgets as well as develop the management programs. Therefore, this thesis focuses on two different aquatic systems including two tropical estuaries and one mid-altitude lake located at different geographical locations and considers the utilization of *n*-alkane proxies as well as investigation of organic compounds (e.g., hopanes, steranes, phthalates) in order to delineate the impact of natural and anthropogenic stressors governing the environment.

The surface sediments from the Mandovi estuary located in Goa were investigated in order to identify the OM sources and examine the depositional processes in the system. The TOC% and $\delta^{13}C_{org}$ were studied so as to understand the productivity changes while grain size parameter and $\delta^{18}O$ were assessed to determine the depositional processes and circulation dynamics respectively. The comprehensive information about OM composition in the estuarine ecosystem was achieved through molecular indices based on *n*-alkanes. The indices such as TAR and P_{aq} were used to know about the presence of terrestrial plants and aquatic productivity changes in the system. Moreover, the anthropogenic loading was delineated using proxies such as CPI, ACL and NAR along with ratios of Pr/Ph. Further, the spatial plots of multiple proxies were studied in order to understand the abundance of OM in the upper and lower reaches of the estuary. The traces of oil pollution were confirmed with the presence of UCM and a diagnostic compound such as hopane. The data suggest the lower reaches of the estuary are highly influenced by the petroleum contamination. Moreover, the LULC results suggest rise in the built-up area as well as increase in urbanization along with tourist influx that has resulted in accumulation of organic pollutants in the estuary.

Additionally, the other petroleum compounds such as sterane and diasterane were also examined from the Mandovi estuary. Likewise, similar set of petroleum hydrocarbons were also investigated from surface sediments collected from the Ramsar site i.e., Ashtamudi estuary located in Kerala. The concentration levels of compounds were compared between both the estuaries and sources responsible for the oil pollution were also assessed. The UCM profiles

along with distribution of petroleum hydrocarbons highlight dominance of petroleum markers in the middle and lower ends of both the estuaries. Oil pollutants in the Ramsar site are majorly derived from oil seepage and fishing activities while in the Mandovi estuary the contamination can be attributed to boating, tourism and mining activities. Along with hydrocarbon contaminants, presence of plastic derived chemicals such as phthalates were also observed in both the systems, and the concentration levels were abundant in the upper and middle zones of both the estuarine ecosystems. Out of all the phthalates, DIBP and DBP were found to be dominant compounds in Mandovi estuary while DBP and DINP were abundant in the Ashtamudi estuary. The dominance of PAEs in both the systems can be ascribed to land-based waste including domestic and industrial waste. Notably, the presence of petroleum hydrocarbons was detected to be higher in the Mandovi estuary as compared to the Ashtamudi estuary. Further, phthalate compounds were highly concentrated in the Ramsar site thereby, indicating intensified plastic pollution.

Further, to investigate the level of plastic contamination in an aquatic system other than estuaries, the presence of microplastics was examined in shallow mid-altitude freshwater environment i.e., Rewalsar lake. The concentration of MPs was detected from both the media including sediments and water, and the MPs levels were higher in the sediments as compared to water. Also, the majority of polymers occurred as polystyrene, polyethylene and polypropylene and the dominant shape types were pellets and fragments. Moreover, the MPs were higher in the proximity of anthropogenic sites. Along with MPs, three phthalate compounds involving DIBP, DBP and isomer, DEHP were also identified from the study site and among the detected compounds, DEHP was abundant. Further, the environment risk assessment based on phthalates was also calculated and the DEHP values exceeded the risk limit, thereby suggesting controlling human intervention. Further, the comparison data retrieved from Indian and global mountain lake systems highlight that Rewalsar lake is highly impacted by microplastic pollution. Overall, the results in the thesis point towards the fact that rise in urbanization and industrialization is negatively impacting the aquatic ecosystems as well as the biota of the system.

Collectively, my work discussed that the lacustrine and estuarine environments in the Indian subcontinent have been substantially impacted by natural and anthropogenic drivers. The various ecological indicators recorded in the study will help to assess the past variations in OM sources along with deducing past climate and ecological conditions. Moreover, the high human induced activities leading to ecotoxicological effects will urge an immediate adoption

of management strategies. In particular, the dataset from various study sites will serve as baseline for policymakers and environmentalists that will further help to prepare framework for future investigations. Also, the accumulation, distribution and risk assessment of numerous organic contaminants will be crucial for future research performed in different geographic locations.

List of Figures

Chapter 1

Chapter 2

Chapter 3

Chapter 4

List of Tables

Chapter 1

None

Chapter 2

Note: TAR= ($C_{27}+C_{29}+C_{31}$) /($C_{15}+C_{17}+C_{19}$) (Bourbonniere and Meyers, 1996), Paq. = ($C_{23}+C_{25}$) / ($C_{23}+C_{25}+C_{29}+C_{31}$) (Ficken et al., 2000), CPI = [($C_{25}+C_{27}+C_{29}+C_{31}+C_{33}$) / ($C_{24}+C_{26}+C_{28}+C_{30}+C_{32}$) + ($C_{25}+C_{27}+C_{29}+C_{31}+C_{33}$)/($C_{26}+C_{28}+C_{30}+C_{32}+C_{34}$)] / 2 (Bray and Evans, 1961), ACL = ($23 \times C_{23}+25\times C_{25}+27\times C_{27}+29\times C_{29}+31\times C_{31}$) / ($C_{23}+C_{25}+C_{27}+C_{29}+C_{31}$) (Poynter et al., 1989), NAR = [Σ *n*-alk(C_{19-32})-2Σ even *n*-alk(C_{20-32})] / Σ *n*-alk(C_{19-32}) (Mille et al., 2007)

Chapter 3

Note: CPI = [($C_{25}+C_{27}+C_{29}+C_{31}+C_{33}$) / ($C_{24}+C_{26}+C_{28}+C_{30}+C_{32}$) + ($C_{25}+C_{27}+C_{29}+C_{31}+C_{33}$)/($C_{26}+C_{28}+C_{30}+C_{32}+C_{34}$)] / 2 (Bray and Evans, 1961)

Chapter 4

Bibliography

Abrahim, G.M.S., Parker, R.J., Nichol, S.L., 2007. Distribution and assessment of sediment toxicity in Tamaki Estuary, Auckland, New Zealand. Environmental Geology 52(7), 1315-1323.

Adeniji, A.O., Okoh, O.O., Okoh, A.I., 2017. Petroleum hydrocarbon fingerprints of water and sediment samples of Buffalo River Estuary in the Eastern Cape Province, South Africa. Journal of analytical methods in chemistry 2017.

Aeppli, C., Nelson, R.K., Radovic, J.R., Carmichael, C.A., Valentine, D.L., Reddy, C.M., 2014. Recalcitrance and degradation of petroleum biomarkers upon abiotic and biotic natural weathering of Deepwater Horizon oil. Environmental science & technology 48(12), 6726-6734.

Ahad, J.M., Ganeshram, R.S., Bryant, C.L., Cisneros-Dozal, L.M., Ascough, P.L., Fallick, A.E., Slater, G.F., 2011. Sources of n-alkanes in an urbanized estuary: Insights from molecular distributions and compound-specific stable and radiocarbon isotopes. Marine Chemistry 126(1-4), 239-249.

Ajay, K., Behera, D., Bhattacharya, S., Mishra, P.K., Ankit, Y., Anoop, A., 2021. Distribution and characteristics of microplastics and phthalate esters from a fresh water lake system in Lesser Himalayas. Chemosphere 283, 131132.

Alagarsamy, R., 2006. Distribution and seasonal variation of trace metals in surface sediments of the Mandovi estuary, west coast of India. Estuarine, Coastal and Shelf Science 67(1-2), 333-339.

Allen, G.P., 1971. Relationship between grain size parameter distribution and current patterns in the Gironde estuary (France). Journal of Sedimentary Research 41(1), 74-88.

Andrady, A.L., 2015. Persistence of plastic litter in the oceans. In Marine anthropogenic litter. Springer, Cham. 57-72.

Ankit, Y., Mishra, P.K., Kumar, P., Jha, D.K., Kumar, V.V., Ambili, V., Anoop, A., 2017. Molecular distribution and carbon isotope of n-alkanes from Ashtamudi Estuary, South

India: Assessment of organic matter sources and paleoclimatic implications. Marine Chemistry 196, 62-70.

Anooja, S., Padmalal, D., Maya, K., Mohan, S.V., Baburaj, B., 2013. Heavy mineral contents and provenance of Late Quaternary sediments of southern Kerala, Southwest India. Indian Journal of Geo-Marine Sciences 42(6), 749-757.

Antony, M.M. and Ignatius, J., 2016. A hydrological study of Ashtamudi Lake, Kerala, India with special reference to its ecological difference. International Journal of Science and Research 5(8), 1841-1846.

Artifon, V., Zanardi-Lamardo, E., Fillmann, G., 2019. Aquatic organic matter: Classification and interaction with organic microcontaminants. Science of the Total Environment 649, 1620-1635.

Atugoda, T., Vithanage, M., Wijesekara, H., Bolan, N., Sarmah, A.K., Bank, M.S., You, S., Ok, Y.S., 2021. Interactions between microplastics, pharmaceuticals and personal care products: implications for vector transport. Environment International 149, 106367.

Avio, C.G., Gorbi, S., Regoli, F., 2017. Plastics and microplastics in the oceans: from emerging pollutants to emerged threat. Marine environmental research 128, 2-11.

Babu, K.N., Omana, P.K., Mohan, M., 2010. Water and sediment quality of Ashtamudi estuary, a Ramsar site, southwest coast of India—a statistical appraisal. Environmental monitoring and assessment 165(1), 307-319.

Baldwin, A.K., Corsi, S.R., Mason, S.A., 2016. Plastic debris in 29 Great Lakes tributaries: relations to watershed attributes and hydrology. Environmental science & technology 50(19), 10377-10385.

Barse, A.V., Chakrabarti, T., Ghosh, T.K., Pal, A.K., Jadhao, S.B., 2007. Endocrine disruption and metabolic changes following exposure of Cyprinus carpio to diethyl phthalate. Pesticide biochemistry and physiology 88(1), 36-42.

Bhattacharya, S., Ankit, Y., Murthy, S., Kushwaha, V., 2021. Biotic response to environmental shift during the Permian-Triassic transition: Assessment from organic geochemical proxies and palynomorphs in terrestrial sediments from Raniganj Sub-basin, India. Palaeogeography, Palaeoclimatology, Palaeoecology 110483.

Behera, D., Bhattacharya, S., Rahman, A., Kumar, S., Anoop, A., 2022. Molecular tracers for characterization and distribution of organic matter in a freshwater lake system from the Lesser Himalaya. Biogeochemistry 1-20.

Bernard, L., Décaudin, B., Lecoeur, M., Richard, D., Bourdeaux, D., Cueff, R., Sautou, V., Armed Study Group, 2014. Analytical methods for the determination of DEHP plasticizer alternatives present in medical devices: a review. Talanta 129, 39-54.

Bertolet, B.L., West, W.E., Armitage, D.W., Jones, S.E., 2019. Organic matter supply and bacterial community composition predict methanogenesis rates in temperate lake sediments. Limnology and Oceanography Letters 4(5), 164-172.

Bianchi, T. S., M. A. Allison, M.A., 2009. Large-river delta-front estuaries as natural "recorders" of global environmental change, Proc. Natl. Acad. Sci. U.S.A. 106, 8085–8092.

Biedermann-Brem, S., Biedermann, M., Pfenninger, S., Bauer, M., Altkofer, W., Rieger, K., Hauri, U., Droz, C., Grob, K., 2008. Plasticizers in PVC toys and childcare products: What succeeds the phthalates? Market survey 2007. Chromatographia 68(3), 227-234.

Bieger, T., Hellou, J., Abrajano Jr, T.A., 1996. Petroleum biomarkers as tracers of lubricating oil contamination. Marine Pollution Bulletin 32(3), 270-274.

Blumer, M., Mullin, M.M., Thomas, D.W., 1963. Pristane in zooplankton. Science 140(3570), 974.

Bost, F.D., Frontera-Suau, R., McDonald, T.J., Peters, K.E., Morris, P.J., 2001. Aerobic biodegradation of hopanes and norhopanes in Venezuelan crude oils. Organic Geochemistry 32(1), 105-114.

Bouloubassi, I., Fillaux, J., Saliot, A., 2001. Hydrocarbons in surface sediments from the Changjiang (Yangtze river) estuary, East China Sea. Marine Pollution Bulletin 42(12), 1335-1346.

Bouloubassi, I., Saliot, A., 1993. Investigation of anthropogenic and natural organic inputs. Oceanologica acta 16(2), 2-145.

Bourbonniere, R.A., Meyers, P.A., 1996. Sedimentary geolipid records of historical changes in the watersheds and productivities of Lakes Ontario and Erie.Limnology and Oceanography 41(2), 352-359.

Borch, J., Axelstad, M., Vinggaard, A.M., Dalgaard, M., 2006. Diisobutyl phthalate has comparable anti-androgenic effects to di-n-butyl phthalate in fetal rat testis. Toxicology letters 163(3), 183-190.

Brassell, S.C., Eglinton, G., 1980. Environmental chemistry —An interdisciplinary subject. Natural and pollutant organic compounds in contemporary aquatic environments. In: Albaiges, J. (Ed.), Analytical Techniques in Environmental Chemistry. Pergamon Press, Oxford.1–22.

Bray, E.E., Evans, E.D., 1961. Distribution of *n*-paraffins as a clue to recognition of source beds. Geochimica et Cosmochimica Acta 22(1), 2-15.

Bruno, D.O., Riccialdelli, L., Acha, E.M., Fernández, D.A., 2023. Seasonal variation of autochthonous and allochthonous carbon sources for the first levels of the Beagle Channel system's food web. Journal of Marine Systems, 103859.

Bukhari, S. S., Nayak, G. N. 1996. Clay minerals in identification of provenance of sediments of Mandovi estuary, Goa, west coast of India. Indian Journal of Marine Sciences 25**,** 341–345.

Bulbul, M., Ankit, Y., Basu, S., Anoop, A., 2021. Characterization of sedimentary organic matter and depositional processes in the Mandovi estuary, western India: An integrated lipid biomarker, sedimentological and stable isotope approach. Applied Geochemistry 131, 105041.

Bulbul, M., Bhattacharya, S., Ankit, Y., Yadav, P., Anoop, A., 2022. Occurrence, distribution and sources of phthalates and petroleum hydrocarbons in tropical estuarine sediments (Mandovi and Ashtamudi) of western Peninsular India. Environmental Research 214, 113679.

Campanale, C., Stock, F., Massarelli, C., Kochleus, C., Bagnuolo, G., Reifferscheid, G., Uricchio, V.F., 2020. Microplastics and their possible sources: The example of Ofanto river in southeast Italy. Environmental Pollution 258, 113284.

Chen, H., Chen, K., Qiu, X., Xu, H., Mao, G., Zhao, T., Feng, W., Okeke, E.S., Wu, X., Yang, L., 2020. The reproductive toxicity and potential mechanisms of combined exposure to dibutyl phthalate and diisobutyl phthalate in male zebrafish (Danio rerio). Chemosphere 258, 127238.

Chen, H., Wang, C., Wang, X., Hao, N., Liu, J., 2005. Determination of phthalate esters in cosmetics by gas chromatography with flame ionization detection and mass spectrometric detection. International journal of cosmetic science 27(4), 205-210.

Cheung, P.K., Fok, L., 2017. Characterisation of plastic microbeads in facial scrubs and their estimated emissions in Mainland China. Water research 122, 53-61.

Chinnadurai, S., Campos, C.J., Geethalakshmi, V., Sharma, J., Kripa, V., Mohamed, K.S., 2020. Microbiological quality of shellfish harvesting areas in the Ashtamudi and Vembanad estuaries (India): Environmental influences and compliance with international standards. Marine Pollution Bulletin 156, 111255.

Clara, M., Windhofer, G., Hartl, W., Braun, K., Simon, M., Gans, O., Scheffknecht, C., Chovanec, A., 2010. Occurrence of phthalates in surface runoff, untreated and treated wastewater and fate during wastewater treatment. Chemosphere 78(9), 1078-1084.

Cole, M., Lindeque, P., Fileman, E., Halsband, C., Goodhead, R., Moger, J., Galloway, T.S., 2013. Microplastic ingestion by zooplankton. Environmental science & technology 47(12), 6646-6655.

Cole, M., Lindeque, P., Halsband, C., Galloway, T.S., 2011. Microplastics as contaminants in the marine environment: a review. Marine pollution bulletin 62(12), 2588-2597.

Cózar, A., Echevarría, F., González-Gordillo, J.I., Irigoien, X., Úbeda, B., Hernández-León, S., Palma, Á.T., Navarro, S., García-de-Lomas, J., Ruiz, A., Fernández-de-Puelles, M.L., 2014. Plastic debris in the open ocean. Proceedings of the National Academy of Sciences 111(28), 10239-10244.

Crump, B.C., Kling, G.W., Bahr, M., Hobbie, J.E., 2003. Bacterioplankton community shifts in an arctic lake correlate with seasonal changes in organic matter source. Applied and Environmental Microbiology 69(4), 2253-2268.Dąbrowska, A., 2021. Raman Spectroscopy of Marine Microplastics-A short comprehensive compendium for the environmental scientists. Marine Environmental Research 168, 105313.

Dar, S.A., Bhat, S.U., Rashid, I., 2021. The status of current knowledge, distribution, and conservation challenges of wetland ecosystems in Kashmir Himalaya, India. Wetlands Conservation: Current Challenges and Future Strategies 175-200.

Das, B.K., Haake, B.G., 2003. Geochemistry of Rewalsar Lake sediment, Lesser Himalaya, India: implications for source-area weathering, provenance and tectonic setting. Geosciences Journal 7(4), 299-312.

Das, M.T., Kumar, S.S., Ghosh, P., Shah, G., Malyan, S.K., Bajar, S., Thakur, I.S., Singh, L., 2021. Remediation strategies for mitigation of phthalate pollution: Challenges and future perspectives. Journal of Hazardous Materials 409, 124496.

Deshpande, R.D., Muraleedharan, P.M., Singh, R.L., Kumar, B., Rao, M.S., Dave, M., Sivakumar, K.U., Gupta, S.K., 2013. Spatio-temporal distributions of δ18O, δD and salinity in the Arabian Sea: Identifying processes and controls. Marine Chemistry 157, 144-161.

Dessai, D.V., Nayak, G.N., Basavaiah, N., 2009. Grain size, geochemistry, magnetic susceptibility: proxies in identifying sources and factors controlling distribution of metals in a tropical estuary, India. Estuar Coast Shelf Sci. 85(2), 307–318.

Dehghani, S., Moore, F., Akhbarizadeh, R., 2017. Microplastic pollution in deposited urban dust, Tehran metropolis, Iran. Environmental Science and Pollution Research 24(25), 20360-20371.

Dey, T.K., Uddin, M.E., Jamal, M., 2021. Detection and removal of microplastics in wastewater: evolution and impact. Environmental Science and Pollution Research 28, 16925-16947.

Dhavamani, J., Beck, A.J., Gledhill, M., El-Shahawi, M.S., Kadi, M.W., Ismail, I.M., Achterberg, E.P., 2022. The effects of salinity, temperature, and UV irradiation on leaching and adsorption of phthalate esters from polyethylene in seawater. Science of The Total Environment 838, 155461.

Díaz-Mendoza, C., Mouthon-Bello, J., Pérez-Herrera, N.L., Escobar-Díaz, S.M., 2020. Plastics and microplastics, effects on marine coastal areas: a review. Environmental Science and Pollution Research 27(32), 39913-39922.

Eglinton, G., Hamilton, R.J., 1967. Leaf epicuticular waxes. Science 156(3780), 1322-1335.

Fernandes, L., Nayak, G.N., 2009. Distribution of sediment parameters and depositional environment of mudflats of Mandovi estuary, Goa, India. Journal of Coastal research 25(2 (252)), 273-284.

Ficken, K.J., Li, B., Swain, D.L., Eglinton, G., 2000. An n-alkane proxy for the sedimentary input of submerged/floating freshwater aquatic macrophytes. Organic geochemistry 31(7-8), 745-749.

Fine, P., Graber, E.R., Yaron, B., 1997. Soil interactions with petroleum hydrocarbons: abiotic processes. Soil Technology 10(2), 133-153.

Folk, R.L., Ward, W.C., 1957. Brazos River bar [Texas]; a study in the significance of grain size parameters. Journal of Sedimentary Research 27(1), 3-26.

Friedl, M.A., McIver, D.K., Hodges, J.C., Zhang, X.Y., Muchoney, D., Strahler, A.H., Woodcock, C.E., Gopal, S., Schneider, A., Cooper, A., Baccini, A., 2002. Global land cover mapping from MODIS: algorithms and early results. Remote sensing of Environment 83(1-2), 287-302.

Friedl, M.A., Sulla-Menashe, D., Tan, B., Schneider, A., Ramankutty, N., Sibley, A., Huang, X., 2010. MODIS Collection 5 global land cover: Algorithm refinements and characterization of new datasets. Remote sensing of Environment 114(1), 168-182.

Fry, B., Sherr, E.B., 1989. $\delta^{13}C$ measurements as indicators of carbon flow in marine and freshwater ecosystems. In Stable isotopes in ecological research. Springer, New York, NY. 196-229.

Frias, J.P.G.L., Sobral, P., Ferreira, A.M., 2010. Organic pollutants in microplastics from two beaches of the Portuguese coast. Marine pollution bulletin 60(11), 1988-1992.

Gao, H.T., Shi, H.Y., Dai, Q.M., Li, A.Q., Yang, L., Sun, Y., Jin, S.Y., Xia, L.Z., 2019. Glycerin monostearate aggravates male reproductive toxicity caused by di (2-ethylhexyl) phthalate in rats. Current medical science 39(6), 1003-1008.

Gao, X., Chen, S., 2008. Petroleum pollution in surface sediments of Daya Bay, South China, revealed by chemical fingerprinting of aliphatic and alicyclic hydrocarbons. Estuarine, Coastal and Shelf Science 80(1), 95-102.

Gao, X., Chen, S., Xie, X., Long, A., Ma, F., 2007. Non-aromatic hydrocarbons in surface sediments near the Pearl River estuary in the South China Sea. Environmental Pollution 148(1), 40-47.

Garcia-Garin, O., Sahyoun, W., Net, S., Vighi, M., Aguilar, A., Ouddane, B., Víkingsson, G.A., Chosson, V., Borrell, A., 2022. Intrapopulation and temporal differences of phthalate

concentrations in North Atlantic fin whales (Balaenoptera physalus). Chemosphere 300, 134453.

Gaury, P.K., Meena, N.K., Mahajan, A.K., 2018. Hydrochemistry and water quality of Rewalsar Lake of Lesser Himalaya, Himachal Pradesh, India. Environmental monitoring and assessment 190(2), 1-22.

Geyer, W.R., MacCready, P., 2014. The estuarine circulation. Annual review of fluid mechanics 46, 175-197.

Ghosh, K., 2021. A framework to assess the benefits and challenges of ecosystem services of a reservoir-based wetland in the Himalayan foothills. Environmental Development 40, 100669.

Ghosh, P., Chakrabarti, R., Bhattacharya, S.K., 2013. Short-and long-term temporal variations in salinity and the oxygen, carbon and hydrogen isotopic compositions of the Hooghly Estuary water, India. Chemical Geology 335, 118-127.

Gilde, K., Pinckney, J.L., 2012. Sublethal effects of crude oil on the community structure of estuarine phytoplankton. Estuaries and Coasts 35(3), 853-861.

Gireeshkumar, T.R., Deepulal, P.M., Chandramohanakumar, N., 2015. Distribution and sources of aliphatic hydrocarbons and fatty acids in surface sediments of a tropical estuary south west coast of India (Cochin estuary). Environmental monitoring and assessment 187(3), 1-17.

Gnanamoorthy, P., Selvam, V., Burman, P.K.D., Chakraborty, S., Karipot, A., Nagarajan, R., Ramasubramanian, R., Song, Q., Zhang, Y., Grace, J., 2020. Seasonal variations of net ecosystem (CO2) exchange in the Indian tropical mangrove forest of Pichavaram. Estuarine, Coastal and Shelf Science 243, 106828.

Gogou, A., Bouloubassi, I., Stephanou, E.G., 2000. Marine organic geochemistry of the Eastern Mediterranean: 1. Aliphatic and polyaromatic hydrocarbons in Cretan Sea surficial sediments. Marine Chemistry 68(4), 265-282.

Gopinath, K., Seshachalam, S., Neelavannan, K., Anburaj, V., Rachel, M., Ravi, S., Bharath, M., Achyuthan, H., 2020. Quantification of microplastic in red hills lake of Chennai city, Tamil Nadu, India. Environmental Science and Pollution Research 27(26), 33297-33306.

Green, D.S., 2020. Biological and ecological impacts of plastic debris in aquatic ecosystems. In Plastics in the Aquatic Environment-Part I. Springer, Cham. 111-133.

Guerrero-Bosagna, C., Skinner, M.K., 2014. Environmentally induced epigenetic transgenerational inheritance of male infertility. Current opinion in genetics & development 26, 79-88.

Gupta, P., Saha, M., Rathore, C., Suneel, V., Ray, D., Naik, A., Unnikrishnan, K., Dhivya, M., Daga, K., 2021. Spatial and seasonal variation of microplastics and possible sources in the estuarine system from central west coast of India. Environmental Pollution 288, 117665.

Hahladakis, J.N., Velis, C.A., Weber, R., Iacovidou, E., Purnell, P., 2018. An overview of chemical additives present in plastics: Migration, release, fate and environmental impact during their use, disposal and recycling. Journal of hazardous materials 344, 179-199.

Hammer, Ø., Harper, D.A. and Ryan, P.D., 2001. PAST: Paleontological statistics software package for education and data analysis. Palaeontologia electronica 4(1), 9.

Han, D., Cheng, J., Hu, X., Jiang, Z., Mo, L., Xu, H., Ma, Y., Chen, X., Wang, H., 2017. Spatial distribution, risk assessment and source identification of heavy metals in sediments of the Yangtze River Estuary, China. Marine Pollution Bulletin 115(1-2), 141-148.

Harji, R.R., Yvenat, A., Bhosle, N.B., 2008. Sources of hydrocarbons in sediments of the Mandovi estuary and the Marmugoa harbour, west coast of India. Environment International 34(7), 959-965.

Harris, C.A., Henttu, P., Parker, M.G., Sumpter, J.P., 1997. The estrogenic activity of phthalate esters in vitro. Environmental health perspectives 105(8), 802-811.

Hemminga, M.A., Mateo, M.A., 1996. Stable carbon isotopes in seagrasses: variability in ratios and use in ecological studies. Marine Ecology Progress Series 140, 285-298.

Heudorf, U., Mersch-Sundermann, V., Angerer, J., 2007. Phthalates: toxicology and exposure. International journal of hygiene and environmental health 210(5), 623-634.

Hitchcock, J.N., 2020. Storm events as key moments of microplastic contamination in aquatic ecosystems. Science of The Total Environment 734, 139436.

Ho, E.S., Meyers, P.A., 1994. Variability of early diagenesis in lake sediments: evidence from the sedimentary geolipid record in an isolated tarn. Chemical Geology 112(3-4), 309-324.

Hong, E.J., Ji, Y.K., Choi, K.C., Manabe, N., Jeung, E.B., 2005. Conflict of estrogenic activity by various phthalates between in vitro and in vivo models related to the expression of Calbindin-D9k. Journal of Reproduction and Development 51(2), 253-263.

Hopewell, J., Dvorak, R., Kosior, E., 2009. Plastics recycling: challenges and opportunities. Philosophical Transactions of the Royal Society B: Biological Sciences 364(1526), 2115-2126.

Howarth, R., Chan, F., Conley, D.J., Garnier, J., Doney, S.C., Marino, R., Billen, G., 2011. Coupled biogeochemical cycles: eutrophication and hypoxia in temperate estuaries and coastal marine ecosystems. Frontiers in Ecology and the Environment 9(1), 18-26.

Hussain, S.M., Anbalagan, S., Kumar, K.S., Neelavannan, K., Pradhap, D., Radhakrishnan, K., Godson, P.S., Krishnakumar, S., 2020. A baseline study on elemental concentration and potential ecological risk status of the surface sediments of Ashtamudi Lake, south west coast of India. Marine Pollution Bulletin 158, 111410.

Hwang, R.J., Heidrick, T., Mertani, B., Qivayanti, Li, M., 2002. Correlation and migration studies of North Central Sumatra oils. Organic Geochemistry 33, 1361–1379.

Ines, Z., Amina, B., Mahmoud, R., Dalila, S.M., 2013. Aliphatic and aromatic biomarkers for petroleum hydrocarbon monitoring in Khniss Tunisian-Coast,(Mediterranean Sea). Procedia Environmental Sciences 18, 211-220.

Ito, R., Seshimo, F., Haishima, Y., Hasegawa, C., Isama, K., Yagami, T., Nakahashi, K., Yamazaki, H., Inoue, K., Yoshimura, Y., Saito, K., 2005. Reducing the migration of di-2-ethylhexyl phthalate from polyvinyl chloride medical devices. International journal of pharmaceutics 303(1-2), 104-112.

Ivleva, N.P., Wiesheu, A.C., Niessner, R., 2017. Microplastic in aquatic ecosystems. Angewandte Chemie International Edition 56(7), 1720-1739.

Jabeen, K., Su, L., Li, J., Yang, D., Tong, C., Mu, J., Shi, H., 2017. Microplastics and mesoplastics in fish from coastal and fresh waters of China. Environmental Pollution 221, 141-149.

Jagtap, T.G., 1991. Distribution of seagrasses along the Indian coast. Aquatic Botany 40(4), 379-386.

Jeng, W.L., 2006. Higher plant n-alkane average chain length as an indicator of petrogenic hydrocarbon contamination in marine sediments. Marine Chemistry 102(3-4), 242-251.

Jeng, W.L., Lin, S., Kao, S.J., 2003. Distribution of terrigenous lipids in marine sediments off northeastern Taiwan. Deep Sea Research Part II: Topical Studies in Oceanography 50(6-7), 1179-1201.

Jennerjahn, T.C., Soman, K., Ittekkot, V., Nordhaus, I., Sooraj, S., Priya, R.S., Lahajnar, N., 2008. Effect of land use on the biogeochemistry of dissolved nutrients and suspended and sedimentary organic matter in the tropical Kallada River and Ashtamudi estuary, Kerala, India. Biogeochemistry 90(1), 29-47.

Jensen, E.S. (1991) Evaluation of automated analysis of ^{15}N and total N in plant material and soil. Plant and Soil 133, 83-92.

Jindal, R., Thakur, R.K., Singh, U.B., Ahluwalia, A.S., 2014. Phytoplankton dynamics and species diversity in a shallow eutrophic, natural mid-altitude lake in Himachal Pradesh (India): role of physicochemical factors. Chemistry and Ecology 30(4), 328-338.

Jindal, R., Thakur, R.K., 2013. Diurnal variations of plankton diversity and physico-chemical characteristics of Rewalsar Wetland, Himachal Pradesh, India. Recent Research in Science and Technology 5(3).

Jolliffe, I.T., Cadima, J., 2016. Principal component analysis: a review and recent developments. Philosophical Transactions of the Royal Society A: Mathematical, Physical and Engineering Sciences 374(2065), 20150202.

Joshi, A.K., Joshi, P.K., 2019. Forest ecosystem services in the Central Himalaya: Local benefits and global relevance. Proceedings of the National Academy of Sciences, India Section B: Biological Sciences 89(3), 785-792.

Joy, N.M., Paul, S.K., 2021. Analysis of the Economic Value and Status of the Ecosystem Services Provided by the Ashtamudi Wetland Region, a Ramsar Site in Kerala. Journal of the Indian Society of Remote Sensing 49(4), 897-912.

Kaewlaoyoong, A., Vu, C.T., Lin, C., Liao, C.S., Chen, J.R., 2018. Occurrence of phthalate esters around the major plastic industrial area in southern Taiwan. Environmental Earth Sciences *77*(12), 1-11.

Karthik, R., R. S. Robin, R. Purvaja, D. Ganguly, I. Anandavelu, R. Raghuraman, G. Hariharan, A. Ramakrishna, R., Ramesh, 2018. Microplastics along the beaches of southeast coast of India. Science of the Total Environment 645, 1388-1399.

Kashyap, R., Verma, K.S., Chand, H., 2015. Heavy metal contamination and their seasonal variations in Rewalsar Lake of Himachal Pradesh, India. Ecoscan 9(1&2), 31-36.

Kastner, J., Cooper, D.G., Marić, M., Dodd, P. and Yargeau, V., 2012. Aqueous leaching of di-2-ethylhexyl phthalate and "green" plasticizers from poly (vinyl chloride). Science of the total environment 432, 357-364.

Kennicutt II, M.C., Barker, C., Brooks, J.M., DeFreitas, D.A., Zhu, G.H., 1987b. Selected organic matter source indicators in the Orinoco, Nile and Changjiang deltas. Organic Geochemistry 11(1), 41-51.

Kennicutt II, M.C., Sericano, J.L., Wade, T.L., Alcazar, F., Brooks, J.M., 1987a. High molecular weight hydrocarbons in Gulf of Mexico continental slope sediments. Deep Sea Research Part A. Oceanographic Research Papers 34(3), 403-424.

Kennish, M.J., 2002. Environmental threats and environmental future of estuaries. Environmental conservation 29(1), 78-107.

Keshavarzifard, M., Zakaria, M.P., Sharifinia, M., Grathwohl, P., Keshavarzifard, S., Sharifi, R., Abbasi, S., Mehr, M.R., 2020. Determination of hydrocarbon sources in major rivers and estuaries of peninsular Malaysia using aliphatic hydrocarbons and hopanes as biomarkers. Environmental Forensics 1-14.

Kessarkar, P.M., Rao, V.P., Shynu, R., Ahmad, I.M., Mehra, P., Michael, G.S., Sundar, D., 2009. Wind-driven estuarine turbidity maxima in Mandovi Estuary, central west coast of India. Journal of Earth System Science 118(4), 369.

Kessarkar, P.M., Suja, S., Sudheesh, V., Srivastava, S., Rao, V.P., 2015. Iron ore pollution in Mandovi and Zuari estuarine sediments and its fate after mining ban. Environmental monitoring and assessment 187(9), 572.

Koniecki, D., Wang, R., Moody, R.P., Zhu, J., 2011. Phthalates in cosmetic and personal care products: concentrations and possible dermal exposure. Environmental research 111(3), 329-336.

Kowalski, N., Reichardt, A.M., Waniek, J.J., 2016. Sinking rates of microplastics and potential implications of their alteration by physical, biological, and chemical factors. Marine pollution bulletin 109(1), 310-319.

Kim, Y., Ha, E.H., Kim, E.J., Park, H., Ha, M., Kim, J.H., Hong, Y.C., Chang, N., Kim, B.N., 2011. Prenatal exposure to phthalates and infant development at 6 months: prospective Mothers and Children's Environmental Health (MOCEH) study. Environmental health perspectives 119(10), 1495-1500.

Kim, Y.K., 2017. The use of polyolefins in industrial and medical applications. In Polyolefin Fibres, Woodhead Publishing 135-155.

Kueseng, P., Thavarungkul, P., Kanatharana, P., 2007. Trace phthalate and adipate esters contaminated in packaged food. Journal of Environmental Science and Health, Part B 42(5), 569-576.

Kumar, A.B., Smrithy, R., Sathasivam, K., 2012. Dolphin-assisted cast net fishery in the Ashtamudi Estuary, south-west coast of India. Indian Journal of fisheries 59(3), 143-148.

Kumar, P., Mahajan, A.K., 2020. Trophic status and its regulating factor determination at the Rewalsar Lake, northwest Himalaya (HP), India, based on selected parameters and multivariate statistical analysis. SN Applied Sciences 2(7), 1-11.

Kumari, V.R., Rao, I.M., 2013. Hypoxia in Indian estuaries—Krishna and Godavari estuarine systems—A case study. In: Sundaresan, J., Sreekesh, S., Ramanathan, A.L., Sonnenschein, L, Boojh, R., (Eds.), Climate Change Impact on Ecosystem 110-132.

Kummu, M., De Moel, H., Salvucci, G., Viviroli, D., Ward, P.J., Varis, O., 2016. Over the hills and further away from coast: global geospatial patterns of human and environment over the 20th–21st centuries. Environmental Research Letters 11(3), 034010.

Kyrikou, I., Briassoulis, D., 2007. Biodegradation of agricultural plastic films: a critical review. Journal of Polymers and the Environment 15(2), 125-150.

Lambert, S., Scherer, C., Wagner, M., 2017. Ecotoxicity testing of microplastics: Considering the heterogeneity of physicochemical properties. Integrated environmental assessment and management 13(3), 470-475.

Le Dréau, Y., Jacquot, F., Doumenq, P., Guiliano, M., Bertrand, J.C., Mille, G., 1997. Hydrocarbon balance of a site which had been highly and chronically contaminated by

petroleum wastes of a refinery (from 1956 to 1992). Marine Pollution Bulletin 34(6), 456-468.

Letcher, T.M., 2020. Introduction to plastic waste and recycling. In Plastic Waste and Recycling, Academic Press 3-12.

Liao, W., Hu, J., Zhou, H., Hu, J. and Deng, W., 2018. Sources and distribution of sedimentary organic matter in the Beibu Gulf, China: Application of multiple proxies. Marine Chemistry 206, 74-83.

Liang, T., Lei, Z., Fuad, M.T.I., Wang, Q., Sun, S., Fang, J.K.H., Liu, X., 2022. Distribution and potential sources of microplastics in sediments in remote lakes of Tibet, China. Science of the Total Environment 806, 150526.

Li, D., Xu, Y., Li, Y., Wang, J., Yin, X., Ye, X., Wang, A., Wang, L., 2018. Sedimentary records of human activity and natural environmental evolution in sensitive ecosystems: A case study of a coral nature reserve in Dongshan Bay and a mangrove forest nature reserve in Zhangjiang River estuary, Southeast China. Organic Geochemistry 121, 22-35.

Lin, J., Yan, D., Fu, J., Chen, Y., Ou, H., 2020. Ultraviolet-C and vacuum ultraviolet inducing surface degradation of microplastics. Water Research 186, 116360.

Lin, V.S., 2016. Research highlights: impacts of microplastics on plankton. Environmental Science: Processes & Impacts 18(2), 160-163.

Li, Q., Zeng, A., Jiang, X., Gu, X., 2021. Are microplastics correlated to phthalates in facility agriculture soil? Journal of Hazardous Materials 412, 125164.

Li, R., Liang, J., Gong, Z., Zhang, N., Duan, H., 2017. Occurrence, spatial distribution, historical trend and ecological risk of phthalate esters in the Jiulong River, Southeast China. Science of the Total Environment 580, 388-397.

Li, X., Yin, P., Zhao, L., 2016. Phthalate esters in water and surface sediments of the Pearl River Estuary: distribution, ecological, and human health risks. Environmental Science and Pollution Research 23(19), 19341-19349.

Liu, H., Cui, K., Zeng, F., Chen, L., Cheng, Y., Li, H., Li, S., Zhou, X., Zhu, F., Ouyang, G., Luan, T., 2014. Occurrence and distribution of phthalate esters in riverine sediments from the Pearl River Delta region, South China. Marine pollution bulletin 83(1), 358-365.

Liu, L., Bao, H., Liu, F., Zhang, J., Shen, H., 2012. Phthalates exposure of Chinese reproductive age couples and its effect on male semen quality, a primary study. Environment international 42, 78-83.

Liu, Y., Chen, Z., Shen, J., 2013. Occurrence and removal characteristics of phthalate esters from typical water sources in Northeast China. Journal of Analytical Methods in Chemistry 2013.

Lodi, F., Zare, A., Arora, P., Stevanovic, S., Ristovski, Z.D., Brown, R.J. and Bodisco, T.A., 2022. Gaseous and particulate emissions analysis using microalgae based dioctyl phthalate biofuel during cold, warm and hot engine operation. Fuel 312, 122965.

Lottrup, G., Andersson, A.M., Leffers, H., Mortensen, G.K., Toppari, J., Skakkebaek, N.E., Main, K.M., 2006. Possible impact of phthalates on infant reproductive health. International journal of andrology 29(1), 172-180.

Lubecki, L., Kowalewska, G., 2019. Plastic-derived contaminants in sediments from the coastal zone of the southern Baltic Sea. Marine pollution bulletin 146, 255-262.

Mackenzie, A.S., Lamb, N.A., Maxwell, J.R., 1982. Steroid hydrocarbons and the thermal history of sediments. Nature 295(5846), 223-226.

Mackenzie, A.S., McKenzie, D., 1983. Isomerization and aromatization of hydrocarbons in sedimentary basins formed by extension. Geological Magazine 120(5), 417-470.

Mackenzie, A.S., Patience, R.L., Maxwell, J.R., Vandenbroucke, M., Durand, B., 1980. Molecular parameters of maturation in the Toarcian shales, Paris Basin, France—I. Changes in the configurations of acyclic isoprenoid alkanes, steranes and triterpanes. Geochimica et Cosmochimica Acta 44(11), 1709-1721.

Madondkar, S.G.P., Gomes, H., Parab, S.G., Pednekar, S., Goes, J.I., 2007. Phytoplankton diversity, biomass, and production. In: Shetye S R, Kumar M D and Shankar D (Eds.), The Mandovi and Zuari Estuaries, 67–81.

Ma, H., Pu, S., Liu, S., Bai, Y., Mandal, S., Xing, B., 2020. Microplastics in aquatic environments: toxicity to trigger ecological consequences. Environmental Pollution 261, 114089.

Maioli, O.L., Rodrigues, K.C., Knoppers, B.A., Azevedo, D.A., 2011. Distribution and sources of aliphatic and polycyclic aromatic hydrocarbons in suspended particulate matter in

water from two Brazilian estuarine systems. Continental Shelf Research 31(10), 1116-1127.

Ma, J., Xiao, X., Miao, R., Li, Y., Chen, B., Zhang, Y., Zhao, B., 2019. Trends and controls of terrestrial gross primary productivity of China during 2000–2016. Environmental Research Letters 14(8), 084032.

Malone, T.C., Crocker, L.H., Pike, S.E., Wendler, B.W., 1988. Influences of river flow on the dynamics of phytoplankton production in a partially stratified estuary. Marine ecology progress series. Oldendorf 48, 235–49.

Malygina, N., Mitrofanova, E., Kuryatnikova, N., Biryukov, R., Zolotov, D., Pershin, D., Chernykh, D., 2021. Microplastic pollution in the surface waters from plain and mountainous lakes in Siberia, Russia. Water 13(16), 2287.

Manikanda Bharath, K., Srinivasalu, S., Natesan, U., Ayyamperumal, R., Kalam, N., Anbalagan, S., Sujatha, K., Alagarasan, C., 2021. Microplastics as an emerging threat to the freshwater ecosystems of Veeranam lake in south India: a multidimensional approach. Chemosphere 264, 128502.

Mankidy, R., Wiseman, S., Ma, H., Giesy, J.P., 2013. Biological impact of phthalates. Toxicology letters 217(1), 50-58.

Maya, M.V., Soares, M.A., Agnihotri, R., Pratihary, A.K., Karapurkar, S., Naik, H., Naqvi, S.W.A., 2011. Variations in some environmental characteristics including C and N stable isotopic composition of suspended organic matter in the Mandovi estuary. Environmental Monitoring and Assessment 175(1), 501-517.

Mayer, L.M., 1994. Surface area control of organic carbon accumulation in the continental shelf sediments. Geochemica et Cosmochimica Acta 58(4), 12711284.

Medeiros, P.M., Bícego, M.C., 2004. Investigation of natural and anthropogenic hydrocarbon inputs in sediments using geochemical markers. I. Santos, SP—Brazil. Marine pollution bulletin 49(9-10), 761-769.

Meng, Y., Kelly, F.J., Wright, S.L., 2020. Advances and challenges of microplastic pollution in freshwater ecosystems: A UK perspective. Environmental Pollution 256, 113445.

Mille, G., Asia, L., Guiliano, M., Malleret, L., Doumenq, P., 2007. Hydrocarbons in coastal sediments from the Mediterranean Sea (Gulf of Fos area, France). Marine pollution bulletin 54(5), 566-575.

Miller, T.H., Ng, K.T., Lamphiere, A., Cameron, T.C., Bury, N.R., Barron, L.P., 2021. Multicompartment and cross-species monitoring of contaminants of emerging concern in an estuarine habitat. Environmental Pollution 270, 116300.

Mishra, P.K., Parth, S., Ankit, Y., Kumar, S., Ambili, V., Kumar, V.V., Singh, S., Anoop, A., 2019. Geochemical and sedimentological characteristics of surface sediments from Ashtamudi Estuary, Southern India: implications for provenance and modern sedimentary dynamics. Environmental Earth Sciences 78(14), 1-11.

Misra, S., Bhattacharya, S., Mishra, P.K., Misra, K.G., Agrawal, S., Anoop, A., 2020. Vegetational responses to monsoon variability during Late Holocene: Inferences based on carbon isotope and pollen record from the sedimentary sequence in Dzukou valley, NE India. Catena 194, 104697.

Mohammadi, A., Malakootian, M., Dobaradaran, S., Hashemi, M., Jaafarzadeh, N., 2022. Occurrence, seasonal distribution, and ecological risk assessment of microplastics and phthalate esters in leachates of a landfill site located near the marine environment: Bushehr port, Iran as a case. Science of The Total Environment 842, 156838.

Montoto-Martínez, T., De la Fuente, J., Puig-Lozano, R., Marques, N., Arbelo, M., Hernández-Brito, J.J., Fernández, A., Gelado-Caballero, M.D., 2021. Microplastics, bisphenols, phthalates and pesticides in odontocete species in the Macaronesian Region (Eastern North Atlantic). Marine Pollution Bulletin 173, 113105.

Mote, S., Kumar, R., Naik, B.G., Ingole, B.S., 2015. Polycyclic aromatic hydrocarbons (PAHs) and *n*-alkanes in beaked sea snake Enhydrina schistose (Daudin, 1803) from the Mandovi Estuary, Goa. Bulletin of environmental contamination and toxicology 94(2), 171-177.

Müller, B., Bryant, L.D., Matzinger, A., Wüest, A., 2012. Hypolimnetic oxygen depletion in eutrophic lakes. Environmental science & technology 46(18), 9964-9971.Nair, N.B., Azis, P.A., Dharmaraj, K., Arunachalam, M., Kumar, K.K., Balasubramanian, N.K., 1984a. Ecology of Indian estuaries—V: Primary productivity of the Ashtamudi estuary, south-west coast of India. Proceedings: Animal Sciences 93(1), 9-23.

Nair, N.B., Dharmaraj, K., Azis, P.A., Arunachalam, M., Krishnakumar, K., Balasubramanian, N.K., 1984b. Ecology of Indian estuaries: 8. Inorganic nutrients in the Ashtamudi Estuary. Mahasagar 17(1), 19-32.

Napper, I.E., Thompson, R.C., 2016. Release of synthetic microplastic plastic fibres from domestic washing machines: Effects of fabric type and washing conditions. Marine pollution bulletin 112(1-2), 39-45.

Napper, I.E., Thompson, R.C., 2020. Plastic debris in the marine environment: history and future challenges. Global Challenges 4(6), 1900081.

Neelavannan, K., Sen, I.S., Lone, A.M., Gopinath, K., 2022. Microplastics in the high-altitude Himalayas: Assessment of microplastic contamination in freshwater lake sediments, Northwest Himalaya (India). Chemosphere 290, 133354.

Negrete Velasco, A.D.J., Rard, L., Blois, W., Lebrun, D., Lebrun, F., Pothe, F., Stoll, S., 2020. Microplastic and fibre contamination in a remote mountain lake in Switzerland. Water 12(9) 2410.

Net, S., Delmont, A., Sempéré, R., Paluselli, A., Ouddane, B., 2015b. Reliable quantification of phthalates in environmental matrices (air, water, sludge, sediment and soil): a review. Science of the Total Environment 515, 162-180.

Net, S., Dumoulin, D., El-Osmani, R., Rabodonirina, S., Ouddane, B., 2014. Case study of PAHs, Me-PAHs, PCBs, phthalates and pesticides contamination in the Somme River water, France. International Journal of Environmental Research 8(4), 1159-1170.

Net, S., Sempere, R., Delmont, A., Paluselli, A., Ouddane, B., 2015a. Occurrence, fate, behavior and ecotoxicological state of phthalates in different environmental matrices. Environmental Science & Technology 49(7), 4019-4035.

Niu, L., Xu, Y., Xu, C., Yun, L., Liu, W., 2014. Status of phthalate esters contamination in agricultural soils across China and associated health risks. Environmental Pollution 195, 16-23.

Nogales, B., Lanfranconi, M.P., Piña-Villalonga, J.M., Bosch, R., 2011. Anthropogenic perturbations in marine microbial communities. FEMS Microbiology reviews 35(2), 275-298.

Nor, N.H.M., Obbard, J.P., 2014. Microplastics in Singapore's coastal mangrove ecosystems. Marine pollution bulletin 79(1-2), 278-283.

Oni, B.A., Ayeni, A.O., Agboola, O., Oguntade, T., Obanla, O., 2020. Comparing microplastics contaminants in (dry and raining) seasons for Ox-Bow Lake in Yenagoa, Nigeria. Ecotoxicology and environmental safety 198, 110656.

Ou, S., Zheng, J., Zheng, J., Richardson, B.J., Lam, P.K., 2004. Petroleum hydrocarbons and polycyclic aromatic hydrocarbons in the surficial sediments of Xiamen Harbour and Yuan Dan Lake, China. Chemosphere 56(2), 107-112

Paluselli, A., Fauvelle, V., Schmidt, N., Galgani, F., Net, S., Sempere, R., 2018. Distribution of phthalates in marseille bay (NW Mediterranean Sea). Science of the total environment 621, 578-587.

Pancost, R.D., Boot, C.S., 2004. The palaeoclimatic utility of terrestrial biomarkers in marine sediments. Marine Chemistry 92(1-4), 239-261.

Pannetier, P., Morin, B., Le Bihanic, F., Dubreil, L., Clérandeau, C., Chouvellon, F., Van Arkel, K., Danion, M., Cachot, J., 2020. Environmental samples of microplastics induce significant toxic effects in fish larvae. Environment international 134, 105047.

Parab, S.G., Matondkar, S.P., Gomes, H.D.R., Goes, J.I., 2013. Effect of freshwater influx on phytoplankton in the Mandovi estuary (Goa, India) during monsoon season: Chemotaxonomy. Journal of Water Resource and Protection 5, 349–361.

Pastorino, P., Pizzul, E., Bertoli, M., Anselmi, S., Kušće, M., Menconi, V., Prearo, M., Renzi, M., 2021. First insights into plastic and microplastic occurrence in biotic and abiotic compartments, and snow from a high-mountain lake (Carnic Alps). Chemosphere 265, 129121.

Pastorino, P., Prearo, M., Pizzul, E., Elia, A.C., Renzi, M., Ginebreda, A., Barceló, D., 2022. High-mountain lakes as indicators of microplastic pollution: current and future perspectives. Water Emerging Contaminants & Nanoplastics 1(1), 3.

Petersen, K., Hultman, M.T., Rowland, S.J., Tollefsen, K.E., 2017. Toxicity of organic compounds from unresolved complex mixtures (UCMs) to primary fish hepatocytes. Aquatic Toxicology 190, 150-161.

Peters, K.E., Moldowan, J.M., 1993. The biomarker guide: interpreting molecular fossils in petroleum and ancient sediments. Prentice Hall, Englewood Cliffs, NJ, USA.

Peters, K.E., Walters, C.C., Moldowan, J.M., 2005. The Biomarker Guide: Biomarkers and Isotopes in Petroleum Exploration and Earth History, vol. 2. Cambridge University Press, UK, 612-613.

PlasticsEurope, 2018. An Analysis of European plastics production, Demand and Waste Data. Plastics-the Facts 2018. https://www.plasticseurope.org/en/resources/market-data

PlasticsEurope, 2019. An Analysis of European plastics production, Demand and Waste Data. Plastics - the Facts 2019 https://www.plasticseurope.org/en/resources/market-data

Potdar, S.S., Kulkarni, S., Patil, P., Pawar, R.P., Jakhalekar, V.V., Nade, D.P., 2019. The long-term trend analysis of rainfall data from 1901 to 2015 for Maharashtra and Goa region from India. International Journal of Water 13(3), 293-309.

Poynter, J., Eglinton, G., 1990. 14. Molecular composition of three sediments from hole 717c: The Bengal fan. In Proceedings of the Ocean Drilling Program: Scientific results 116, 155-161.

Poynter, J.G., Farrimond, P., Robinson, N., Eglinton, G., 1989. Aeolian-derived higher plant lipids in the marine sedimentary record: links with palaeoclimate. In: Paleoclimatology and Paleometeorology: Modern and Past Patterns of Global Atmospheric Transport, Springer, Netherlands, 435–462.

Pradhan, U.K., Wu, Y., Shirodkar, P.V., Zhang, J., Zhang, G., 2014. Sources and distribution of organic matter in thirty five tropical estuaries along the west coast of India-a preliminary assessment. Estuarine, Coastal and Shelf Science 151, 21-33.

Prajith, A., Rao, V.P., Chakraborty, P., 2016. Distribution, provenance and early diagenesis of major and trace metals in sediment cores from the Mandovi estuary, western India. Estuarine, Coastal and Shelf Science 170, 173-185.

Prajith, A., Rao, V.P., Chakraborty, P., 2016. Distribution, provenance and early diagenesis of major and trace metals in sediment cores from the Mandovi estuary, western India. Estuarine, Coastal and Shelf Science 170, 173-185.

Premke, K., Wurzbacher, C., Felsmann, K., Fabian, J., Taube, R., Bodmer, P., Attermeyer, K., Nitzsche, K.N., Schroer, S., Koschorreck, M., Hübner, E., 2022. Large-scale sampling of the freshwater microbiome suggests pollution-driven ecosystem changes. Environmental Pollution 308, 119627.

Przybylinska, P.A., Wyszkowski, M., 2016. Environmental contamination with phthalates and its impact on living organisms. Ecological Chemistry and Engineering 23(2), 347.

Qasim, S.Z., Gupta, R.S., 1981. Environmental characteristics of the Mandovi-Zuari estuarine system in Goa. Estuarine, Coastal and Shelf Science 13(5), 557-578.

Raghavan, T.M., Furtado, I., 2000. Tolerance of an estuarine halophilic archaebacterium to crude oil and constituent hydrocarbons. Bulletin of environmental contamination and toxicology 65(6), 725-731

Raghunathan, M.B., 2007. Faunal Diversity of Ashtatnudi Wetlands, Kerala, India. Rec. zool. Surv. India, Occ. Paper No, 276, 1-38.

Ram, A., Jaiswar, J.R.M., Rokade, M.A., Bharti, S., Vishwasrao, C., Majithiya, D., 2014. Nutrients, hypoxia and mass fishkill events in Tapi Estuary, India. Estuarine, Coastal and Shelf Science148, 48-58.

Ramzi, A., Gireeshkumar, T.R., Rahman, K.H., Manu, M., Balachandran, K.K., Chacko, J., Chandramohanakumar, N., 2018. Distribution and contamination status of phthalic acid esters in the sediments of a tropical monsoonal estuary, Cochin–India. Chemosphere 210, 232-238.

Ramirez, M.M.B., Caamal, R.D., von Osten, J.R., 2019. Occurrence and seasonal distribution of microplastics and phthalates in sediments from the urban channel of the Ria and coast of Campeche, Mexico. Science of the Total Environment 672, 97-105.

Renjan, S., Rao, V.P., Kessarkar, P.M., 2017. Major and trace metals in suspended and bottom sediments of the Mandovi and Zuari estuaries, western India: distribution, source, and pollution. Environmental Science and Pollution Research 24(35), 27409-27429.

Reshmi, R.R., Nair, K.D., Zachariah, E.J., Vincent, S.G.T., 2015. Methanogenesis: Seasonal changes in human impacted regions of Ashtamudi estuary (Kerala, South India). Estuarine, Coastal and Shelf Science 156, 144-154

Rhind, S., 2009. Anthropogenic pollutants: a threat to ecosystem sustainability?. Philosophical Transactions of the Royal Society B: Biological Sciences 364(1534), 3391-3401.

Ridgway, J., Shimmield, G., 2002. Estuaries as repositories of historical contamination and their impact on shelf seas. Estuarine, Coastal and Shelf Science 55(6), 903-928.

Rodrigues, M.O., Gonçalves, A.M.M., Gonçalves, F.J.M., Nogueira, H., Marques, J.C., Abrantes, N., 2018. Effectiveness of a methodology of microplastics isolation for environmental monitoring in freshwater systems. Ecological Indicators 89, 488-495.

Rogge, W.F., Hildemann, L.M., Mazurek, M.A., Cass, G.R., Simoneit, B.R., 1993. Sources of fine organic aerosol. 3. Road dust, tire debris, and organometallic brake lining dust: roads as sources and sinks. Environmental Science & Technology, 27(9), 1892-1904.

Royer, S.J., Ferrón, S., Wilson, S.T., Karl, D.M., 2018. Production of methane and ethylene from plastic in the environment. PloS one 13(8), e0200574.

Saha, M., Naik, A., Desai, A., Nanajkar, M., Rathore, C., Kumar, M., Gupta, P., 2021. Microplastics in seafood as an emerging threat to marine environment: A case study in Goa, west coast of India. Chemosphere 270, 129359.

Saha, M., Togo, A., Mizukawa, K., Murakami, M., Takada, H., Zakaria, M.P., Chiem, N.H., Tuyen, B.C., Prudente, M., Boonyatumanond, R., Sarkar, S.K., 2009. Sources of sedimentary PAHs in tropical Asian waters: differentiation between pyrogenic and petrogenic sources by alkyl homolog abundance. Marine pollution bulletin 58(2), 189-200.

Saliu, F., Lasagni, M., Andò, S., Ferrero, L., Pellegrini, C., Calafat, A., Sanchez-Vidal, A., 2022. A baseline assessment of the relationship between microplastics and plasticizers in sediment samples collected from the Barcelona continental shelf. Environmental Science and Pollution Research 1-14.

Samant, S., Naik, M., Parulekar, K., Charya, L., Vaigankar, D., 2018. Selenium reducing Citrobacter fruendii strain KP6 from Mandovi estuary and its potential application in selenium nanoparticle synthesis. Proceedings of the National Academy of Sciences, India Section B: Biological Sciences 88(2), 747-754.

Samelak, I., Balaban, M., Antić, M., Šolević Knudsen, T., Jovančićević, B., 2020. Geochromatographic migration of oil pollution from a heating plant to river sediments. Environmental Chemistry Letters 18, 459-466.

Santhosh, S., Badusha, M., 2017. Water Quality Assessment of Ashtamudi Lake with Special Reference to Environmental Pollution. ECO CHRONICLE 12, 105-110

Saranya, J.S., Roxy, M.K., Dasgupta, P., Anand, A., 2022. Genesis and trends in marine heatwaves over the tropical Indian Ocean and their interaction with the Indian summer monsoon. Journal of Geophysical Research: Oceans 127(2), 2021JC017427.

Sarkar, D.J., Sarkar, S.D., Manna, R.K., Samanta, S., Das, B.K., 2020. Microplastics pollution: an emerging threat to freshwater aquatic ecosystem of India. J Inland Fish Soc India 52(1), 05-15.

Sarkar, S., Prakasam, M., Upasana, S., Bhushan, R., Gaury, P.K., Meena, N.K., 2016. Rapid sedimentation history of Rewalsar Lake, Lesser Himalaya, India during the last fifty

years-estimated using Cs and Pb dating techniques: a comparative study with other North-Western Himalayan Lakes. Himal Geol. 37(1), 1-7.

Schmidt, N., Castro-Jiménez, J., Oursel, B., Sempéré, R., 2021. Phthalates and organophosphate esters in surface water, sediments and zooplankton of the NW Mediterranean Sea: exploring links with microplastic abundance and accumulation in the marine food web. Environmental Pollution 272, 115970.

Schrank, I., Trotter, B., Dummert, J., Scholz-Böttcher, B.M., Löder, M.G., Laforsch, C., 2019. Effects of microplastic particles and leaching additive on the life history and morphology of Daphnia magna. Environmental Pollution *255*, 113233.

Schubert, C.J., Calvert, S.E., 2001. Nitrogen and carbon isotopic composition of marine and terrestrial organic matter in Arctic Ocean sediments: implications for nutrient utilization and organic matter composition. Deep Sea Research Part I: Oceanographic Research Papers 48(3), 789-810.

Sedlak, D., 2017. Three lessons for the microplastics voyage. Environmental Science & Technology 51(14), 7747-7748.

Selvakumar, R.A., Nair, V.R., Madhupratap, M., 1980. Seasonal variations in the secondary production of the Mandovi–Zuari estuarine system of Goa. Ind J Mar Sci. 1980. 9, 27–34.

Shetye, S.R., 1999. Propagation of tides in the Mandovi and Zuari estuaries. Sadhana 24(1-2), 5-16.

Seifert, W.K., Moldowan, J.M., 1980. The effect of thermal stress on source-rock quality as measured by hopane stereochemistry. Physics and Chemistry of the Earth 12, 229-237.

Selvaraj, K.K., Sundaramoorthy, G., Ravichandran, P.K., Girijan, G.K., Sampath, S., Ramaswamy, B.R., 2015. Phthalate esters in water and sediments of the Kaveri River, India: environmental levels and ecotoxicological evaluations. Environmental geochemistry and health 37(1), 83-96.

Sharma, S., Chatterjee, S., 2017. Microplastic pollution, a threat to marine ecosystem and human health: a short review. Environmental Science and Pollution Research 24(27), 21530-21547.

Shetye, S.R., Shankar, D., Neetu, S., Suprit, K., Michael, G.S., Chandramohan, P., 2007. The environment that conditions the Mandovi and Zuari estuaries. In Shetye, S.R., Kumar,

M.D., Shankar, D., (Eds.), The Mandovi and Zuari estuaries. National Institute of oceanography, Goa, India, 3-27.

Shetye, S.R., 1999. Propagation of tides in the Mandovi and Zuari estuaries. Sadhana, 24(1-2), 5-16.

Shetye, S.R., Vijith, V., 2013. Sub-tidal water-level oscillations in the Mandovi estuary, west coast of India. Estuarine, Coastal and Shelf Science 134, 1-10.

Shynu, R., Rao, V.P., Kessarkar, P.M., Rao, T.G., 2012. Temporal and spatial variability of trace metals in suspended matter of the Mandovi estuary, central west coast of India. Environmental Earth Sciences 65(3), 725-739.

Shynu, R., Rao, V.P., Sarma, V.V.S.S., Kessarkar, P.M., ManiMurali, R., 2015. Sources and fate of organic matter in suspended and bottom sediments of the Mandovi and Zuari estuaries, western India. Current Science 226-238.

Sigler, M., 2014. The effects of plastic pollution on aquatic wildlife: current situations and future solutions. Water, Air, & Soil Pollution 225, 1-9.

Silva, T.R., Lopes, S.R., Spörl, G., Knoppers, B.A., Azevedo, D.A., 2013. Evaluation of anthropogenic inputs of hydrocarbons in sediment cores from a tropical Brazilian estuarine system. Microchemical Journal 109, 178-188.

Silveira, M.J., Thomaz, S.M., 2015. Growth of a native versus an invasive submerged aquatic macrophyte differs in relation to mud and organic matter concentrations in sediment. Aquatic Botany 124, 85-91.

Sinclair, M., Sagar, M.V., Knudsen, C., Sabu, J., Ghermandi, A., 2021. Economic appraisal of ecosystem services and restoration scenarios in a tropical coastal Ramsar wetland in India. Ecosystem Services 47, 101236.

Singh, I.J., Singh, S.K., Kushwaha, S.P.S., Ashutosh, S., Singh, R.K., 2004. Assessment and monitoring of estuarine mangrove forests of Goa using satellite remote sensing. Journal of the Indian Society of Remote Sensing 32(2), 167-174.

Singh, K.T., Nayak, G.N., Fernandes, L.L., Borole, D.V., Basavaiah, N., 2014. Changing environmental conditions in recent past - Reading through the study of geochemical characteristics, magnetic parameters and sedimentation rate of mudflats, central west coast of India. Palaeogeography, Palaeoclimatology, Palaeoecology 397, 61-74.

Sitaram, N., 2014. Impact of urbanisation on water quality parameters–a case study of Ashtamudi Lake, Kollam. International Journal of Research in Engineering and Technology, 3(6), 140-147.

Smith, B.N., Epstein, S., 1971. Two categories of 13C/12C ratios for higher plants. Plant physiology 47(3), 380-384.

Sousa, T.D., Ingole, B., Sousa, S.D., Bhosle, S., 2013. Seasonal variations of nitrate reducing and denitrifying bacteria utilizing hexadecane in Mandovi estuary, Goa, West Coast of India. Indian J Geo Mar Sci 42, 587–592.

Sreekanth, G.B., Madhu, V.R., Jha, P.N., Thomas, S.N., 2017. Quantitative and qualitative assessment of hook and line fishery in estuaries of Goa: A preliminary analysis. 107-108.

Srivastava, A., Sharma, V.P., Tripathi, R., Kumar, R., Patel, D.K., Mathur, P.K., 2010. Occurrence of phthalic acid esters in Gomti River Sediment, India. Environmental monitoring and assessment 169(1), 397-406.

Steinhauer, M.S., Boehm, P.D., 1992. The composition and distribution of saturated and aromatic hydrocarbons in nearshore sediments, river sediments, and coastal peat of the Alaskan Beaufort Sea: Implications for detecting anthropogenic hydrocarbon inputs. Marine Environmental Research 33(4), 223-253.

Sundarapandian, S.M., Swamy, P.S., 1999. Litter production and leaf-litter decomposition of selected tree species in tropical forests at Kodayar in the Western Ghats, India. Forest Ecology and Management 123(2-3), 231-244.

Sundar, D., Shetye, S.R., 2005. Tides in the Mandovi and Zuari estuaries, Goa, west coast of India. Journal of Earth System Science 114(5), 493-503.

Sündermann, J., Feng, S., 2004. Analysis and modelling of the Bohai sea ecosystem—a joint German–Chinese study. Journal of marine systems 44(3-4), 127-140.

Staples, C.A., Peterson, D.R., Parkerton, T.F., Adams, W.J., 1997. The environmental fate of phthalate esters: a literature review. Chemosphere 35(4), 667-749.

Steinsberger, T., Schwefel, R., Wüest, A., Müller, B., 2020. Hypolimnetic oxygen depletion rates in deep lakes: Effects of trophic state and organic matter accumulation. Limnology and Oceanography 65(12), 3128-3138.

Sun, J., Huang, J., Zhang, A., Liu, W., Cheng, W., 2013. Occurrence of phthalate esters in sediments in Qiantang River, China and inference with urbanization and river flow regime. Journal of hazardous materials 248, 142-149.

Swan, S.H., 2008. Environmental phthalate exposure in relation to reproductive outcomes and other health endpoints in humans. Environmental research 108(2), 177-184.

Talsness, C.E., Andrade, A.J., Kuriyama, S.N., Taylor, J.A., Vom Saal, F.S., 2009. Components of plastic: experimental studies in animals and relevance for human health. Philosophical Transactions of the Royal Society B: Biological Sciences 364(1526), 2079-2096.

Tan, X., Yu, X., Cai, L., Wang, J., Peng, J., 2019. Microplastics and associated PAHs in surface water from the Feilaixia Reservoir in the Beijiang River, China. Chemosphere 221, 834-840.

Teil, M.J., Blanchard, M., Dargnat, C., Larcher-Tiphagne, K., Chevreuil, M., 2007. Occurrence of phthalate diesters in rivers of the Paris district (France). Hydrological Processes: An International Journal 21(18), 2515-2525.

Teng, J., Zhao, J., Zhang, C., Cheng, B., Koelmans, A.A., Wu, D., Gao, M., Sun, X., Liu, Y., Wang, Q., 2020. A systems analysis of microplastic pollution in Laizhou Bay, China. Science of the Total Environment 745, 140815.

Ten Haven, H.L., De Leeuw, J.W., Rullkötter, J., Damsté, J.S., 1987. Restricted utility of the pristane/phytane ratio as a palaeoenvironmental indicator. Nature 330(6149), 641-643.

Thakur, R.K., Jindal, R., Singh, U.B., Ahluwalia, A.S., 2013. Plankton diversity and water quality assessment of three freshwater lakes of Mandi (Himachal Pradesh, India) with special reference to planktonic indicators. Environmental monitoring and assessment 185(10), 8355-8373.

Thompson, R.C., 2015. Microplastics in the marine environment: sources, consequences and solutions. In Marine anthropogenic litter. Springer, Cham. 185-200.

Thornton, S.F., McManus, J., 1994. Application of organic carbon and nitrogen stable isotope and C/N ratios as source indicators of organic matter provenance in estuarine systems: evidence from the Tay estuary, Scotland. Estuar. Coast. Shelf Sci. 38, 219-233.

Tsering, T., Sillanpää, M., Viitala, M., Reinikainen, S.P., 2022. Variation of microplastics in the shore sediment of high-altitude lakes of the Indian Himalaya using different pretreatment methods. Science of The Total Environment 849, 157870.

Untawale, A.G., Dwivedi, S.N., Singbal, S.Y.S., 1973. Ecology of mangroves in Mandovi and Zuari estuaries and the interconnecting Cumbarjua canal of Goa. Indian J Geo Mar Sci 2, 47–573.

Untawale, A.G., Jagtap, T.G., 1977. A new record of Halophila beccarii Aschers from Indian coast. Mahasagar 10(1-2), 91-93.

USEPA 2010. National primary drinking water regulation. United States Environmental Protection Agency.

Vaezzadeh, V., Zakaria, M.P., Shau-Hwai, A.T., Ibrahim, Z.Z., Mustafa, S., Abootalebi-Jahromi, F., Masood, N., Magam, S.M., Alkhadher, S.A.A., 2015. Forensic investigation of aliphatic hydrocarbons in the sediments from selected mangrove ecosystems in the west coast of Peninsular Malaysia. Marine pollution bulletin 100(1), 311-320.

Vanapalli, K.R., Dubey, B.K., Sarmah, A.K., Bhattacharya, J., 2021. Assessment of microplastic pollution in the aquatic ecosystems–An indian perspective. Case Studies in Chemical and Environmental Engineering 3, 100071.

Van Cauwenberghe, L., Devriese, L., Galgani, F., Robbens, J., Janssen, C.R., 2015. Microplastics in sediments: a review of techniques, occurrence and effects. Marine environmental research 111, 5-17.

Van Leussen, W., Dronkers, J., 1988. Physical processes in estuaries: An introduction. In Physical processes in estuaries. Springer, Berlin, Heidelberg, 1-18.

Van Wezel, A.P., Van Vlaardingen, P., Posthumus, R., Crommentuijn, G.H., Sijm, D.T.H.M., 2000. Environmental risk limits for two phthalates, with special emphasis on endocrine disruptive properties. Ecotoxicology and Environmental Safety 46(3), 305-321.

Veerasingam, S., Saha, M., Suneel, V., Vethamony, P., Rodrigues, A.C., Bhattacharyya, S., Naik, B.G., 2016. Characteristics, seasonal distribution and surface degradation features of microplastic pellets along the Goa coast, India. Chemosphere 159, 496-505.

Veerasingam, S., Vethamony, P., ManiMurali, R., Babu, M.T., 2015b. Sources, vertical fluxes and accumulation of petroleum hydrocarbons in sediments from the Mandovi estuary, west coast of India. Int. J. Environ. Res. 9(1), 179-186.

Veerasingam, S., Vethamony, P., Murali, R.M., Fernandes, B., 2015a. Depositional record of trace metals and degree of contamination in core sediments from the Mandovi estuarine mangrove ecosystem, west coast of India. Marine pollution bulletin 91(1), 362-367.

Ventura, G.T., Kenig, F., Reddy, C.M., Frysinger, G.S., Nelson, R.K., Van Mooy, B., Gaines, R.B., 2008. Analysis of unresolved complex mixtures of hydrocarbons extracted from Late Archean sediments by comprehensive two-dimensional gas chromatography (GC× GC). Organic Geochemistry 39(7), 846-867.

Venturini, N., Muniz, P., Bícego, M.C., Martins, C.C., Tommasi, L.R., 2008. Petroleum contamination impact on macrobenthic communities under the influence of an oil refinery: integrating chemical and biological multivariate data. Estuarine, Coastal and Shelf Science 78(3), 457-467.

Venkatramanan, S., Chung, S.Y., Selvam, S., Sivakumar, K., Soundhariya, G.R., Elzain, H.E., Bhuyan, M.S., 2022. Characteristics of microplastics in the beach sediments of Marina tourist beach, Chennai, India. Marine Pollution Bulletin 176, 113409.

Verla, A.W., Enyoh, C.E., Verla, E.N., Nwarnorh, K.O., 2019. Microplastic–toxic chemical interaction: a review study on quantified levels, mechanism and implication. SN Applied Sciences 1(11), 1-30.

Vethamony, P., Sudheesh, K., Babu, M.T., Jayakumar, S., Manimurali, R., Saran, A.K., Sharma, L.H., Rajan, B., Srivastava, M., 2007. Trajectory of an oil spill off Goa, eastern Arabian Sea: Field observations and simulations. Environmental pollution 148(2), 438-444.

Vianello, A., Boldrin, A., Guerriero, P., Moschino, V., Rella, R., Sturaro, A., Da Ros, L., 2013. Microplastic particles in sediments of Lagoon of Venice, Italy: First observations on occurrence, spatial patterns and identification. Estuarine, Coastal and Shelf Science 130, 54-61.

Vijith, V., Shetye, S.R., Baetens, K., Luyten, P., Michael, G.S., 2016. Residual estuarine circulation in the Mandovi, a monsoonal estuary: A three-dimensional model study. Estuarine, Coastal and Shelf Science 173, 79-92.

Vijith, V., Sundar, D., Shetye, S.R., 2009. Time-dependence of salinity in monsoonal estuaries. Estuarine, Coastal and Shelf Science 85(4), 601-608.

Visher, G.S., 1969. Grain size distributions and depositional processes. Journal of Sedimentary Research 39(3).

VishnuRadhan, R., Sagayadoss, J., Seelan, E., Vethamony, P., Shirodkar, P., Zainudin, Z., Shirodkar, S., 2015. Southwest monsoon influences the water quality and waste assimilative capacity in the Mandovi estuary (Goa state, India). Chemistry and Ecology 31(3), 217-234.

Volkman, J.K., Holdsworth, D.G., Neill, G.P., Bavor Jr, H.J., 1992. Identification of natural, anthropogenic and petroleum hydrocarbons in aquatic sediments. Science of the Total Environment 112(2-3), 203-219.

Wagner, M., Scherer, C., Alvarez-Muñoz, D., Brennholt, N., Bourrain, X., Buchinger, S., Fries, E., Grosbois, C., Klasmeier, J., Marti, T., Rodriguez-Mozaz, S., 2014. Microplastics in freshwater ecosystems: what we know and what we need to know. Environmental Sciences Europe 26(1), 1-9.

Wang, J., Tan, Z., Peng, J., Qiu, Q., Li, M., 2016. The behaviors of microplastics in the marine environment. Marine Environmental Research 113, 7-17.

Wang, X.C., Chen, R.F., Berry, A., 2003. Sources and preservation of organic matter in Plum Island salt marsh sediments (MA, USA): long-chain n-alkanes and stable carbon isotope compositions. Estuarine, Coastal and Shelf Science 58(4), 917-928.

Wang, Z., Fingas, M. and Sergy, G., 1994. Study of 22-year-old Arrow oil samples using biomarker compounds by GC/MS. Environmental science & technology 28(9), 1733-1746.

Ward, N.D., Bianchi, T.S., Medeiros, P.M., Seidel, M., Richey, J.E., Keil, R.G., Sawakuchi, H.O., 2017. Where carbon goes when water flows: carbon cycling across the aquatic continuum. Frontiers in Marine Science 4, 7.

Warrier, A.K., Kulkarni, B., Amrutha, K., Jayaram, D., Valsan, G., Agarwal, P., 2022. Seasonal variations in the abundance and distribution of microplastic particles in the surface waters of a Southern Indian Lake. Chemosphere 300, 134556.

WHO 2010. Guidelines for drinking water quality, recommendations. 2nd Edn. Geneva.

Wu Y., Zhang, J., Cho, K.W., Hong, G.H., Chung, C.S., 2004. Origin and transport of sedimentary organic matter in the Yalujiang Estuary, North China. Estuaries 27, 583–92.

Yamada, K., Ishiwatari, R., 1999. Carbon isotopic compositions of long-chain n-alkanes in the Japan Sea sediments: implications for paleoenvironmental changes over the past 85 kyr. Organic Geochemistry 30(5), 367-377.

Yang, C., Harris, S.A., Jantunen, L.M., Kvasnicka, J., Nguyen, L.V., Diamond, M.L., 2020. Phthalates: relationships between air, dust, electronic devices, and hands with implications for exposure. Environmental Science & Technology 54(13), 8186-8197.

Yang, G., Zhou, X., Wang, J., Zhang, W., Zheng, H., Lu, W., Yuan, J., 2012. MEHP-induced oxidative DNA damage and apoptosis in HepG2 cells correlates with p53-mediated mitochondria-dependent signaling pathway. Food and chemical toxicology 50(7), 2424-2431.

Yang, S., Zhou, M., Chen, X., Hu, L., Xu, Y., Fu, W., Li, C., 2022. A comparative review of microplastics in lake systems from different countries and regions. Chemosphere 286, 131806.

Yang, X., Yuan, X., Zhang, A., Mao, Y., Li, Q., Zong, H., Wang, L., Li, X., 2015. Spatial distribution and sources of heavy metals and petroleum hydrocarbon in the sand flats of Shuangtaizi Estuary, Bohai Sea of China. Marine Pollution Bulletin 95(1), 503-512.

Yan, M., Wang, L., Dai, Y., Sun, H. and Liu, C., 2021. Behavior of microplastics in inland waters: aggregation, settlement, and transport. Bulletin of Environmental Contamination and Toxicology, 107(4), pp.700-709.

Yan, Z., Zhang, S., Zhao, Y., Yu, W., Zhao, Y., Zhang, Y., 2022. Phthalates released from microplastics inhibit microbial metabolic activity and induce different effects on intestinal luminal and mucosal microbiota. Environmental Pollution 310, 119884.

Yost, E.E., Euling, S.Y., Weaver, J.A., Beverly, B.E., Keshava, N., Mudipalli, A., Arzuaga, X., Blessinger, T., Dishaw, L., Hotchkiss, A., Makris, S.L., 2019. Hazards of diisobutyl phthalate (DIBP) exposure: A systematic review of animal toxicology studies. Environment international 125, 579-594.

Yuan, D., Yang, D., Wade, T.L., Qian, Y., 2001. Status of persistent organic pollutants in the sediment from several estuaries in China. Environmental Pollution 114(1), 101-111.

Yuan, W., Liu, X., Wang, W., Di, M., Wang, J., 2019. Microplastic abundance, distribution and composition in water, sediments, and wild fish from Poyang Lake, China. Ecotoxicology and environmental safety 170, 180-187.

Yu, F., Zong, Y., Lloyd, J.M., Huang, G., Leng, M.J., Kendrick, C., Lamb, A.L., Yim, W.W.S., 2010. Bulk organic δ13C and C/N as indicators for sediment sources in the Pearl River delta and estuary, southern China. Estuarine, Coastal and Shelf Science 87(4), 618-630.

Zachariah, E.J., Johny, C.J., 2009. Methane in Estuarine Discharges to Coastal Ocean–A Study at Ashtamudi Estuary, Kerala, India. Asian Journal of Water, Environment and Pollution 6(2), 15-22.

Zaghden, H., Kallel, M., Louati, A., Elleuch, B., Oudot, J., Saliot, A., 2005. Hydrocarbons in surface sediments from the Sfax coastal zone, (Tunisia) Mediterranean Sea. Marine Pollution Bulletin 50(11), 1287-1294.

Zakaria, M.P., Takada, H., Tsutsumi, S., Ohno, K., Yamada, J., Kouno, E., Kumata, H., 2002. Distribution of polycyclic aromatic hydrocarbons (PAHs) in rivers and estuaries in Malaysia: a widespread input of petrogenic PAHs. Environmental science & technology 36(9), 1907-1918.

Zeng, F., Cui, K., Xie, Z., Wu, L., Luo, D., Chen, L., Lin, Y., Liu, M., Sun, G., 2009a. Distribution of phthalate esters in urban soils of subtropical city, Guangzhou, China. Journal of hazardous materials 164(2-3), 1171-1178.

Zeng, F., Wen, J., Cui, K., Wu, L., Liu, M., Li, Y., Lin, Y., Zhu, F., Ma, Z., Zeng, Z., 2009b. Seasonal distribution of phthalate esters in surface water of the urban lakes in the subtropical city, Guangzhou, China. Journal of Hazardous Materials 169(1-3), 719-725.

Zhang, H., 2017. Transport of microplastics in coastal seas. Estuarine, Coastal and Shelf Science 19974–86.

Zhang, J., Wang, D.R., Jennerjahn, T., Dsikowitzky, L., 2013. Land–sea interactions at the east coast of Hainan Island, South China Sea: a synthesis. Continental Shelf Research 57, 132-142.

Zhang, K., Hamidian, A.H., Tubić, A., Zhang, Y., Fang, J.K., Wu, C., Lam, P.K., 2021. Understanding plastic degradation and microplastic formation in the environment: A review. Environmental Pollution 274, 116554.

Zhang, Y., Yu, J., Su, Y., Du, Y., Liu, Z., 2020. A comparison of n-alkane contents in sediments of five lakes from contrasting environments. Organic Geochemistry 139, 103943.

Zhang, Y., Sun, Y., Liu, B., Wang, Y., Xie, W., Wang, P., Zhang, C., He, D., 2021. Spatiotemporal distribution and source variations of hydrocarbons in surface sediments

from the Pearl River Estuary, Southern China. Journal of Soils and Sediments 21(1), 499-511.

Zheng, X., Zhang, B.T., Teng, Y., 2014. Distribution of phthalate acid esters in lakes of Beijing and its relationship with anthropogenic activities. Science of the Total Environment 476, 107-113.

Zheng, Y., Li, J., Cao, W., Jiang, F., Zhao, C., Ding, H., Wang, M., Gao, F., Sun, C., 2020. Vertical distribution of microplastics in bay sediment reflecting effects of sedimentation dynamics and anthropogenic activities. Marine Pollution Bulletin 152, 110885.

Zhou, J., Wu, Y., Zhang, J., Kang, Q., Liu, Z., 2006. Carbon and nitrogen composition and stable isotope as potential indicators of source and fate of organic matter in the salt marsh of the Changjiang Estuary, China. Chemosphere 65(2), 310-317.

Zhou, Y., Zhou, L., Zhang, Y., Zhu, G., Qin, B., Jang, K.S., Spencer, R.G., Kothawala, D.N., Jeppesen, E., Brookes, J.D., Wu, F., 2022. Unraveling the role of anthropogenic and natural drivers in shaping the molecular composition and biolability of dissolved organic matter in non-pristine lakes. Environmental Science & Technology 56(7), 4655-4664.

Zimmerman, A.R., Canuel, E.A., 2000. A geochemical record of eutrophication and anoxia in Chesapeake Bay sediments: anthropogenic influence on organic matter composition. Marine Chemistry 69(1-2), 117-137.

Zrafi, I., Hizem, L., Chalghmi, H., Ghrabi, A., Rouabhia, M., Saidane-Mosbahi, D., 2013. Aliphatic and aromatic biomarkers for petroleum hydrocarbon investigation in marine sediment. Journal of Petroleum Science Research (JPSR) 2(4).

Zhang, Y.H., Chen, B.H., Zheng, L.X., Zhu, J.H., Ding, X.C., 2003. Determination of phthalates in environmental samples. Journal of Environmental Health 20(5), 283-286.

Zota, A.R., Calafat, A.M., Woodruff, T.J., 2014. Temporal trends in phthalate exposures: findings from the National Health and Nutrition Examination Survey, 2001–2010. Environmental health perspectives 122(3), 235-241.

Appendix 01

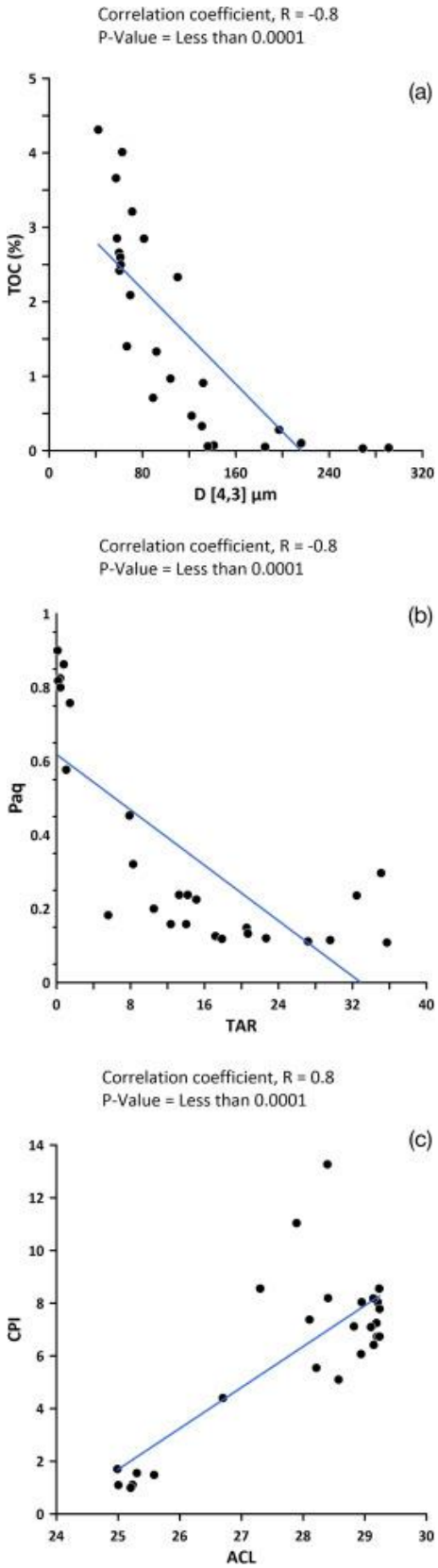

Fig. S2.1. Relationship of (a) D[4,3] and TOC (%), (b) TAR and Paq, (c) CPI and ACL.

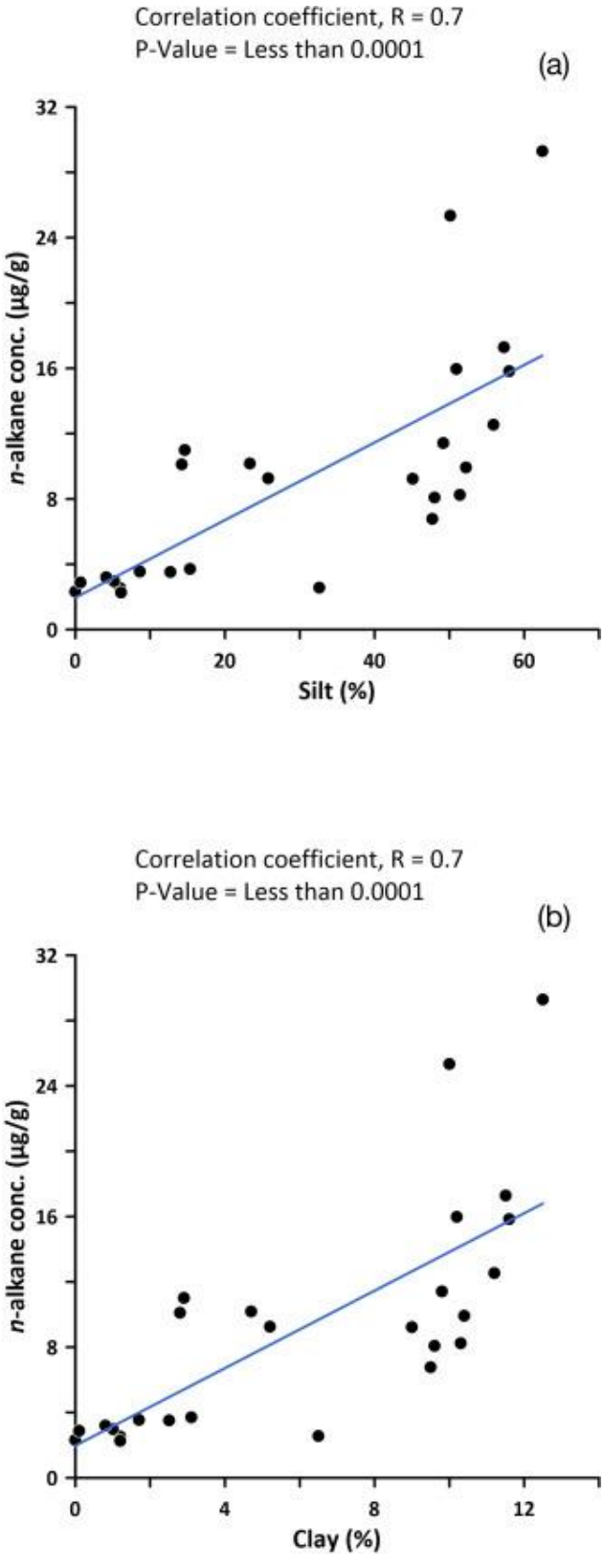

Fig. S2.2. Relationship of (a) silt (%) and *n*-alkane concentrations, (b) clay (%) and *n*-alkane Concentrations.

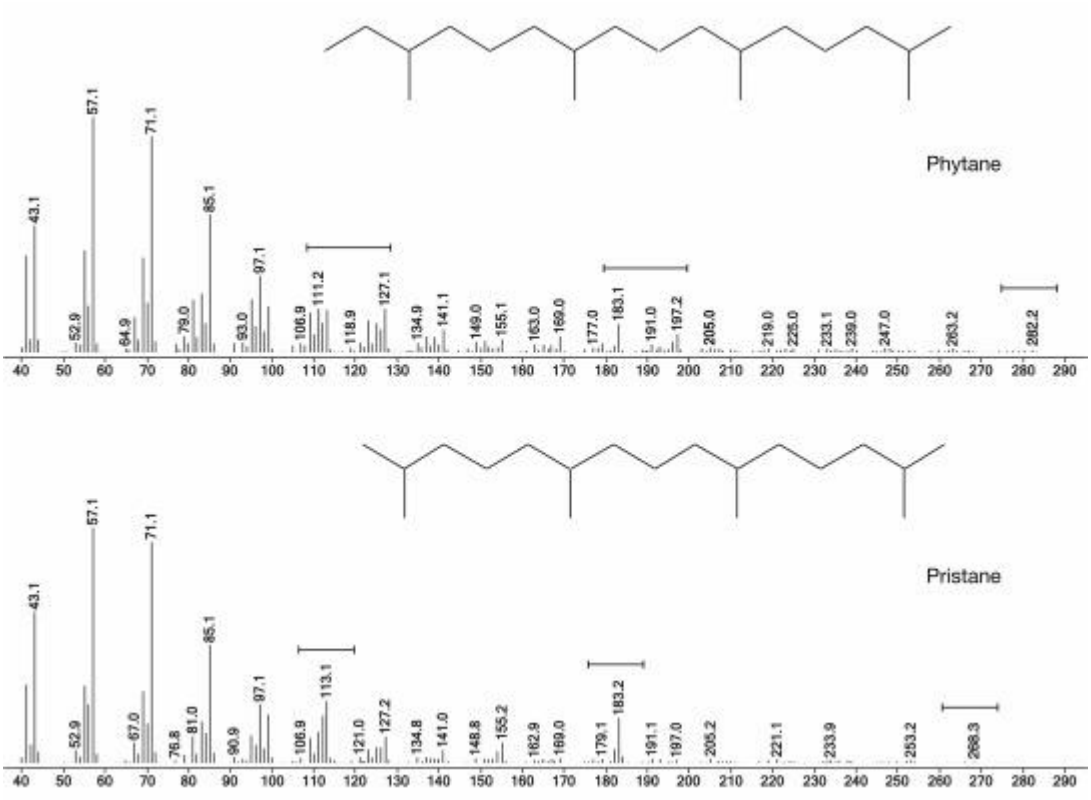

Fig. S2.3. Mass spectra of pristane and phytane.

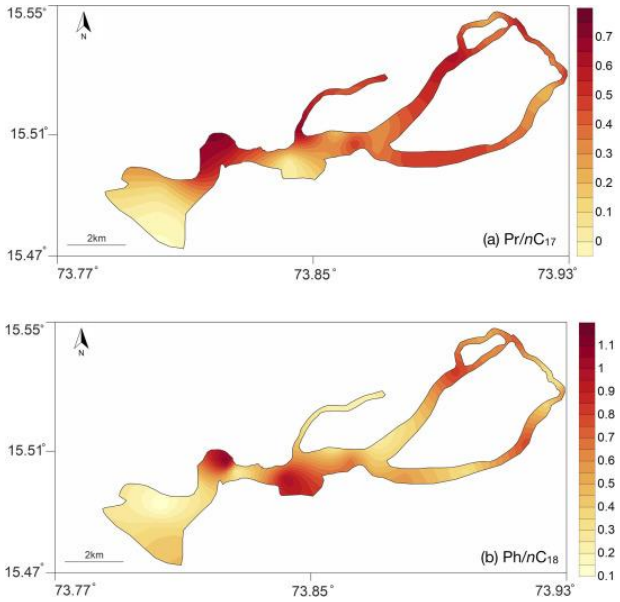

Fig. S2.4. Spatial distribution of (a) Pr/*n*-C17, (b) Ph/*n*-C18 in estuarine surface sediments.

Appendix 02

Supplementary Table S3.1: Information about qualitative method for phthalates identification in Ashtamudi estuary.

S.No.	Retention Time (min.)	Compound Name	Diagnostic Ions
1.	41.66	DIBP	149, 278
2.	43.18-45.0	DBP isomers	149, 278
3.	63.0	DEHP	149, 390
4.	67.1-73.0	DINP isomers	149, 418

Supplementary Table S3.2: Information about qualitative method for phthalates identification in Mandovi estuary

S.No.	Retention Time (min.)	Compound Name	Diagnostic Ions
1.	31.2	DEP	149, 222
2.	44.1	DIBP	149, 278
3.	46.2-48.1	DBP isomers	149, 278
4.	70.1	DEHP	149, 390
5.	76.2	DEHTP	149, 390

Supplementary Table S3.3: The identified hopanes from Ashtamudi and Mandovi estuaries.

S. No.	Retention Time (min.)	Compound Name	Diagnostic Ions
1.	67.759	18α(H)-22,29,30-trisnorneohopane	191, 370
2.	69.423	17α(H)-22,29,30-trisnorhopane	191, 370
3.	71.625	17α(H), 21β(H) C_{29} hopane	191, 398
4.	71.75	17α(H), 21β(H) C_{30} hopane	191, 412
5.	73.426-73.614	C_{31}homohopanes (22S, 22R)	191,426
6.	75.516-75.778	C_{32}homohopanes (22S, 22R)	191, 440
7.	77.167-77.517	C_{33}homohopanes (22S, 22R)	191, 454

Supplementary Table S3.4: The identified steranes and diasteranes from Ashtamudi and Mandovi estuaries.

S.No.	Retention time (min)	Compound name	Diagnostic Ions
1.	64.7-65.5	C27 diasterane	217/259, 372
2.	66.7-66.9	C28 diasterane	217/ 259,386
3.	68.3-68.6	C27 steranes	217/218, 372
4.	68.8	C29 diasterane	217/ 259,400
5.	70.8-71.0	C28 steranes	217/218, 386
6.	72.7-72.9	C29 steranes	217/218, 400

Supplementary Table S3.5: Comparison of phthalates (ng/g) in sediments measured in the present study with other study sites worldwide.

S. No.	Locations	DEP	DIBP	DBP	DEHP	DEHTP	DINP	∑PAEs	References
1.	Kaveri River, India	n.d.-16	-	nd-36	n.d.-278	-	-	2-1,438	Selvaraj et al., 2015
2.	Cochin estuary, India	0-565	-	1-349	0-3650	-	-	44-4,015	Ramzi et al., 2018
3.	Gomti River, India	n.d.-350	-	n.d.-340	n.d.-3240	-	-	0-1,870	Srivastava et al., 2010
4.	Pearl River estuary, China	n.d.-180	-	56-4660	470-8530	-	-	880-13,600	Li et al., 2016
5.	Guanting Reservoir, China	0.2-89.5	n.d.-1370.3	n.d.-570.6	n.d.-278.4	-	-	52.6-6,034.2	Zheng et al., 2014
6.	Jinshan, China	-	-	19-50	32-48	-	-	-	Zhang et al., 2003
7.	Ashtamudi estuary, India	-	2.64-514.5	3.85-739.94	1.28 to 223.73	-	0-359.99	7.77 to 1478.17	This study 2022
8.	Mandovi estuary, India	0-19.25	15.01-	30.02-87.68	15.09-38.13	0-18.98	-	60.13 to 271.93	This study 2022

n.d.- not detected

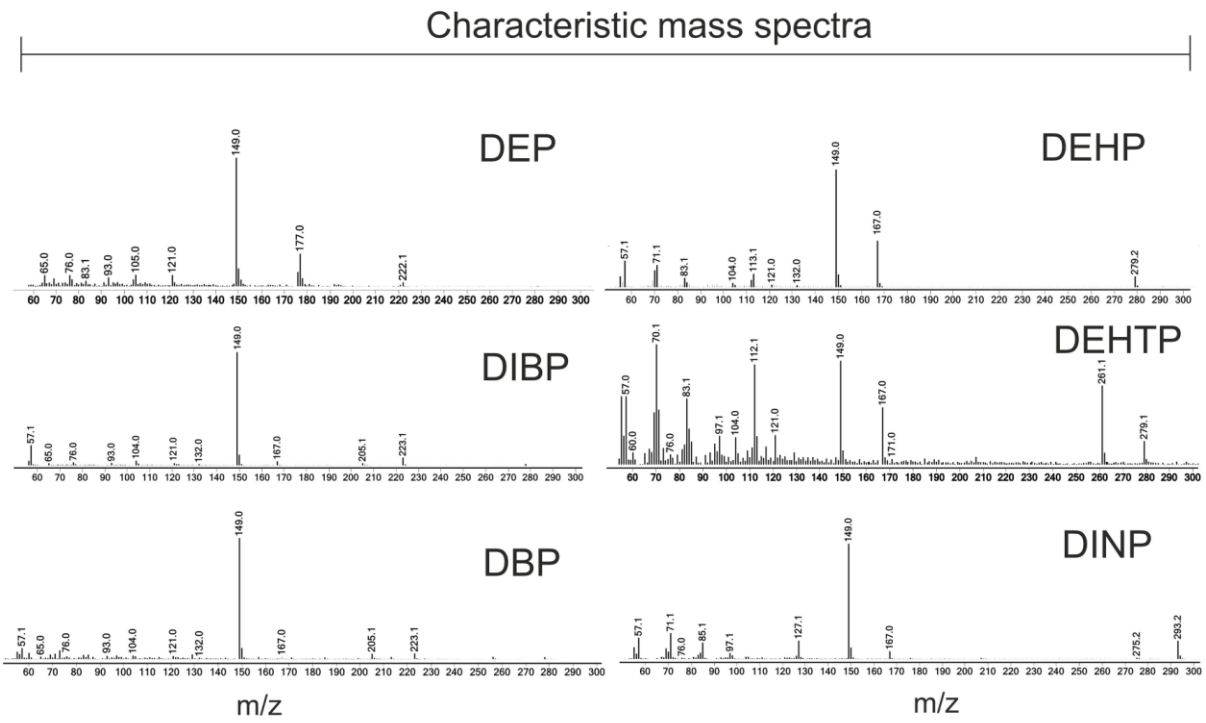

Fig. S3.1. Characteristic mass spectra of phthalate compounds observed in both the tropical estuaries.

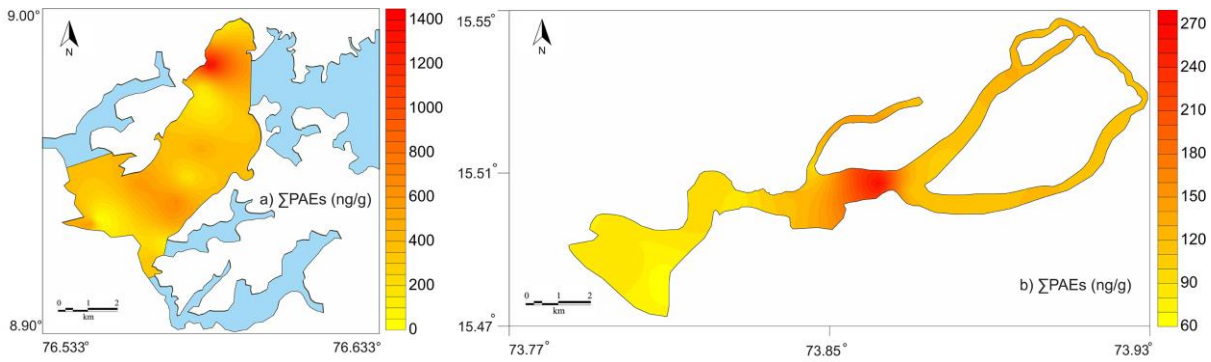

Fig. S3.2. Spatial distribution of phthalates in Ashtamudi estuary (a) and Mandovi estuary (b).

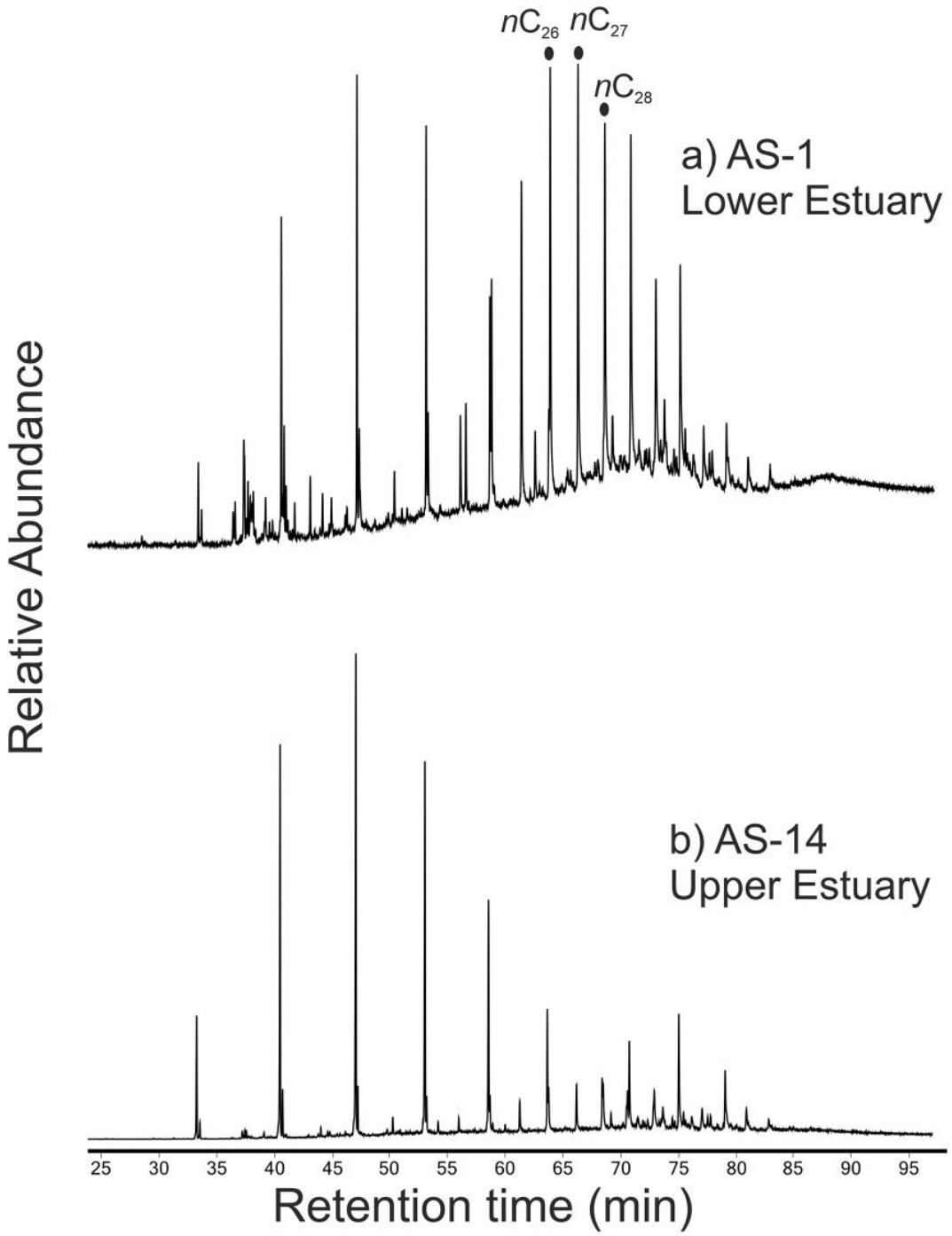

Fig. S3.3. The representative TIC depicting *n*-alkanes distribution in saturated hydrocarbon fraction of surface sediments retrieved from lower and upper Ashtamudi estuary.

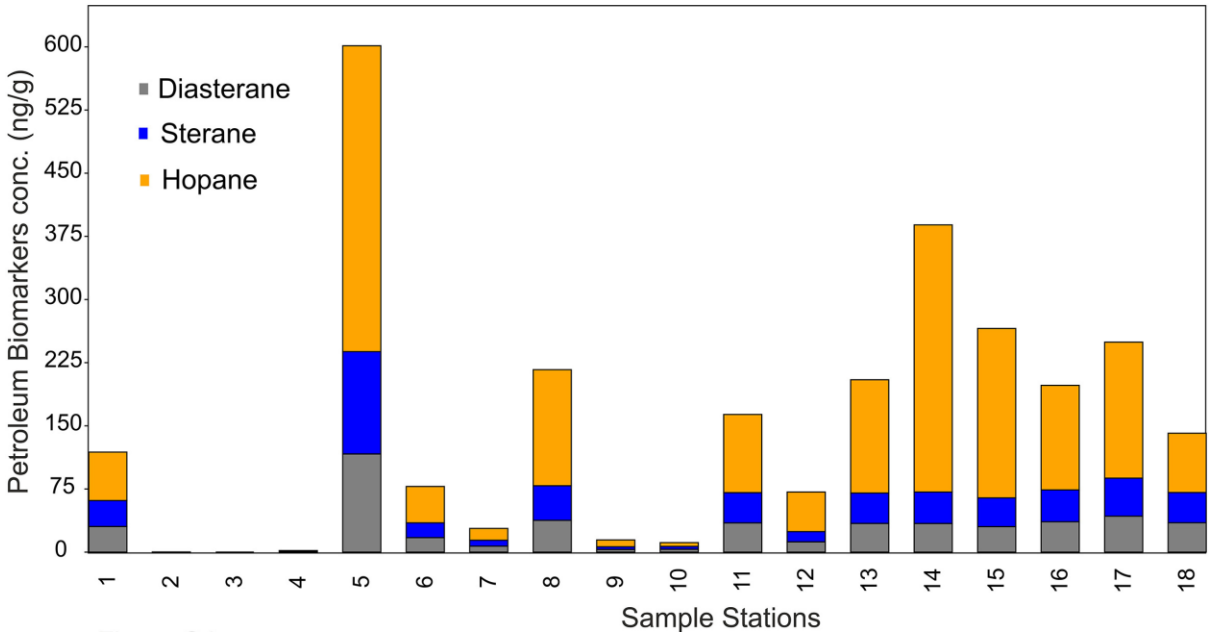

Fig. S3.4. Stacked bar chart representing petroleum biomarker concentrations (ng/g) at different locations of Ashtamudi estuary.

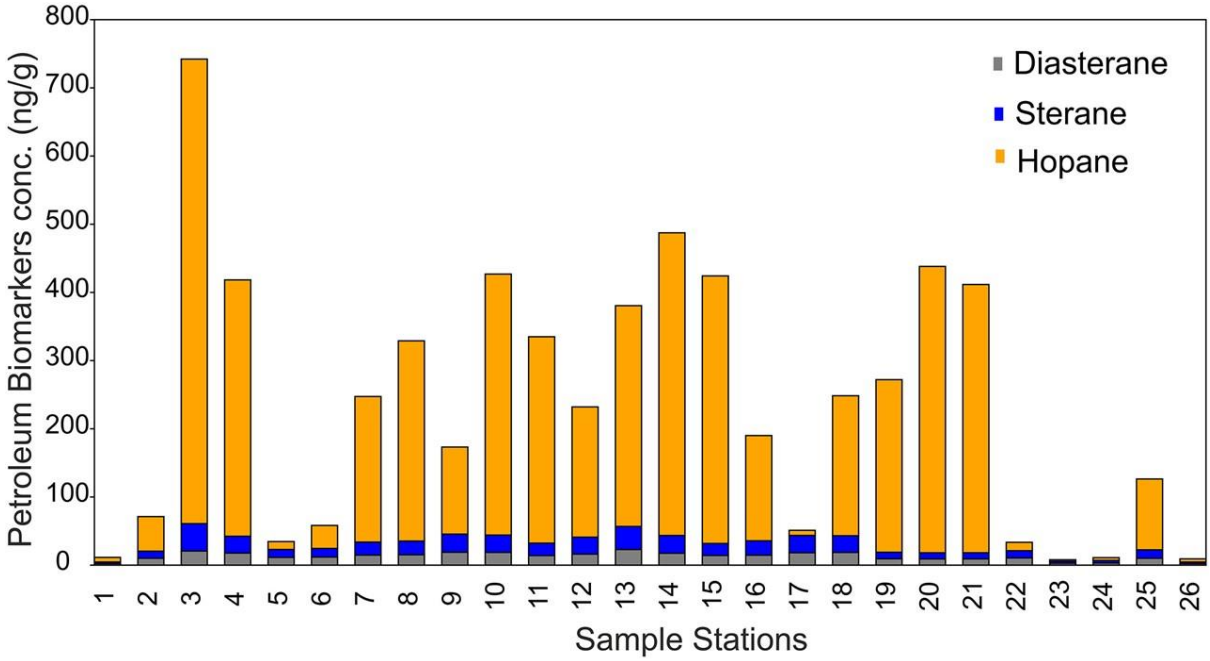

Fig. S3.5. Stacked bar chart depicting petroleum biomarker concentrations (ng/g) at various sampling locations of Mandovi estuary.

Appendix 03

Supplementary Table S4.1: PAE congeners detected in Rewalsar lake.

S.No.	Retention Time (min.)	Compound Name	Diagnostic Ions
1.	41.06	DIBP	149, 278
2.	42.62-44.07	DBP isomers	149, 278
3.	60.51	DEHP	149, 390

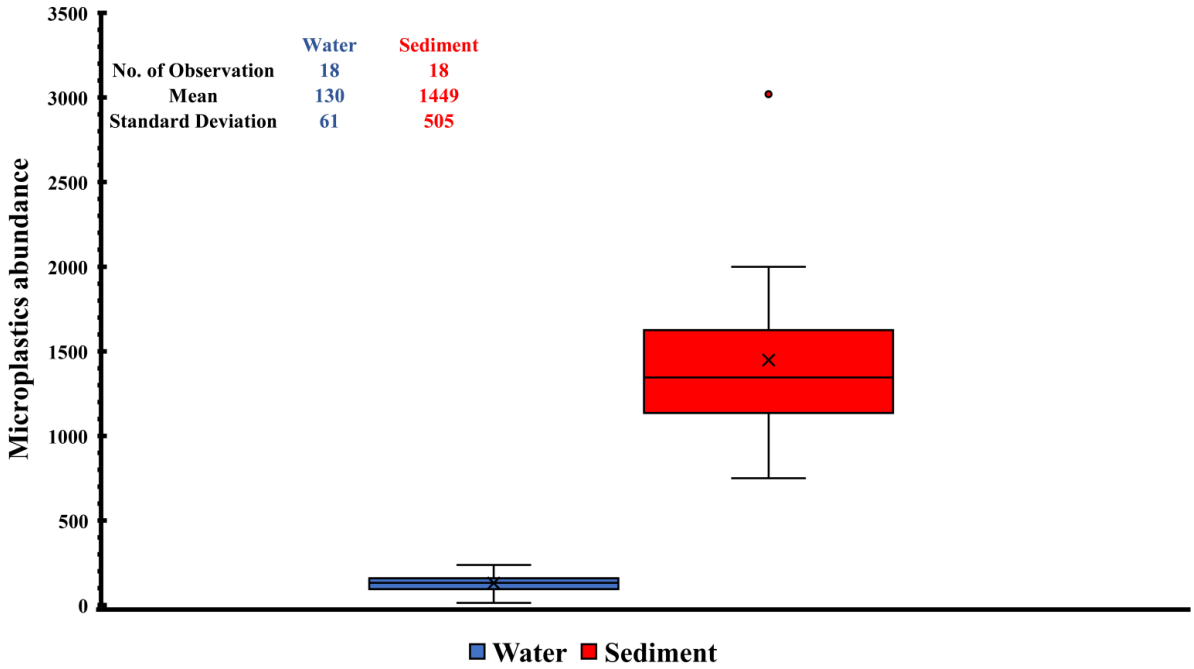

Fig. S4.1: The average abundance of microplastics in surface water and sediment samples of Rewalsar Lake

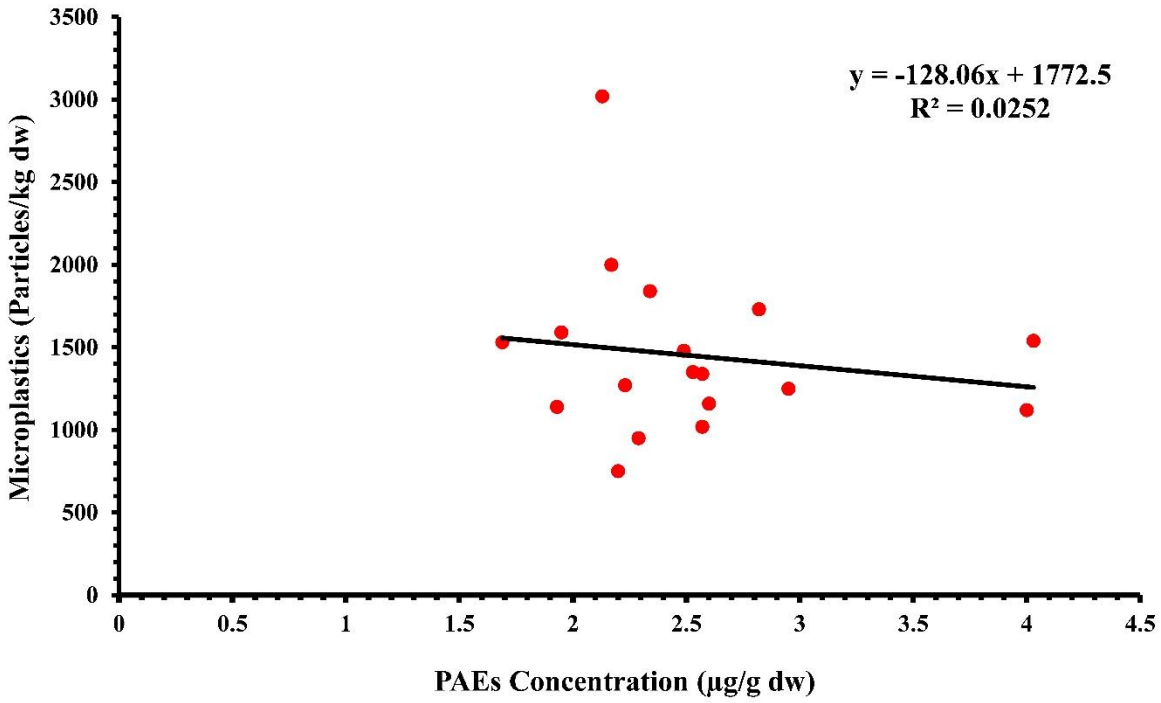

Fig. S4.2: The correlation plot of microplastic abundance and phthalate concentration in surface sediments.